nature chemistry

Article

https://doi.org/10.1038/s41557-022-01124-7

Plasmonic visible–near infrared photothermal activation of olefin metathesis enabling photoresponsive materials

In the format provided by the authors and unedited

Supplementary Information

Plasmonic Vis-NIR photothermal activation of olefin metathesis enabling photoresponsive materials

Nir Lemcoff,[1] Noy B. Nechmad,[1] Or Eivgi,[1] Elad Yehezkel,[1] Ofir Shelonchik,[1] Ravindra S. Phatake,[1] Doron Yesodi,[1]Anna Vaisman,[1] Aritra Biswas,[1] N. Gabriel Lemcoff[1,2] and Yossi Weizmann[1,2]*
[1]Department of Chemistry, Ben-Gurion University of the Negev, Beer-Sheva 84105, Israel
[2]Ilse Katz Institute for Nanotechnology Science, Ben-Gurion University of the Negev, Beer-Sheva 84105, Israel
*Correspondence to: yweizmann@bgu.ac.il (Y.W.)

Table of Contents

1. List of Materials

All materials were purchased from Sigma-Aldrich unless noted otherwise. Ultrapure water (type 1, 18.2 MΩ) from Millipore® Direct-Q® 3 with UV was used.

Cetyltrimethylammonium chloride (CTAC) sodium borohydride ReagentPlus 99 %, sodium citrate tribasic BioUltra ≥ 99.5 %, gold chloride trihydrate 99.9 %, cetyltrimethylammonium bromide (CTAB) ≥ 99 %, ascorbic acid BioXtra ≥ 99.0 %, hydrochloric acid 32 %, silver nitrate BioXtra ≥ 99 %, tetraethyl orthosilicate (TEOS)

reagent grade 98 %, ammonium hydroxide 28 % in water 99.9 %, and dicyclopentadiene (DCPD).

2. Instruments

2.1 Ultra-violet visible (UV-Vis) light spectrophotometer

A BioTek Epoch 2 microplate reader equipped with UV-Vis spectrophotometer was used to determine AuBP solution's localized surface plasmon resonance (LSPR) activation wavelength and optical density (OD). Samples were diluted to less than 1 OD in order to obtain accurate measurements and solvents varied depending on experiment requirements.

2.2 Inductively coupled plasma optical emission spectrometer (ICP-OES)

The amount of Au was determined using a SPECTRO ARCOS ICP-OES. Samples were prepared by dissolving AuBPs in 2 ml of aqua regia and then diluting to obtain a 10 % nitric acid solution.

2.3 Transmission electron microscope (TEM)

TEM images were obtained using a Thermo Fisher Scientific (FEI) Talos F200C transmission electron microscope operating at 200 kV. The images were taken with Ceta 16M CMOS camera. Electron Microscopy Sciences formvar/carbon 200 Mesh, copper grids were prepared by adding 5 µl of an AuBP in ethanol solution (2 OD) to the grid surface and allowing it to evaporate under air.

2.4 Scanning electron microscope (SEM)

SEM images were obtained using a Thermo Fisher Scientific Verios 460L FEI scanning electron microscope. AuBP embedded polymer samples were prepared by cutting a cross section under liquid nitrogen and carbon coating the sample using an Emitech k575x.

2.5 Dynamic Mechanical Analysis (DMA)

DMA measurements were performed using the Mettler-Toledo Dynamic Mechanical Analyzer (DMA) 1 STARe instrument with a rotatable measuring head. The single cantilever bending approach was used for determining the loss factor tan δ for all polymeric films. Runs with frequencies at 1, 5 and 10 Hz were performed at a constant heating rate of 2 °C/min over the temperature ranges from 30 °C to 180 °C. A rectangular specimen was used (length: 20 mm; width: 10 mm; thickness: 1 mm). Viscoelastic properties of the cured polymeric films were estimated from the changes in the storage modulus (E'), mechanical loss (E'') as well as from the changes of tan δ (tan δ = E''/E') at a constant frequency depending on temperature. The T_g was identified as the maximum of the tan δ and the half of the full width from the tan δ curve.

2.6 Tensile Universal Testing Machine (UTM)

Dog-bone-shaped cured specimens of the polymer film were evaluated using a Universal Testing Machine (UTM) (Hounsfield, UK), model H 25 KS, with a maximum load of 25 kN, following the procedure outlined in ASTM D-638 test method. Films were placed between the grips of the testing machine. The grip length was 2.5 cm (the part of the sample held by the instrument), while the loading rate was set to 3 mm/min.

2.7 Matrix-Assisted Laser Desorption/Ionization (MALDI)

Matrix-Assisted Laser Desorption/Ionization (MALDI) mass spectra were recorded on Mass Spectrometer Autoflex speed™ MALDI TOF/TOF. The samples analyzed by MALDI-TOF MS were mixed with NaTFA as additive to improve ion formation.

2.8 Size exclusion chromatography (SEC)

Molecular weights and polydispersity indices (PDIs) of the polymers were determined by size exclusion chromatography (SEC) analyses in tetrahydrofuran (THF) at 35 °C using an Agilent 1260 Infinity II Quaternary system HPLC equipped with two Shodex SEC LF-804 Columns and one Shodex SEC KF-803. The flow rate was set to 1 mL/min. Detection was obtained with Agilent 1260 Infinity II Variable Wavelength Detector G7114A, Wyatt ViscoStar WV4-01 viscometer, Wyatt OPTILAB WOP1-01 refractometer, and Wyatt MALS DAWN WD3-02 laser light-scattering system. Prior to measurements, polymer solutions were filtered through Millipore 0.22 µm filters. Wyatt's Astra 8.0.0.25 64-bit software was used for SEC data analysis and polymer properties calculation.

2.9 Nuclear magnetic resonance spectroscopy (NMR)

NMR spectra were obtained with Bruker DPX 400 or DPX 500 instruments; chemical shifts, given in ppm, are relative to the residual solvent peak.

2.10 Gas chromatography–mass spectrometry (GC-MS)

GC-MS data was obtained using an Agilent 6850 GC equipped with an Agilent 5973 MSD working under standard conditions and an Agilent HP5-MS (30*0.25*0.25) column.

3. AuBP Synthesis and Characterization

3.1 AuBP synthesis

Gold bipyramids were synthesized using the seed mediated method described by Sánchez-Iglesias *et al.*[1] Briefly, 5 ml of $HAuCl_4$ (10 mM), 1 ml of $AgNO_3$ (10 mM) and 2 ml of HCl (1 M) were added to a 100 ml aqueous solution of CTAB (100 mM). Next 0.8 ml of L-ascorbic acid were added under vigorous stirring and the seed solution

was rapidly added. Control over AuBP size was achieved by varying seed solution concentration in the growth solution (100 µl for **AuBP$_{850}$** and 2 ml for **AuBP$_{660}$**), less seed particles lead to larger AuBPs since more gold salt is reduced on each seed particle. The reaction was complete after 2h. The seed solution was also prepared as described in supplementary reference 1. Before beginning the encapsulation process the AuBP solution was washed 3 times (centrifugation at 7000 x g for 15 min) with 1 mM CTAB in water.

3.2 Encapsulating AuBPs

The reason for encapsulating the AuBPs is to prevent degradation of the bipyramidal structure. The encapsulation included two successive steps done immediately after AuBP synthesis. The first step, mesoporous silica encapsulation, was performed by adding to a 10 ml solution of 0.3 mM CTAB and 2 OD AuBPs, 30 µl of 0.1 M NaOH and 10 µl of tetraethyl orthosilicate (TEOS) then shaking (120 rpm) the solution overnight at 30 °C. After the first encapsulation the AuBPs were washed 4 times with ethanol (centrifugation at 7000 x g for 10 min). The second step, a standard Stöber encapsulation, was performed by adding to a 10 ml solution of 4 OD AuBPs in ethanol 250 µl 28 % ammonia in water (18.2 MΩ) and 25 µl of 20 % TEOS in ethanol were added and the solution was left overnight in a shaker at 120 rpm and 30 °C. Finally, encapsulated AuBPs were washed 3 times with ethanol and concentrated for use.

3.3 Supplementary Figure 1: UV-Vis spectrum.

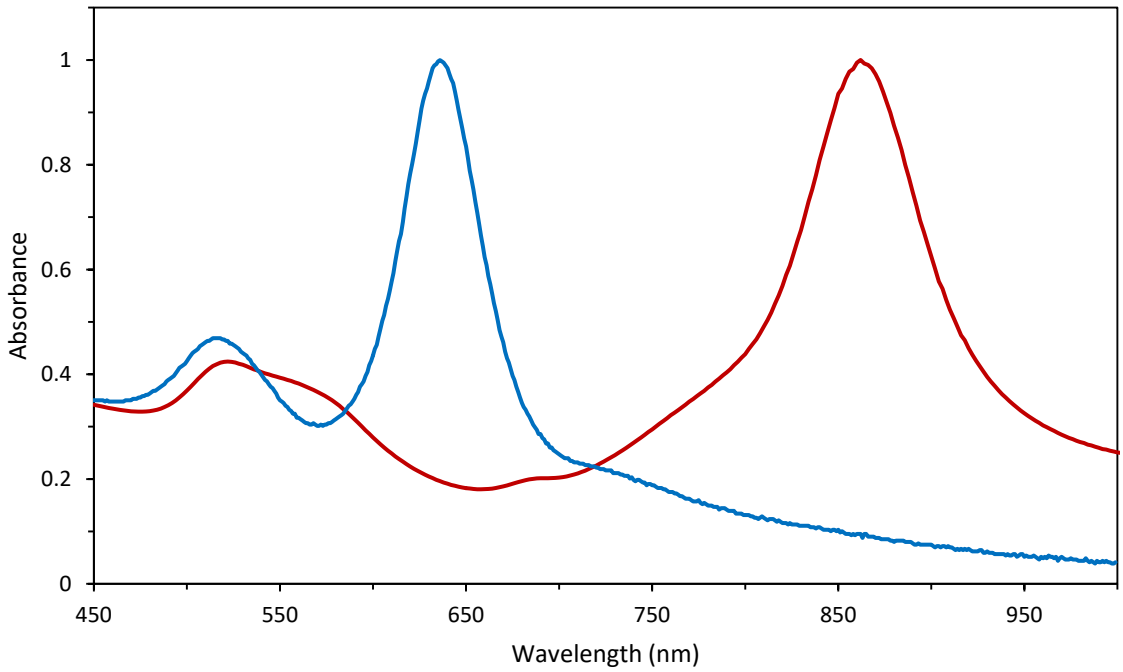

Supplementary figure 1 | Absorption spectrum of **AuBP$_{660}$** (blue line) and **AuBP$_{850}$** (red line).

3.4 Supplementary Figure 2-5: TEM images

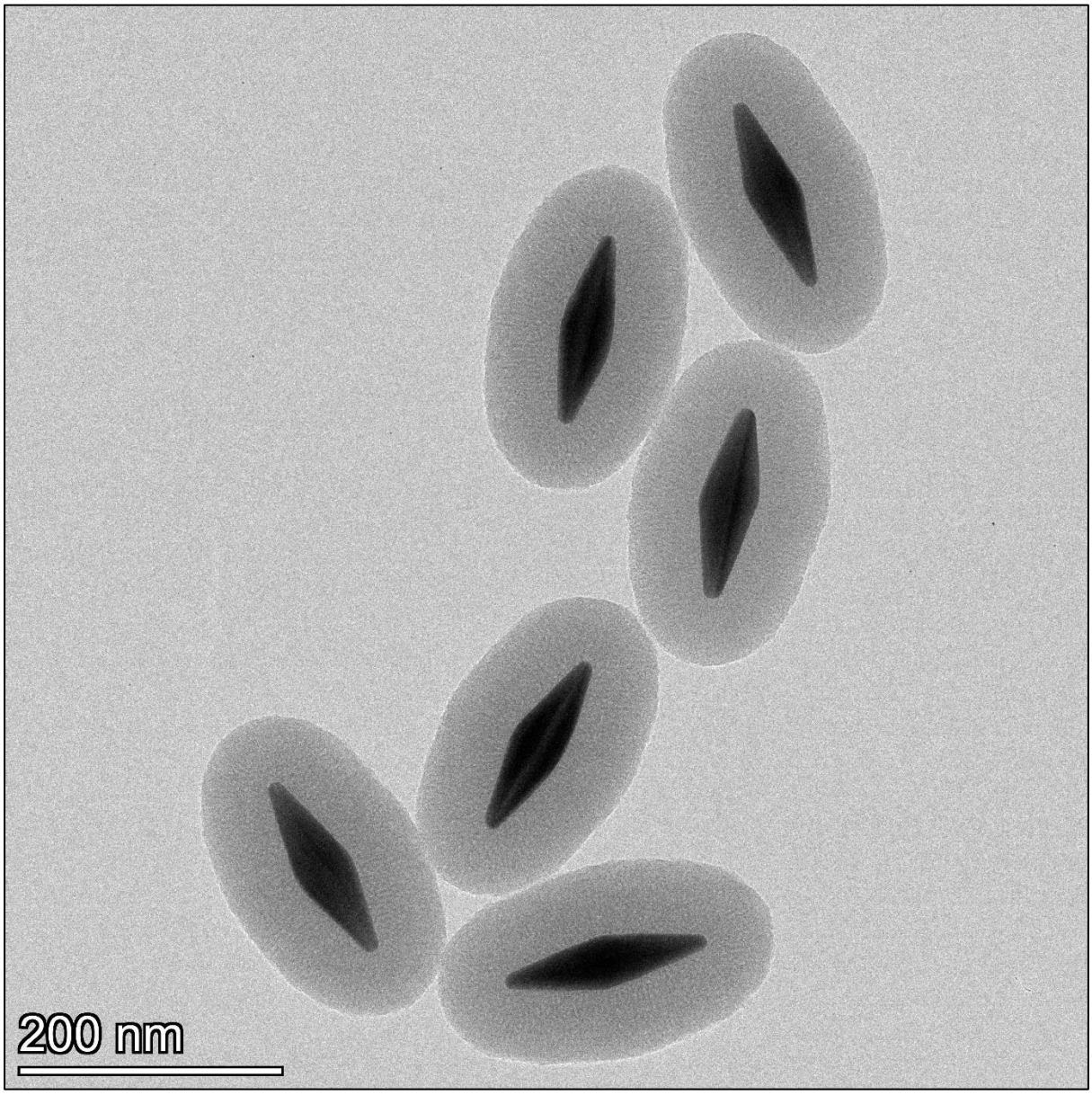

Supplementary figure 2 | TEM image of IR absorbing (850 nm) silica encapsulated AuBPs (**AuBP$_{850}$**). UV-Vis spectrum can be seen in supplementary figure 1 represented by the red curve. IR absorbing AuBPs give the solution a brownish red color.

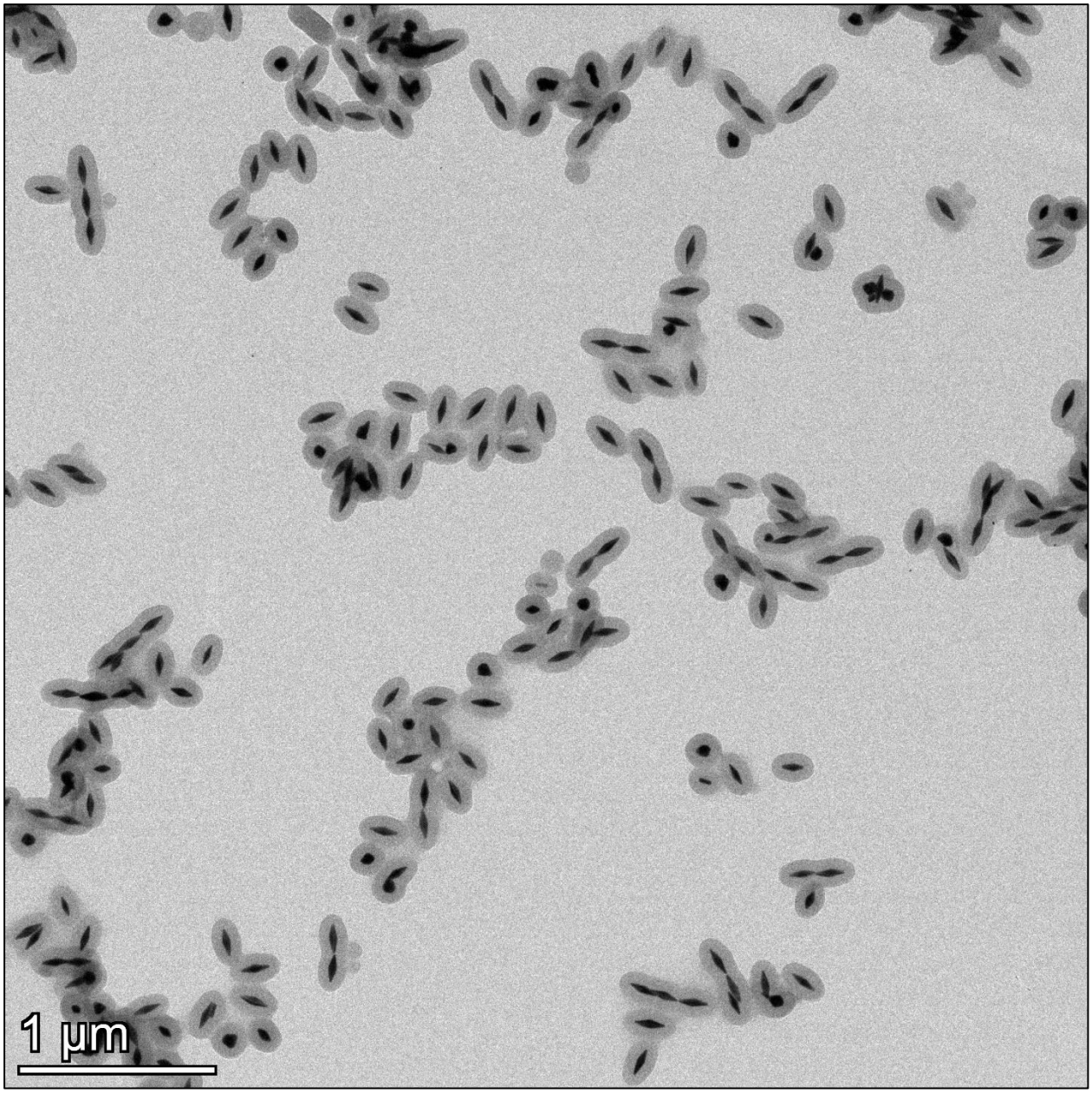

Supplementary figure 3 | Zoomed out TEM image of **AuBP$_{850}$**.

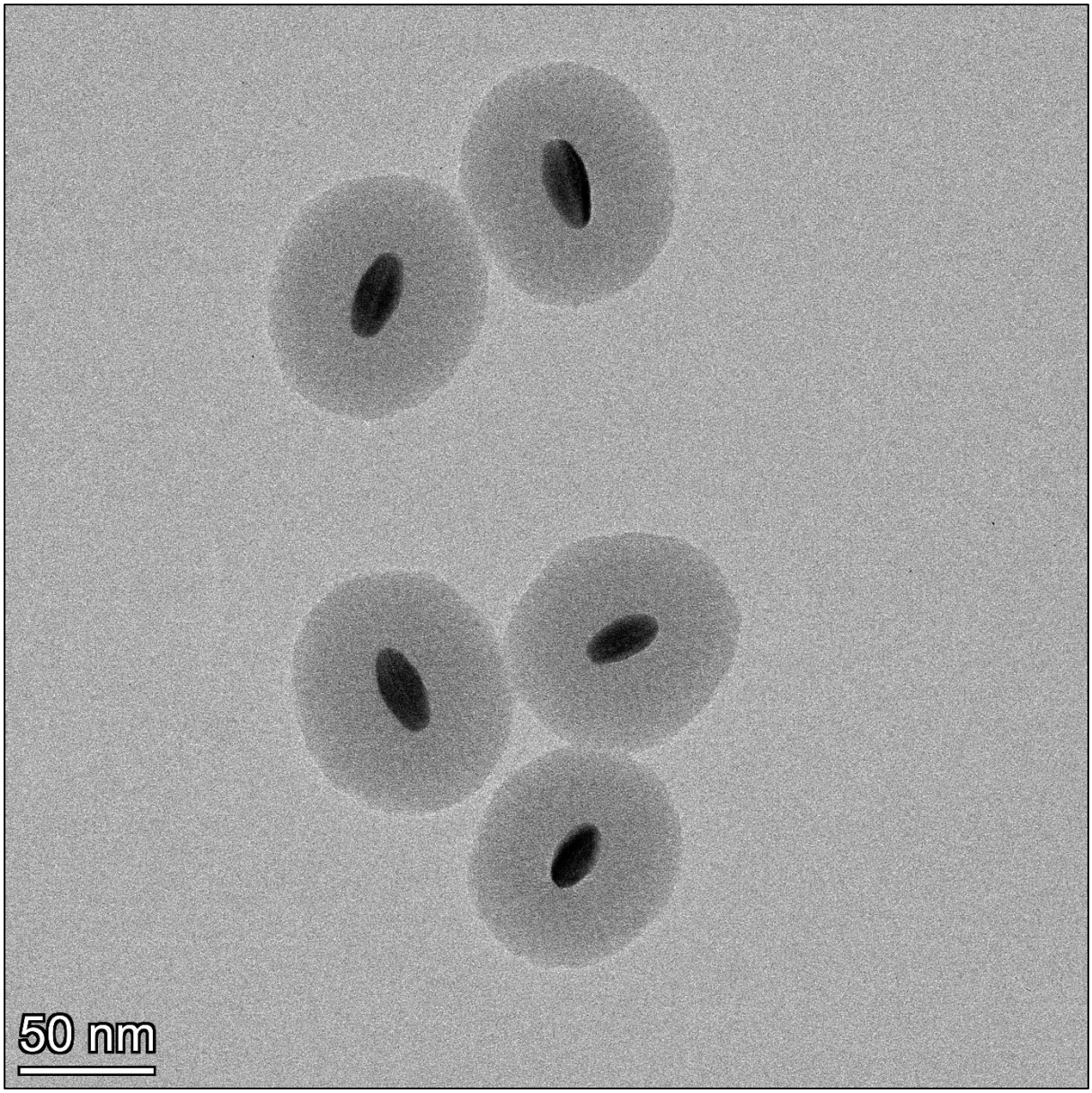

Supplementary figure 4 | TEM image of Vis absorbing (660 nm) silica encapsulated AuBPs (**AuBP$_{660}$**). UV-Vis spectrum can be seen in supplementary figure 1 represented by the blue curve. 660 nm absorbing AuBPs give the solution a blue color.

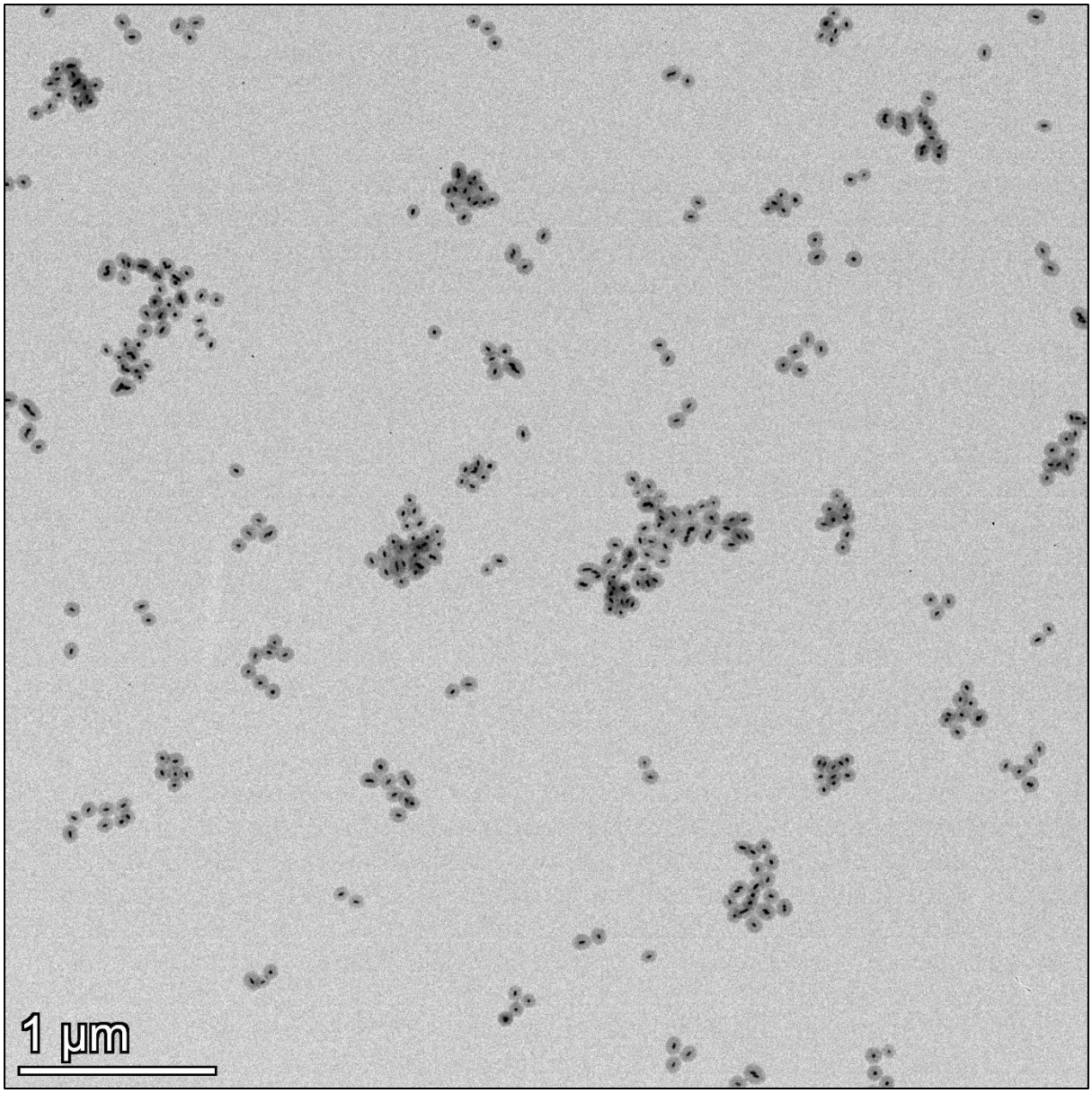

Supplementary figure 5 | Zoomed out TEM image **AuBP$_{660}$**.

4. Relationship of optical density (OD) to Au concentration

The relationship between the OD and Au mass concentration of $AuBP_{850}$ was determined by analyzing 3 samples with different known ODs with an ICP-OES.

Supplementary Table 1

Entry	AuBP concentration (OD)	Au concentration (ppm) Spectral lines (nm)				Average Au conc. per OD (ppm/OD)
		201.265	197.819	267.595	242.795	
Blank	0	0.028	0.05	0.041	0.049	-
1	0.25	3.472	3.358	3.367	3.403	13.6
2	0.5	6.283	6.322	6.368	6.46	12.7
3	0.75	8.972	9.091	9.197	9.066	12.1

The results presented in supplementary table 1 reveal that for a 1 OD solution of $AuBP_{850}$ the concentration of Au is 12.8 ± 0.6 ppm.

5. Comments on olefin metathesis catalysts

Three different latent olefin metathesis catalysts were used throughout the experiments showing that this method can be utilized to activate a wide scope of thermally active catalysts.

5.1 *cis*-Caz-1

Purchased from Strem Chemicals.

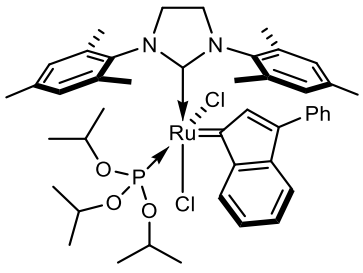

5.2 *cis*-Ru-P(OBn)$_3$

Synthesized as described in the supplementary reference 2.

Eivgi, O., Vaisman, A., Nechmad, N. B., Baranov, M. and Lemcoff, N. G., Latent Ruthenium Benzylidene Phosphite Complexes for Visible Light Induced Olefin Metathesis, *ACS Catal.*, **2020**, 10, 2033-2038.

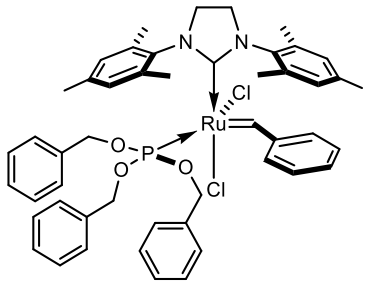

5.3 *cis*-Ru-SCF_3

Synthesized as described in the supplementary reference 3.

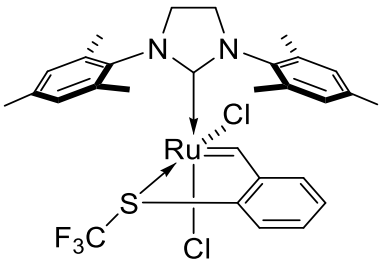

6. Temperature regulation for plasmon induced reactions

6.1 System setup

The temperature measuring system consists of a MLX90614-DF ROBOT IR Thermometer Sensor connected to a computer via an Arduino Mega. The LEDs used for activating plasmonic AuBPs were purchased from LED ENGIN and connected to a 9130B-BK Precision programmable DC power supply. Data from the IR thermometer and power supply unit was relayed to a LabView program, enabling the activation of LEDs as a function of the temperature. The systems accuracy was ensured by measuring the temperature of 5 OD AuBPs in 1 ml ethanol with a conventional thermometer (PT 1000.60 Temperature sensor from a RCT 5 digital IKA plate) while utilizing the system to activate the LED and IR thermometer.

6.2 Supplementary Figure 6: Image of temperature regulation system

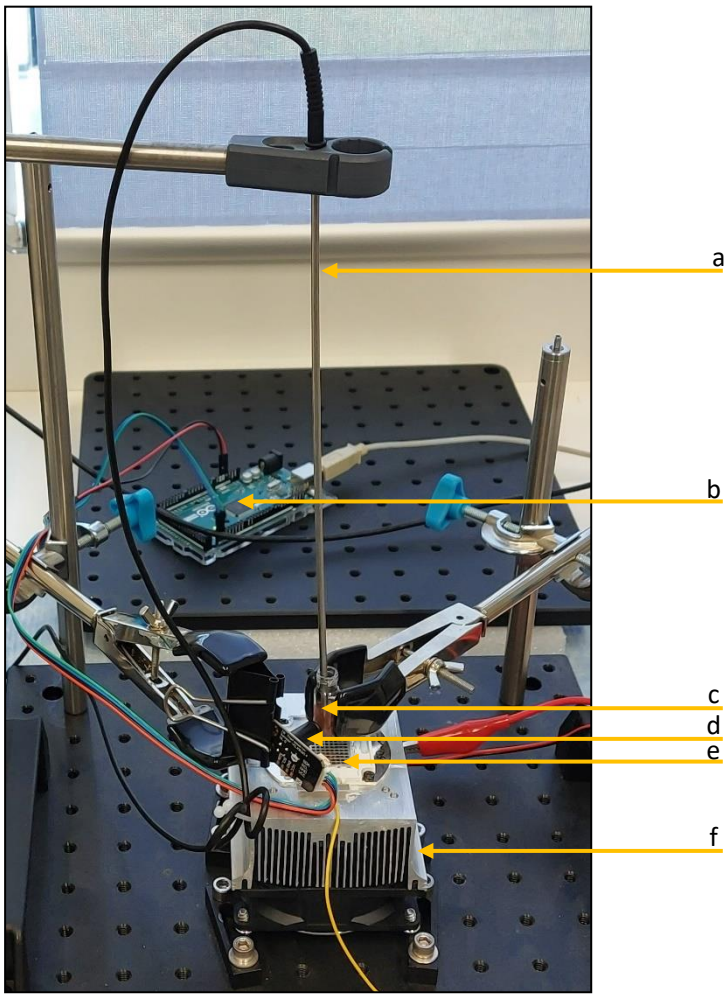

Supplementary figure 6 | As can be seen in the image and is stated above the accuracy of the temperature measurements obtained from the IR thermometer were checked with a conventional thermometer. Additionally, the system setup is clarified. **a,** PT 1000.60 Temperature sensor from a RCT 5 digital IKA plate. **b,** Arduino Mega. **c,** 5 OD AuBPs in 1 ml ethanol. **d,** MLX90614-DF ROBOT IR Thermometer Sensor. **e,** LED ENGIN 100 W, 850 nm LED. f) Aluminum heat-sink with a radiator cooling fan.

7. Ring closing metathesis (RCM)

Supplementary Table 2

Entry	substrate	*cis*-Caz-1 (%mol)	% Conversion		
			$AuBP_{850}$	$AuBP_{660}$	Oil Bath
1	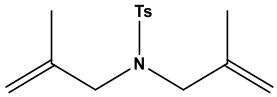	0.5	97	98	80
2	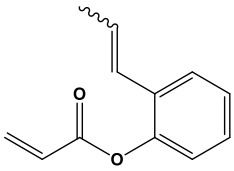	0.5	100	100	85

7.1 Procedures

To a 4 mL vial, an appropriate amount of AuBPs in ethanol was transferred (5 OD in final reaction volume) and the ethanol was evaporated using a rotary evaporator resulting in a powder attached to the vial's sides. To the dry AuBPs, a toluene solution (0.5 mL) of RCM substrate (0.1 M), ***cis*-Caz-1** (0.23 mg, 0.5 mol %) and mesitylene (7 µL) as an internal standard were added. The mixture was sonicated briefly to dissolve the AuBPs and irradiated with 850 nm LED (100 Watt) or 660 nm LED (100 Watt) for 15 minutes to 110 ^{o}C. The reaction temperatures were monitored using the system described in section 5. Reaction conversions were measured using GC-MS, signal integrations are relative to the mesitylene internal standard. The control experiments consisted of an identical solution without AuBPs, heated in an oil bath to 110 ^{o}C for 15 minutes.

7.2 Supplementary Figures 7-10: Temperature profiles for RCM reactions

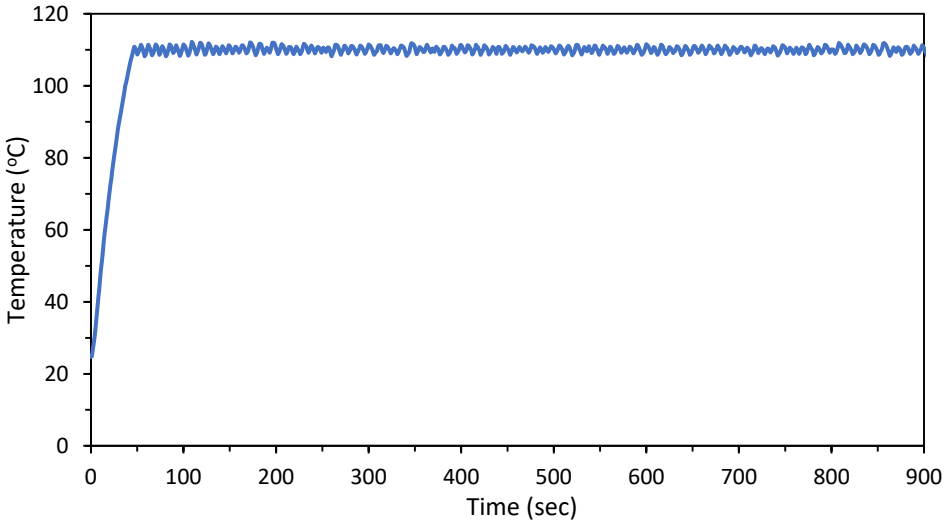

Supplementary figure 7 | Temperature profile for entry 1 when irradiated at 850 nm

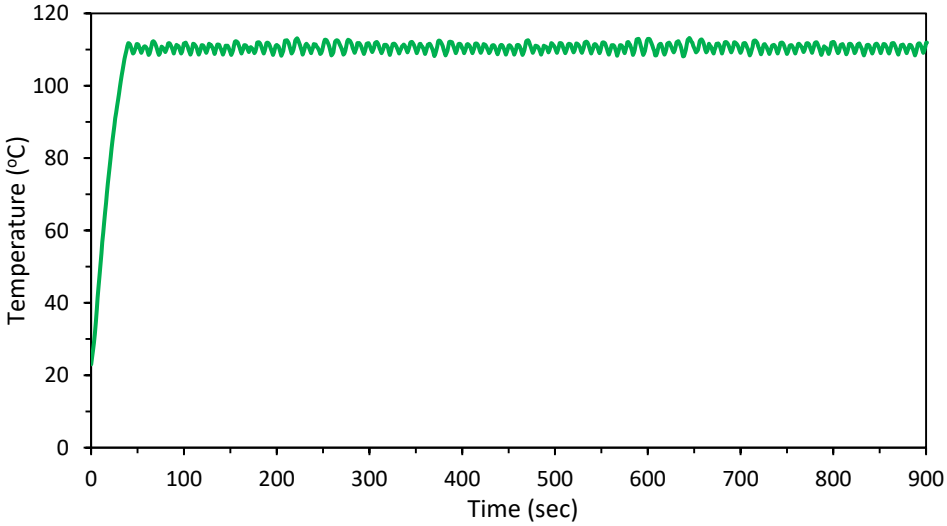

Supplementary figure 8 | Temperature profile for entry 1 when irradiated at 660 nm

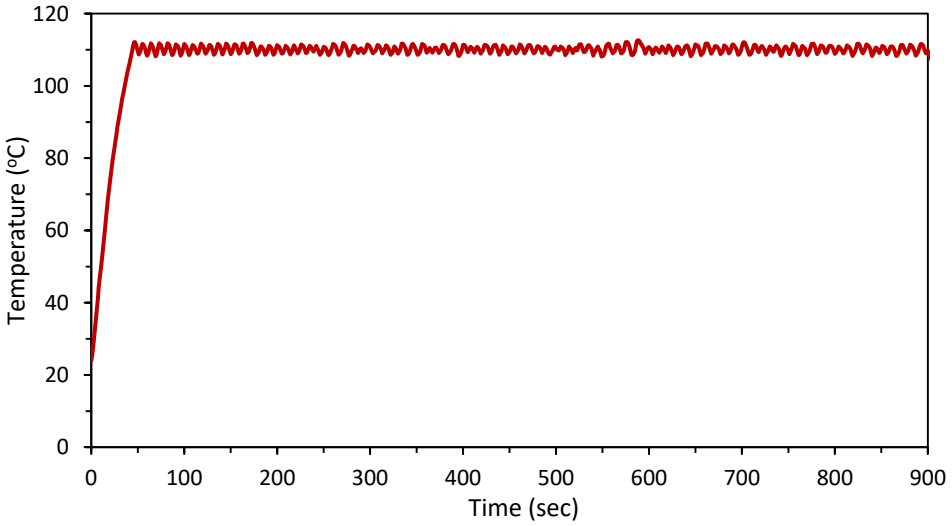

Supplementary figure 9 | Temperature profile for entry 2 when irradiated at 850 nm

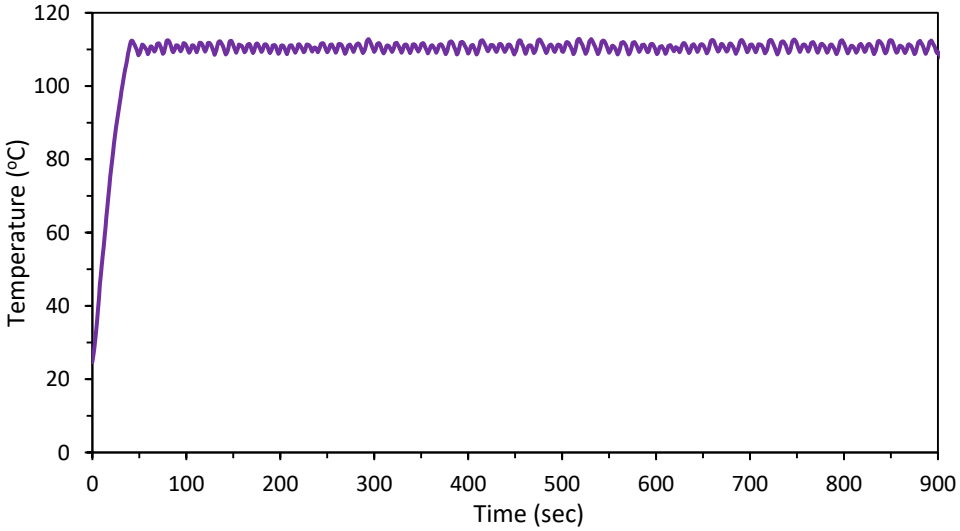

Supplementary figure 10 | Temperature profile for entry 2 when irradiated at 660 nm

7.3 Supplementary Figures 11-16: GC-MS results

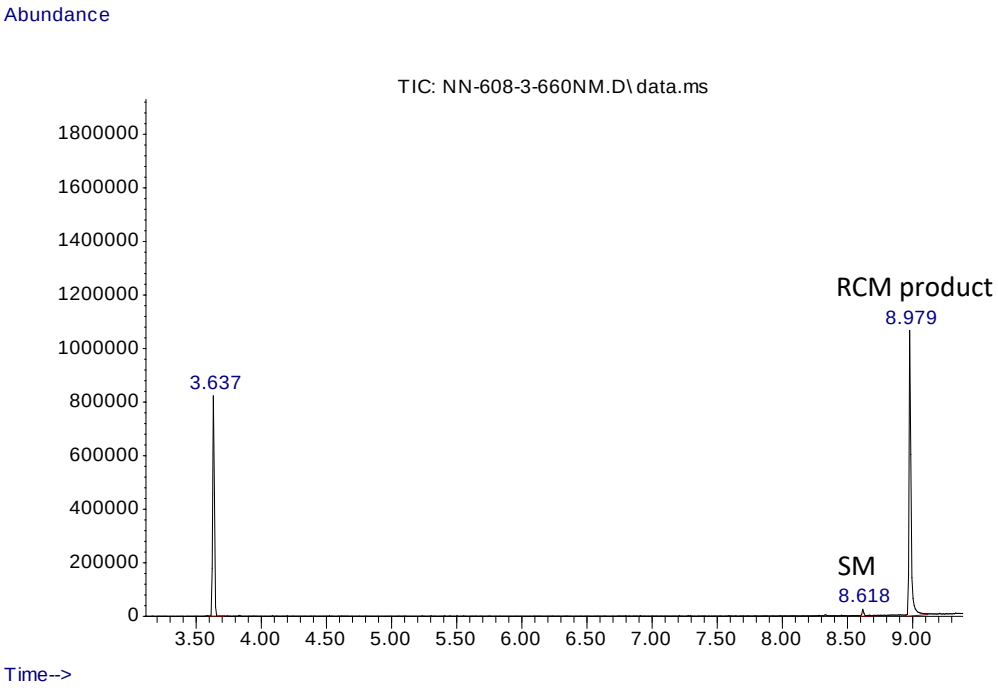

Supplementary figure 11 | GC-MS for entry 1 after irradiation at 850 nm

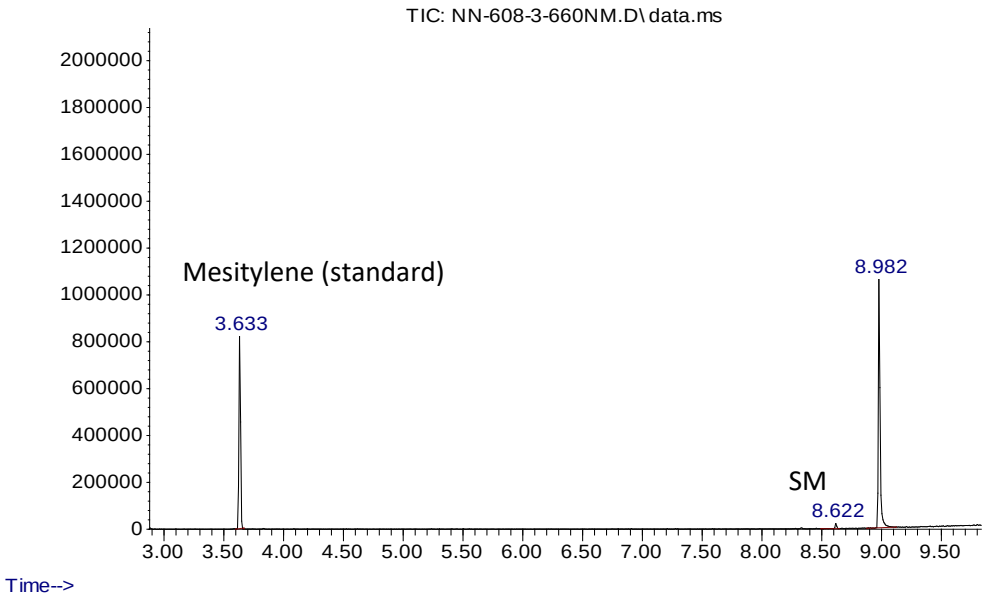

Supplementary figure 12 | GC-MS for entry 1 after irradiation at 660 nm

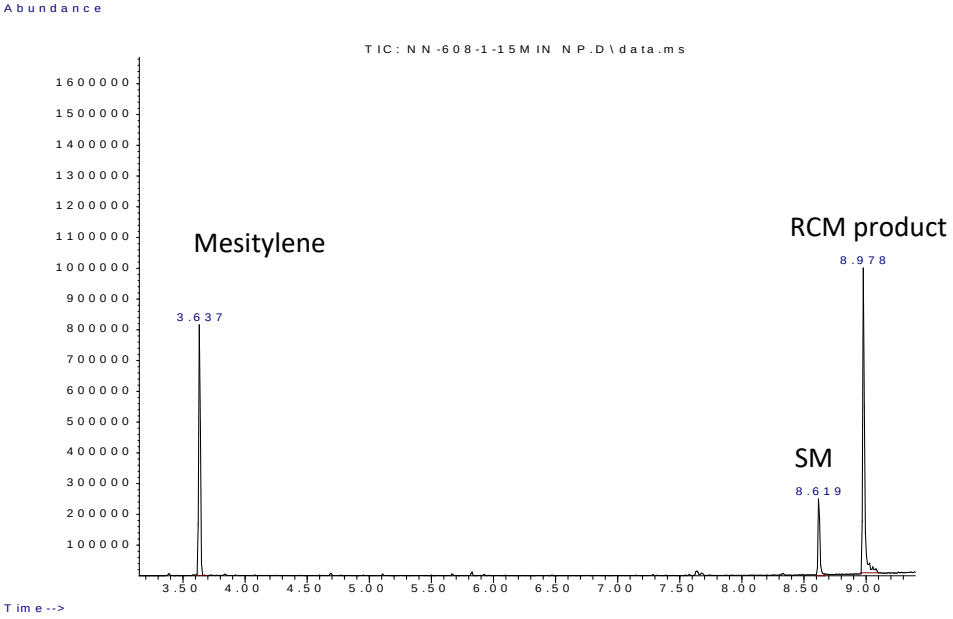

Supplementary figure 13 | GC-MS for entry 1 after completing control experiment (oil bath)

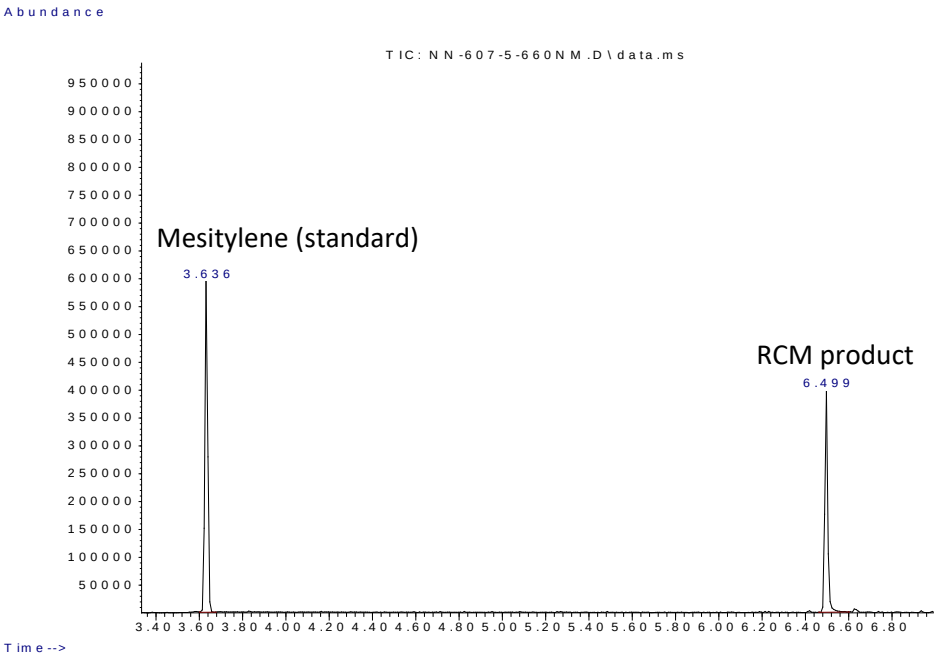

Supplementary figure 14 | GC-MS for entry 2 after irradiation at 850 nm

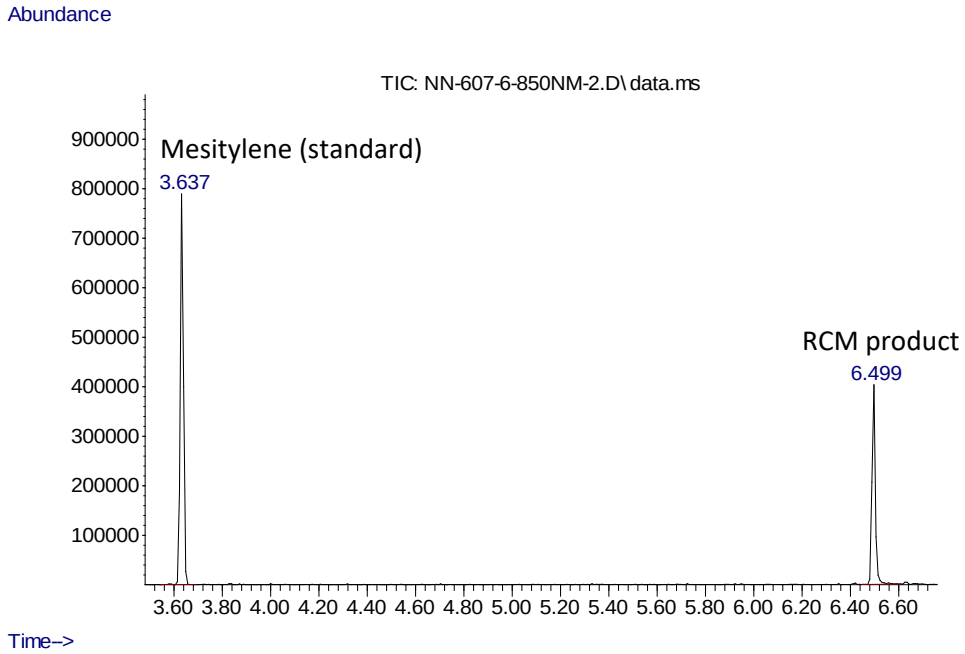

Supplementary figure 15 | GC-MS for entry 2 after irradiation at 660 nm

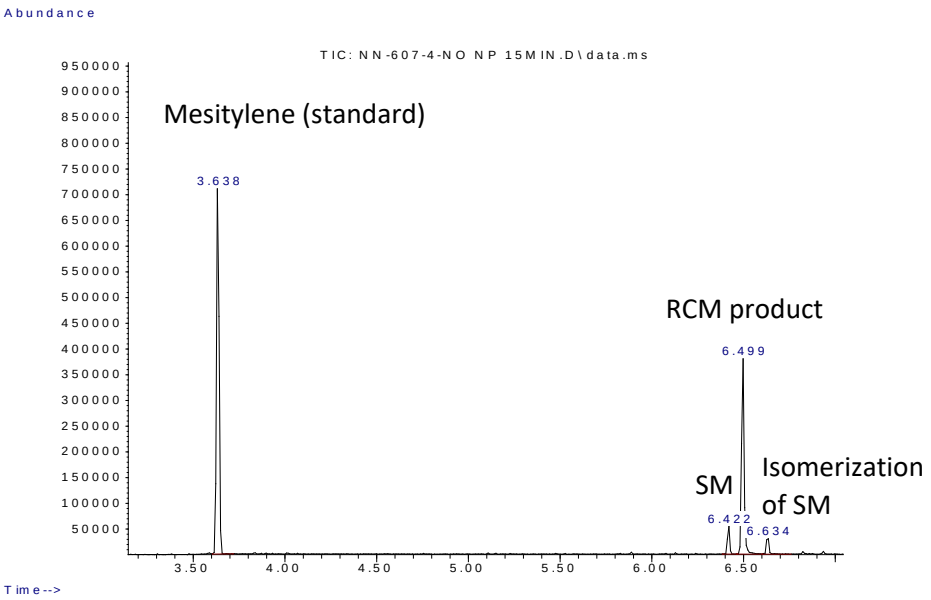

Supplementary figure 16 | GC-MS for entry 2 after completing control experiment (oil bath)

7.4 Supplementary Figure 17: Unprotected $AuBP_{850}$ RCM

To highlight the importance of the silica encapsulation in maintaining the AuBP structure intact when the nanoparticles produce heat, we carried out an RCM reaction as described in section 7.1. TEM images of the AuBPs before and after the reaction and the temperature profile were analyzed. From the images it is clear that the structure of all nanoparticles seen has been degraded to a pseudo-spherical structure. The temperature profile demonstrates that a maximal temperature lower than the targeted 110 °C was reached and steadily decreased throughout the reaction time. The reaction conversion was determined to be 55 % via GC-MS, very low compared to the reaction activated by encapsulated AuBPs.

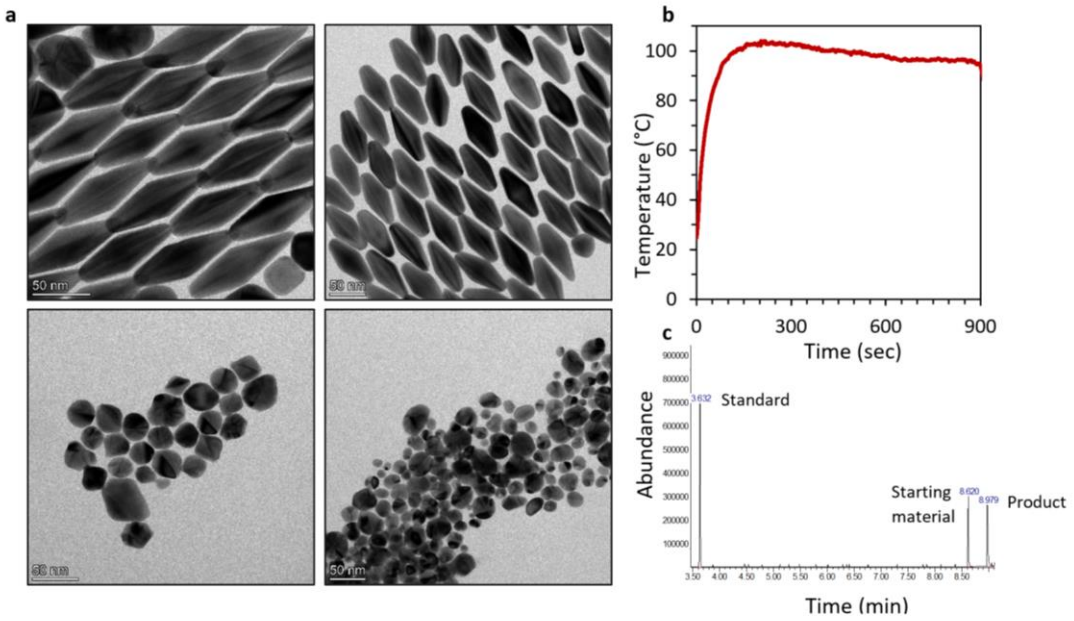

Supplementary figure 17 | Non-encapsulated AuBPs. **a,** TEM images of unprotected **$AuBP_{850}$**. **Top,** Images taken prior to photothermal activation. **Bottom,** Images taken of the AuBPs after conducting the RCM reaction described in Table 1, entry 1. **b,** Temperature profile of the RCM reaction. **c,** GC-MS results for the reaction. Peak integration showed 55 % conversion.

7.5 Supplementary Figures 18, 19: $AuNR_{850}$ and carbon black activated RCM

Showing that the photothermal method is not limited to a single nanostructure, RCM reactions were activated by irradiating NIR light onto solutions containing gold nanorods and carbon black. The reactions were carried out as previously described. The amount of **$AuNR_{850}$** added was set to match the absorbance in the AuBP experiments and the amount of carbon black was set to match the mass of Au as shown by ICP-OES results in section 4.

Gold nanorods (AuNR) were synthesized according to the procedure reported in supplementary reference 4, with slight modification. Briefly, 1.6 mL of $HAuCl_4$ (6mM)

was added in 8 mL of aqueous CTAB solution (200 mM). Next, 160 µL of $AgNO_3$ (10 mM) and 120 µL of ascorbic acid (100 mM) were added stepwise followed by addition of 40 µL of $NaBH_4$ (1mM) solution. The mixture was kept until the color of the solution changed to deep brown. The nanorods were further purified by centrifuging at 1500 rpm for 5 min and washed with water. Finally, the nanorods were coated with silica similarly to the AuBPs.

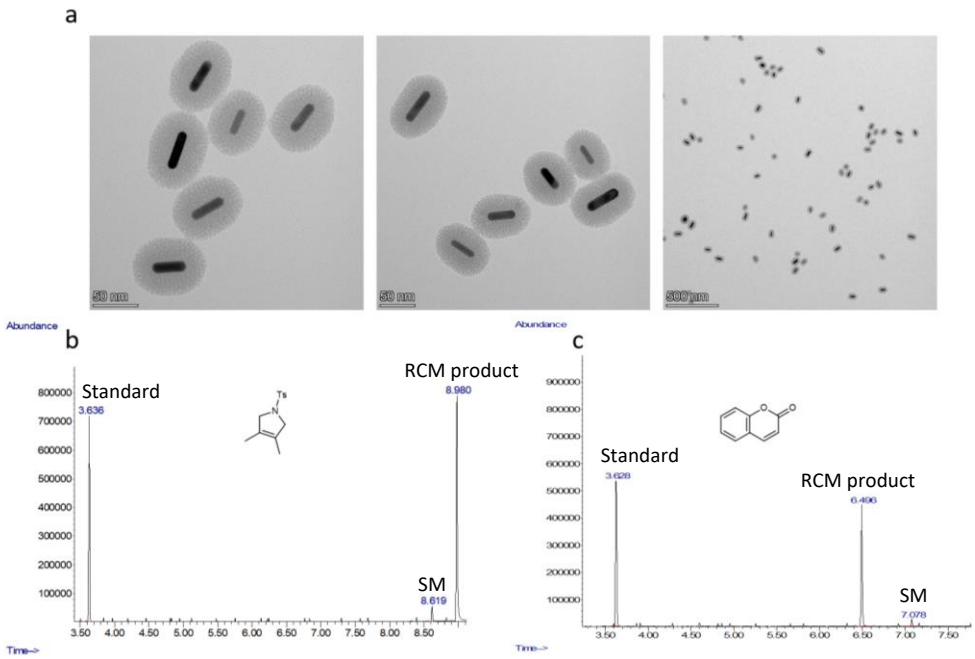

Supplementary figure 18 | AuNR activated RCM **a,** TEM images of encapsulated **$AuNR_{850}$**. **b,** GC-MS results of the reaction described in Table 1 Entry 1 with 5 OD **$AuNR_{850}$**. Peak integration showed 94 % conversion. **c,** GC-MS results of the reaction described in table 1 entry 2 with 5 OD **$AuNR_{850}$**. Peak integration showed 95 % conversion.

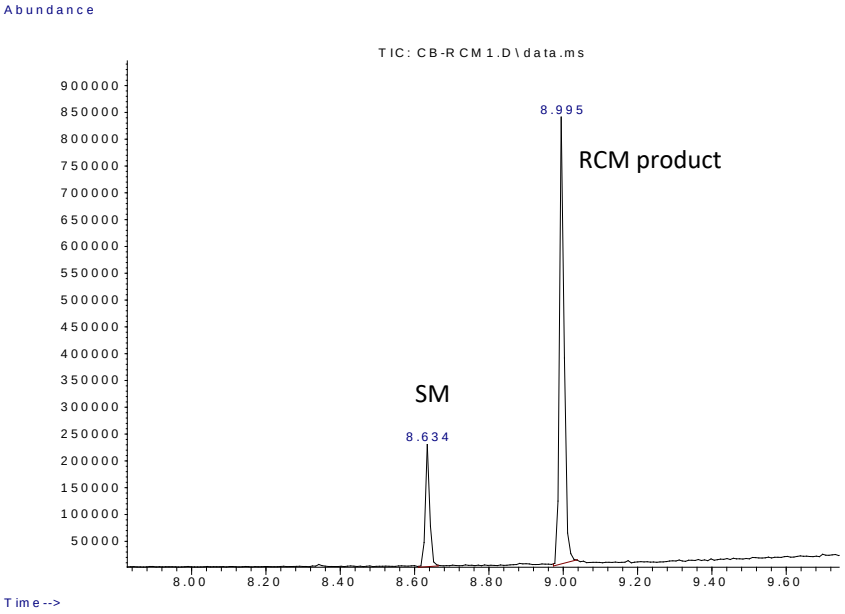

Supplementary figure 19 | Carbon black activated RCM. GC-MS results of the reaction described in Table 1 Entry 1 with 65 ppm of carbon black. Peak integration showed 80 % conversion.

7.6 Supplementary Figure 20: Low catalyst loading RCM

A reaction identical to the one described in Table 1 Entry 1 except for the catalyst loading that was reduced to 0.1 mol% was carried out and the conversion was determined via GC-MS.

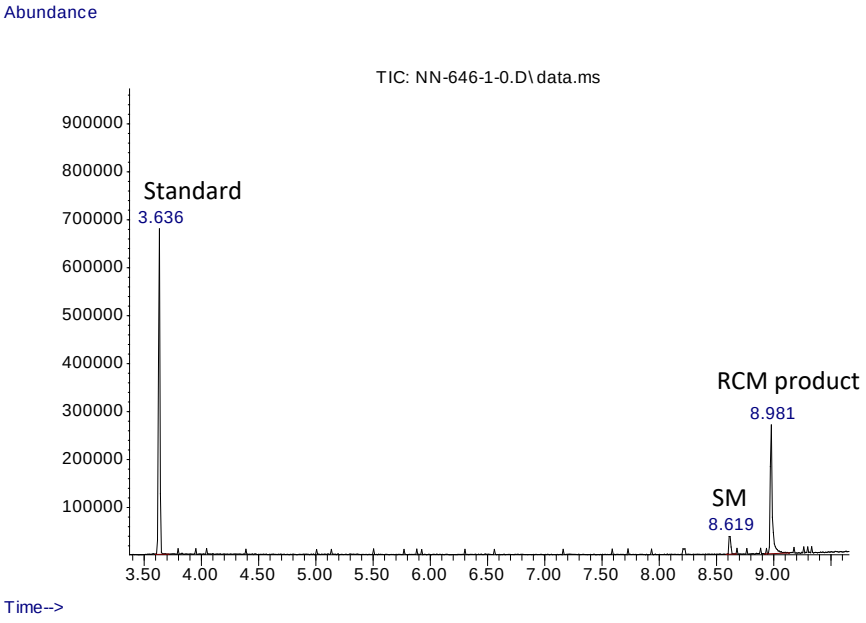

Supplementary figure 20 | GC-MS for low catalyst loading experiment. Peak integration showed 88 % conversion.

7.7 Supplementary Figure 21: Low temperature RCM reaction

A reaction identical to the one described in Table 1, entry 1 except for the temperature that was reduced to 80 °C was carried out and the conversion was determined via GC-MS.

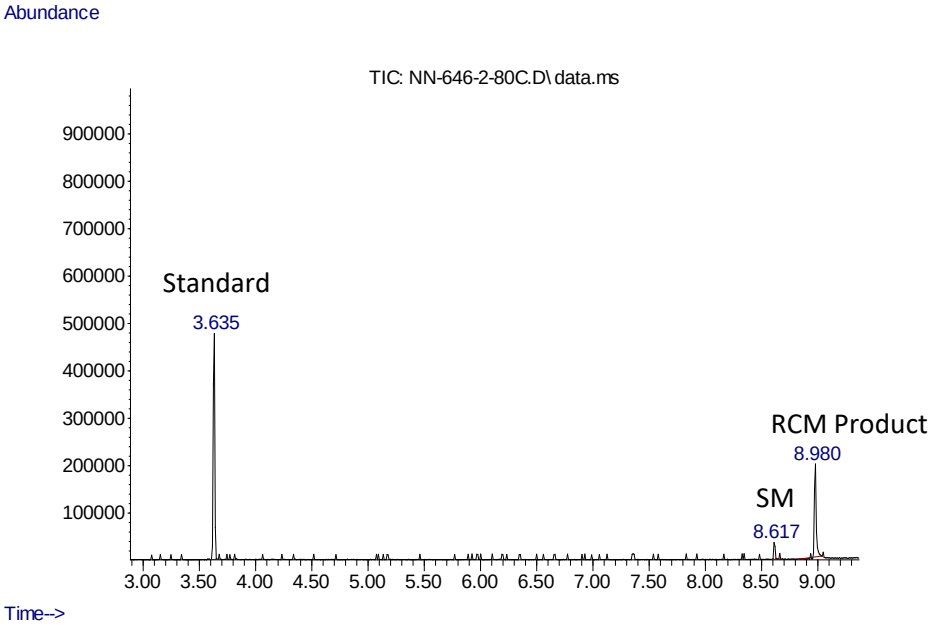

Supplementary figure 21 | GC-MS for low temperature experiment. Peak integration showed 88 % conversion, which is higher than the 80 % conversion of the RCM reaction obtained at 110 °C without the presence of NPs (Table 1 Entry 1).

8. Recycling $AuBP_{850}$

8.1 Procedure

The reaction solution was prepared as described in section 6.1 with **$AuBP_{850}$** and the RCM substrate appearing in entry 1 of table 1. All four cycles were irradiated with 850 nm LED (100 Watt) for 15 min to a temperature of 110 °C as seen in the temperature profiles. After the first three cycles the AuBPs were recycled as follows: A Buchner filtration (0.2 µm Teflon filter) of the reaction contents resulted in the AuBPs attaching to the filter. The filter was submerged in 2 mL of methanol and sonicated for 2-3 min causing the dispersion of the nanoparticles, resulting in a methanol **$AuBP_{850}$** solution. The AuBPs were dried using a rotary evaporator and a new reaction solution was prepared.

8.2 Supplementary Figure 22: Temperature profiles

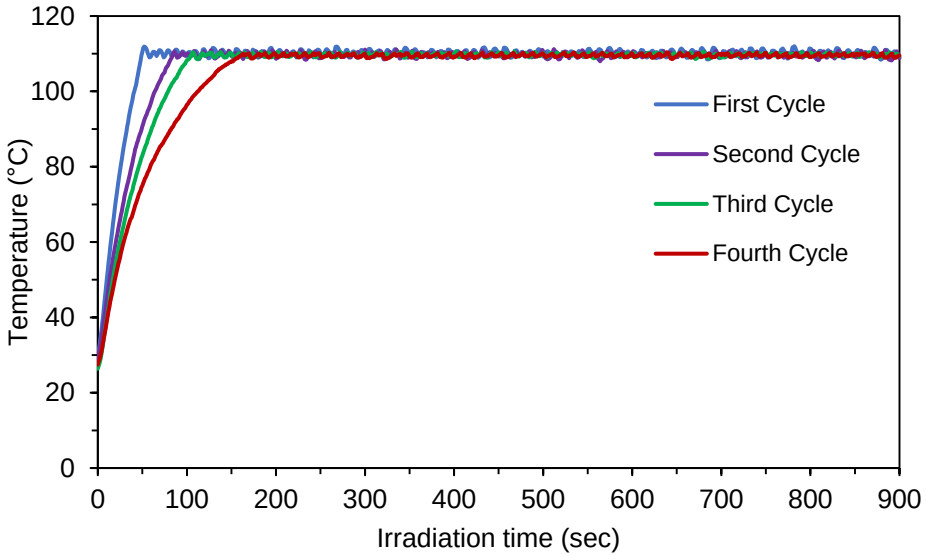

Supplementary figure 22 | Temperature profiles of RCM reactions for all four cycles. Heating ramp gradients slightly decline as minimal amounts of **AuBP$_{850}$** are lost in the recycling process.

8.3 Supplementary Figures 23-26: GC-MS results

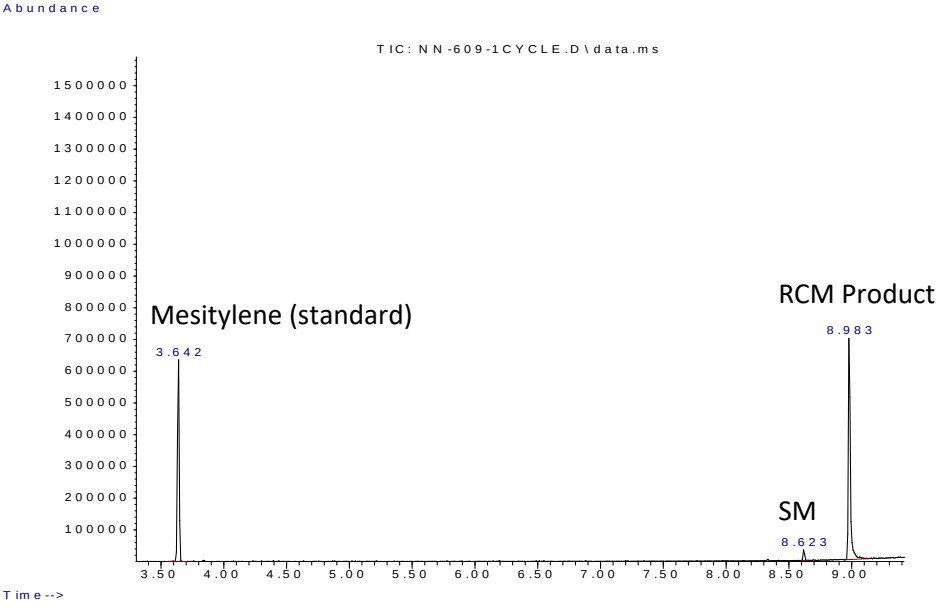

Supplementary figure 23 | GC-MS for RCM reaction after first cycle.

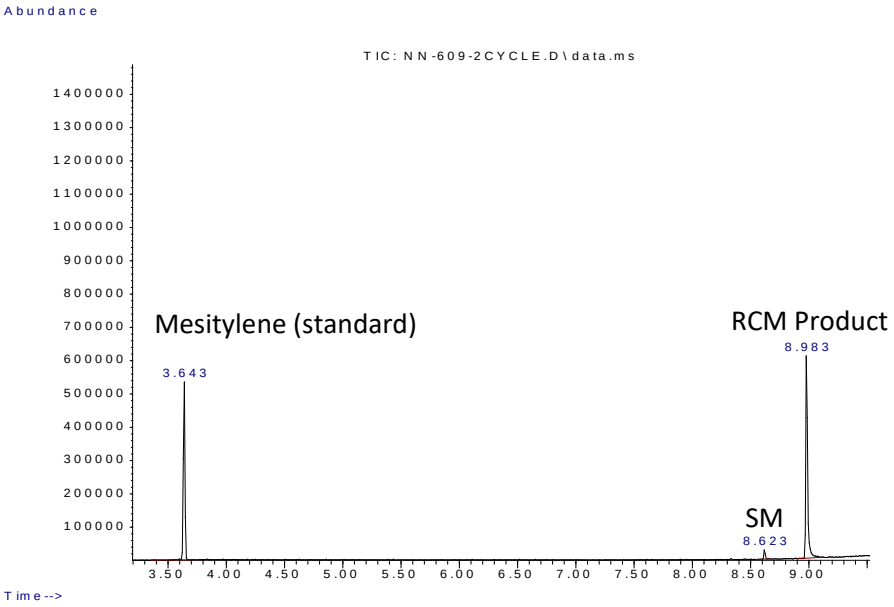

Supplementary figure 24 | GC-MS for RCM reaction after second cycle.

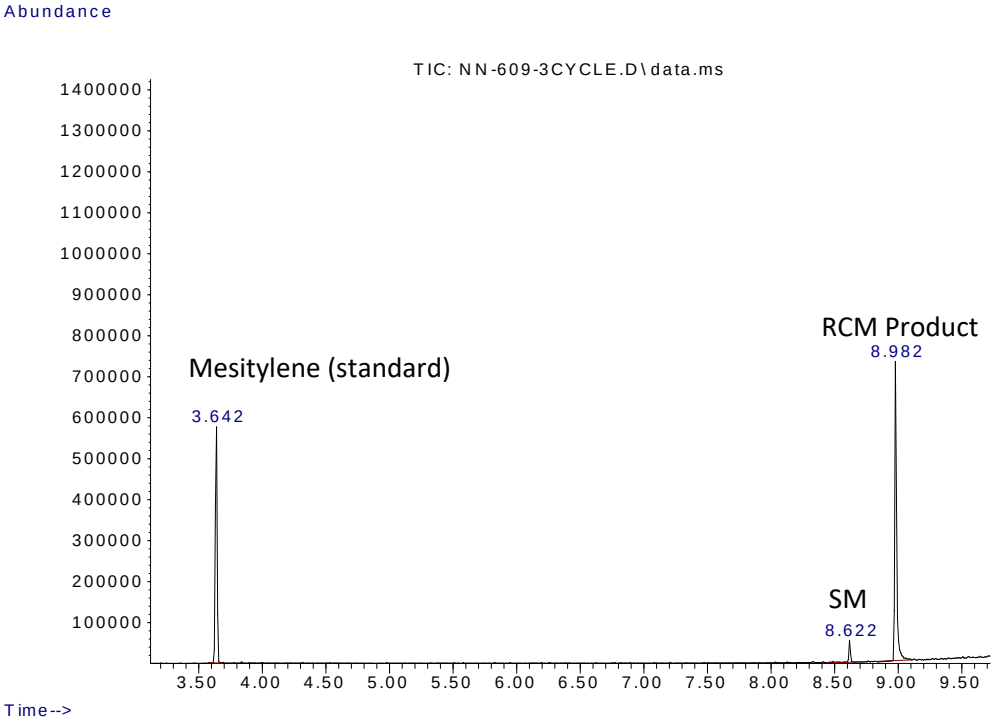

Supplementary figure 25 | GC-MS for RCM reaction after third cycle.

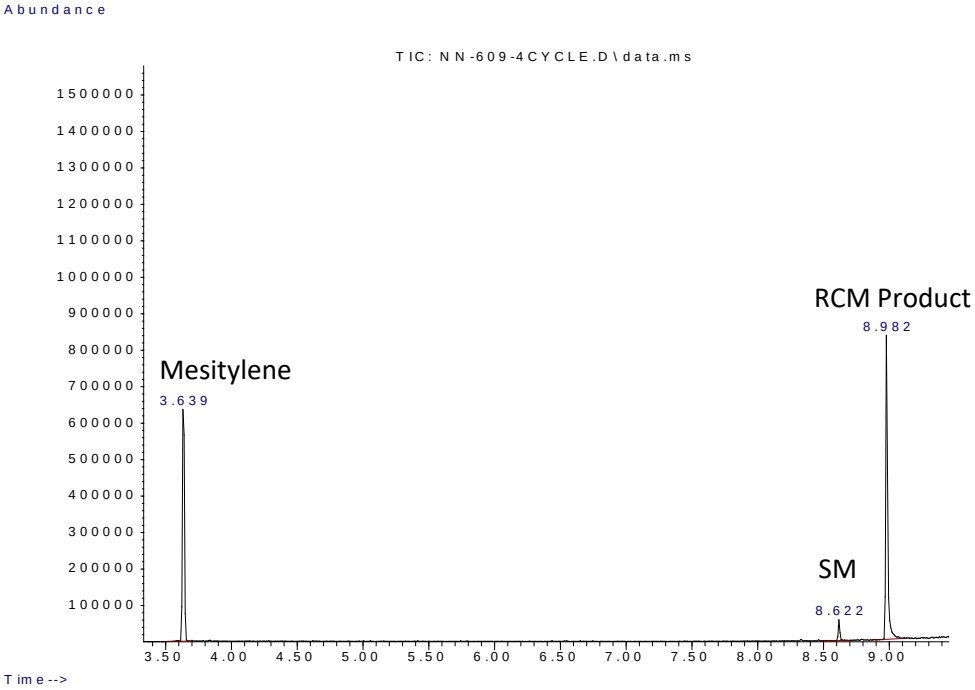

Supplementary figure 26 | GC-MS for RCM reaction after fourth cycle.

9. Recycling $AuBP_{660}$

9.1 Procedure

The recycling procedure is identical to the one described in section 7.1 with the exception that **$AuBP_{660}$** and the RCM substrate from table 1 entry 2 were used.

9.2 Supplementary Figure 27: Temperature profiles

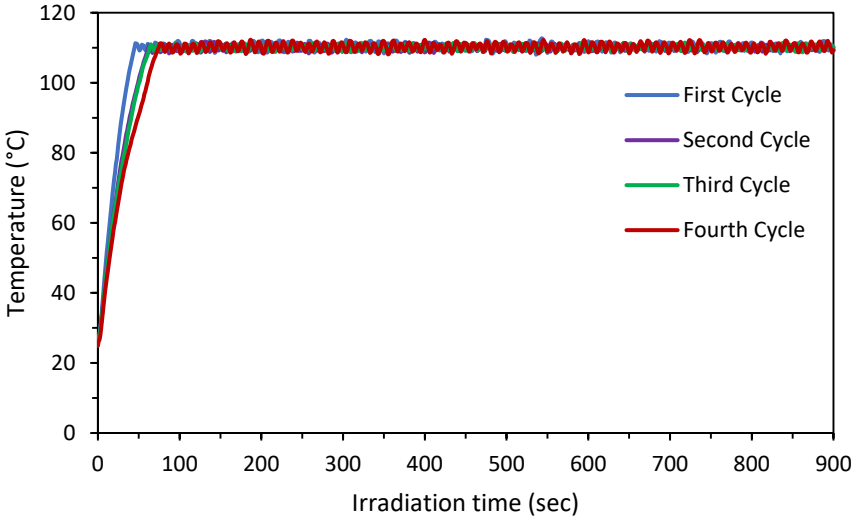

Supplementary figure 27 | Temperature profiles of RCM reactions for all four cycles. Heating ramp gradients slightly decline as minimal amounts of **AuBP$_{660}$** are lost in the recycling process.

9.3 Supplementary Figures 28-31: GC-MS results

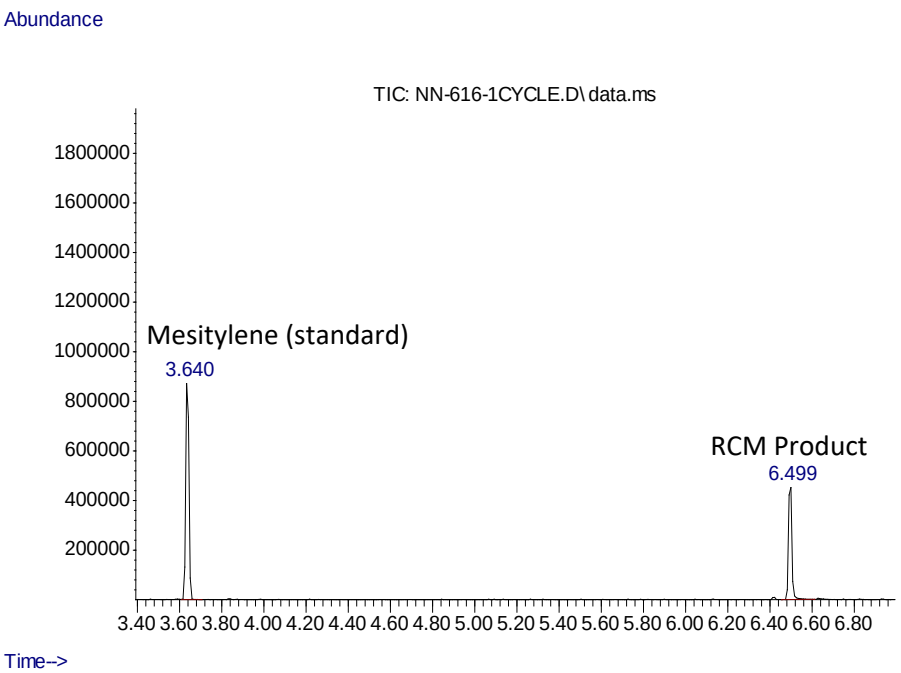

Supplementary figure 28 | GC-MS for RCM reaction after first cycle.

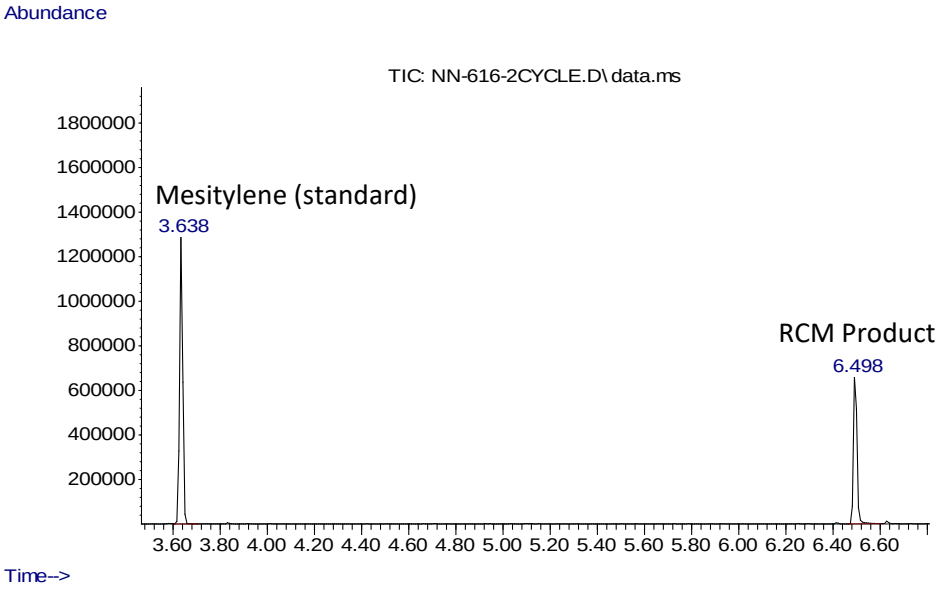

Supplementary figure 29 | GC-MS for RCM reaction after second cycle.

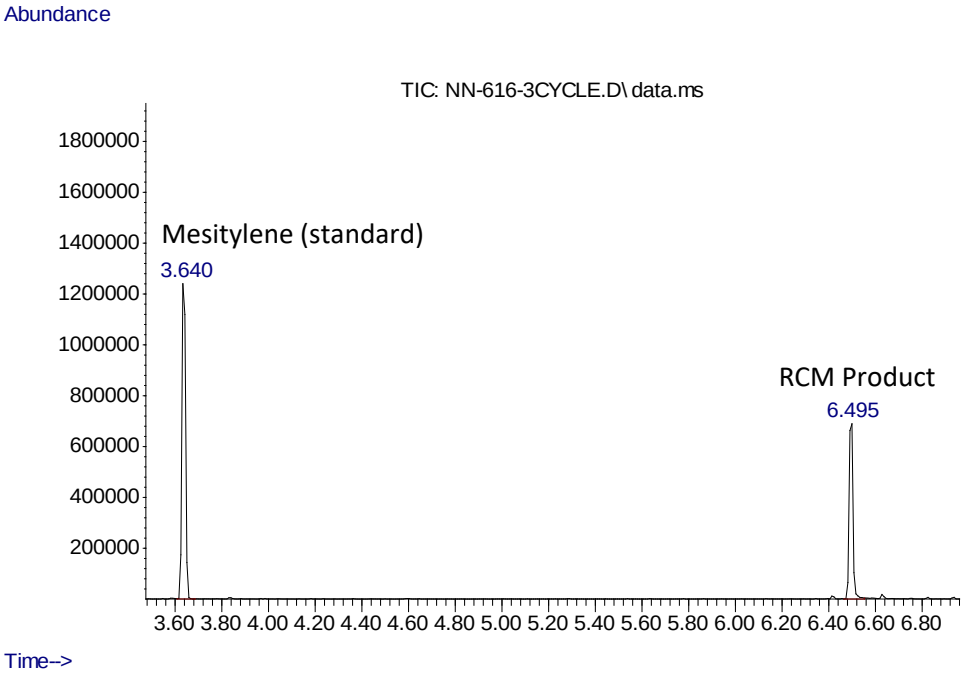

Supplementary figure 30 | GC-MS for RCM reaction after third cycle.

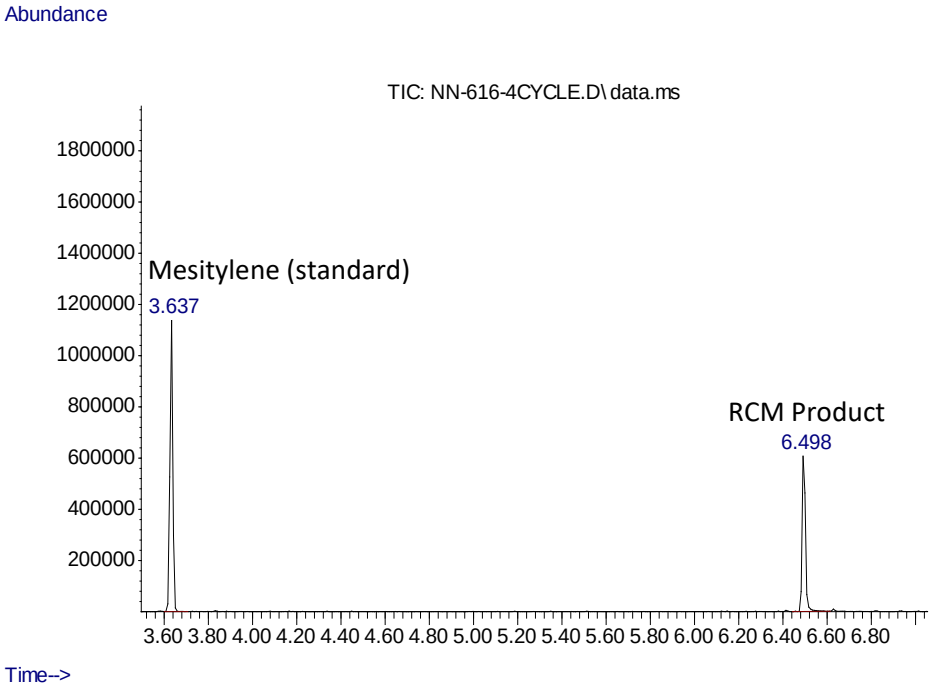

Supplementary figure 31 | GC-MS for RCM reaction after fourth cycle.

10. Supplementary Figure 32: Acyclic Diene Metathesis (ADMET) of Jojoba Oil

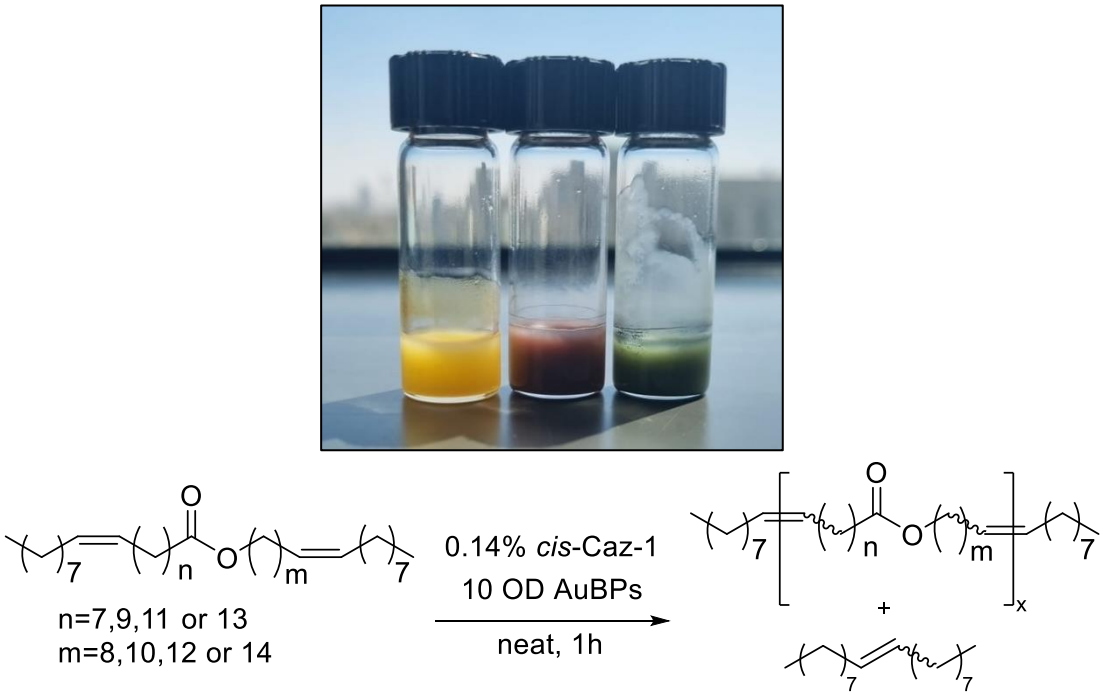

Supplementary figure 32 | Top) Scheme showing the ADMET reaction of jojoba oil. Two products are obtained, a waxy polymer and an 18-carbon alkene. Bottom) Image showing the waxy product with no AuBPs (yellow wax on the left), with **AuBP$_{850}$** (red wax in the middle) and with **AuBP$_{660}$** (greenish-blue wax on the right).

10.1 Procedure

***cis*-Caz-1** (2 mg, 0.14 mol %) was dissolved in a minimal amount of DCM and mixed with 1g of jojoba oil. The solution was added to the appropriate amount of dried AuBPs (10 OD in final reaction volume) then sonicated until a homogeneous mixture was obtained. The solution was irradiated continuously for 1h with 100-watt LED while the temperature was monitored with the system described in section 5 (control experiment was done in a heating block set to 250 °C). The reaction afforded a waxy product after cooling to room temperature.

10.2 Supplementary Figure 33: Temperature profiles

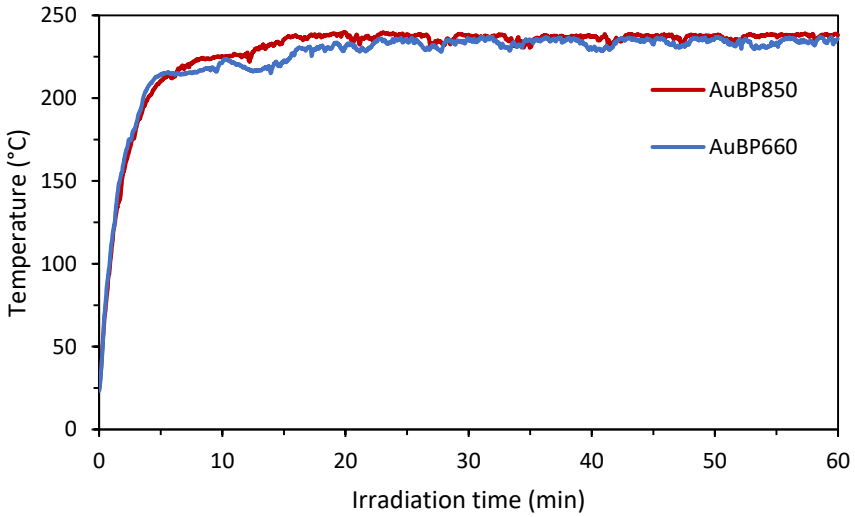

Supplementary figure 33 | Temperature profiles of ADMET reactions of jojoba oil in the presence of **AuBP$_{850}$** (red curve) and **AuBP$_{660}$** (blue curve). For **AuBP$_{850}$** the reaction reached a temperature of 240 °C and for **AuBP$_{660}$** the maximal temperature was 237 °C.

10.3 Supplementary Figure 34: Photoresponsive character

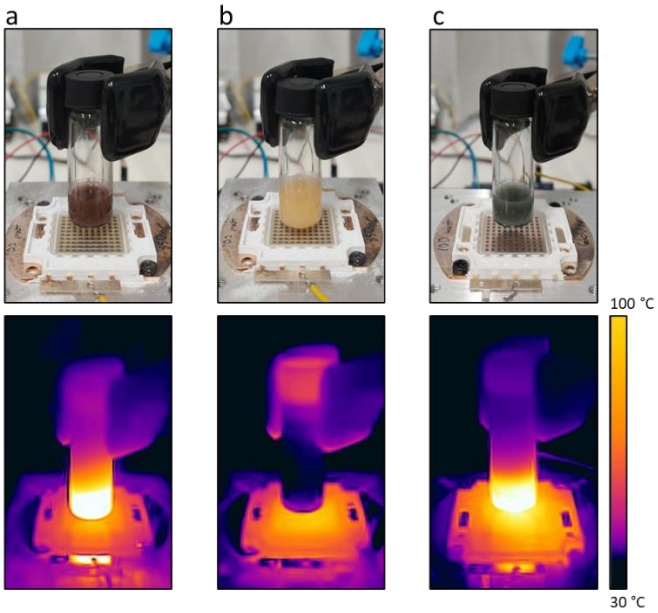

Supplementary figure 34 | Photoresponsive wax. **a,** Wax embedded with a 10 OD concentration of **AuBP$_{850}$**. Top, normal image of wax with 850 nm LED. Bottom, thermal image of wax while irradiated. **b,** Wax without AuBPs. Top, normal image of wax with 850 nm LED. Bottom, thermal image of wax while irradiated. **c,** Wax embedded with a 10 OD concentration of **AuBP$_{660}$**. Top, normal image of wax with 660 nm LED. Bottom, thermal image of wax while irradiated.

10.4 Supplementary Figures 35, 36: SEC Analysis

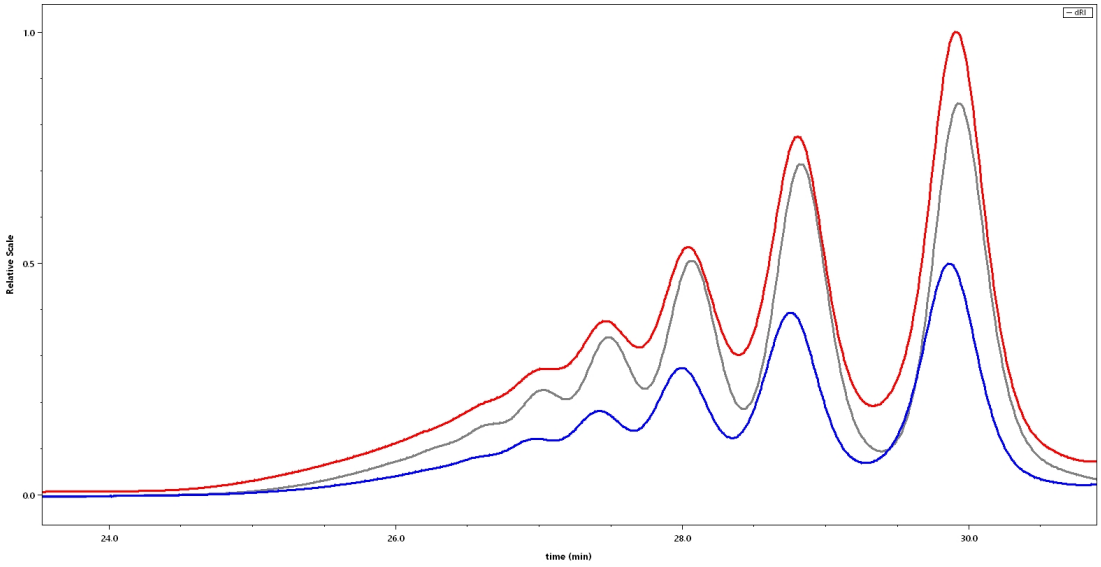

Supplementary figure 35 | SEC spectra of ADMET reaction product, produced from differential refractive index (dRI) detector. **Red curve,** photothermal reaction in the presence of **AuBP$_{850}$** (10 OD) as detailed in the procedure. **Blue curve,** photothermal reaction in the presence of **AuBP$_{660}$** (10 OD). **Grey curve,** reaction carried out in heating block. Temperature profiles can be seen in supplementary figure 33.

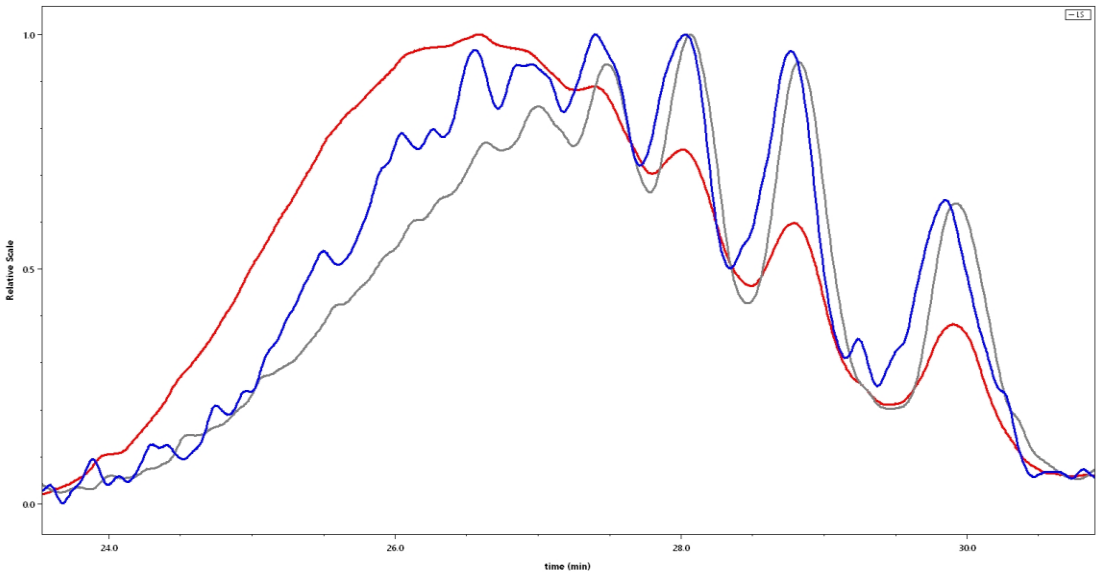

Supplementary figure 36 | SEC spectra of ADMET reaction product, produced from the light scattering (LS) detector. The curves represent the same samples as in supplementary figure 30.

Supplementary Table 3

Entry	AuBP	Mn (g/mol)	Mw (g/mol)	PDI
1	No AuBPs	1500	2100	1.4
2	**AuBP$_{850}$**	1800	3300	1.8
3	**AuBP$_{660}$**	1450	3300	1.8

The data shown here was derived from SEC analysis (Supplementary Fig. 35, 36).

10.5 Supplementary Figures 37-39: MALDI Analysis

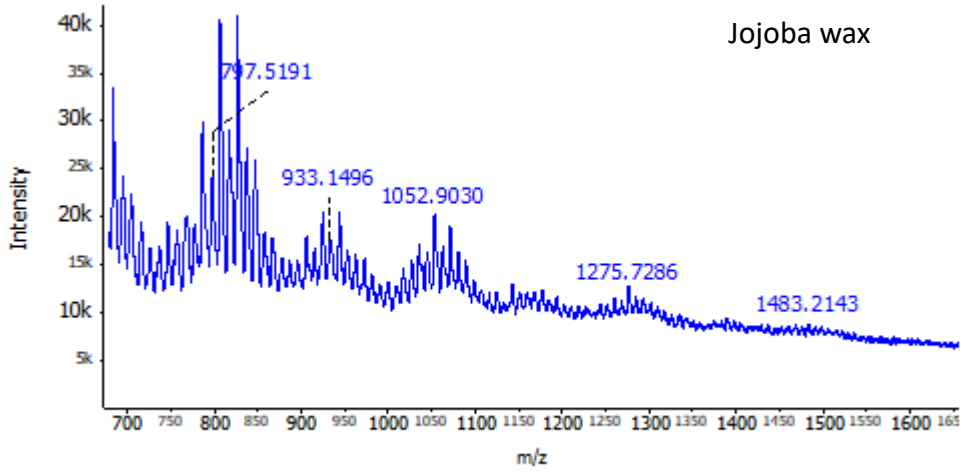

Supplementary figure 37 | MALDI results for ADMET product of jojoba oil without AuBPs.

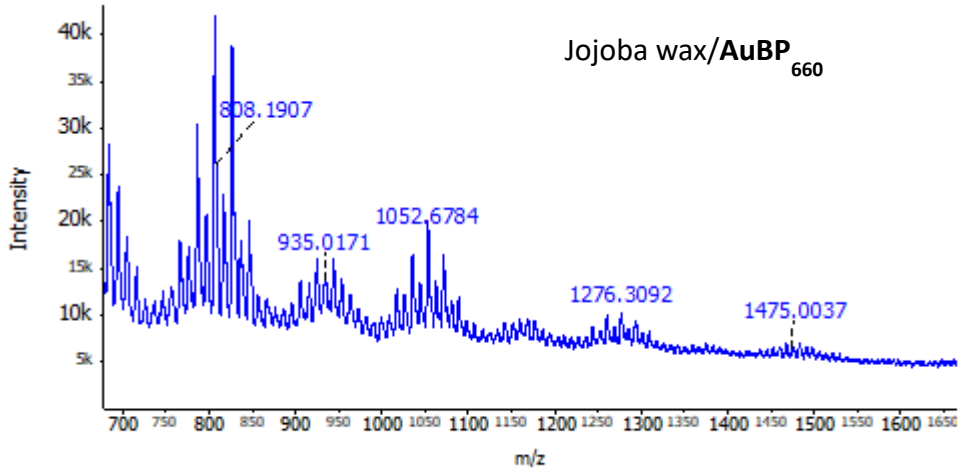

Supplementary figure 38 | MALDI results for ADMET product of jojoba oil with **AuBP$_{660}$**.

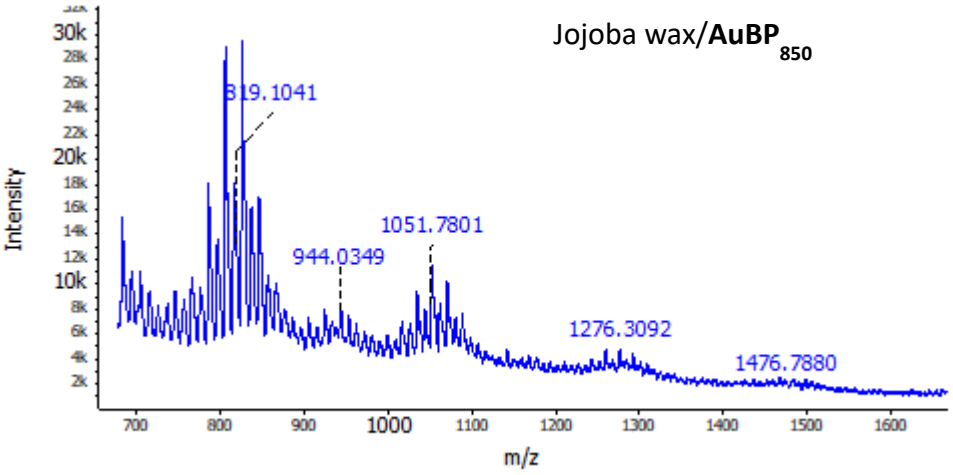

Supplementary figure 39 | MALDI results for ADMET product of jojoba oil with **AuBP$_{850}$**.

10.6 Supplementary Figure 40: Methyl oleate experiments

To neat methyl oleate (0.2 mL), ***cis*-Caz-1** was added (0.14% mol, 0.76 mg) and mixed with **AuBP$_{850}$** (5 OD). The solution was then heated to the specified temperature for 1h with the selected heating method (NIR or oil bath).

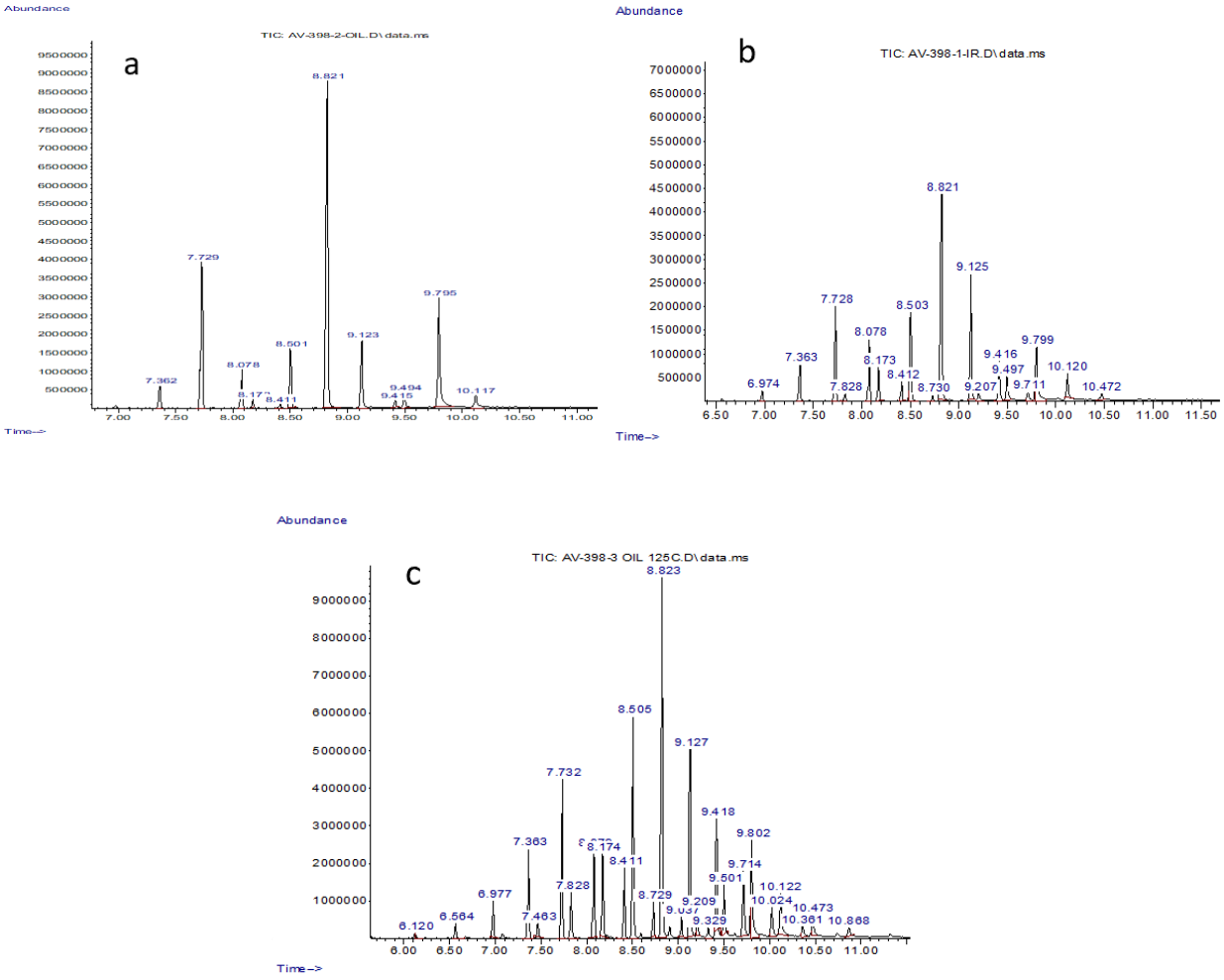

Sample	Activation method	Temperature (°C)
a	Oil bath	100
b	NIR irradiation	100
c	Oil bath	125

Supplementary figure 40 | GC-MS results showing the degree of isomerization. The less peaks the less products indicating decreased isomerization.

11. DCPD polymerization reaction

11.1 Procedure

1.04 mg of ***cis*-Ru-P(OBn)$_3$** (0.03 mol %) were dissolved in 30 µL of dichloromethane and added to 0.5 g of DCPD. This mixture was added to dried AuBPs (or AuNRs, CB) at the appropriate amount (depending on desired OD in final reaction volume) and the mixture was sonicated until homogenous. The formulation was then irradiated for 10 min at the corresponding wavelength (5-watt LED for 850 nm light and 660 nm light) and the temperature profiles were obtained with the set up mentioned above (section 5).

11.2 Supplementary Figure 41: Testing for FROMP

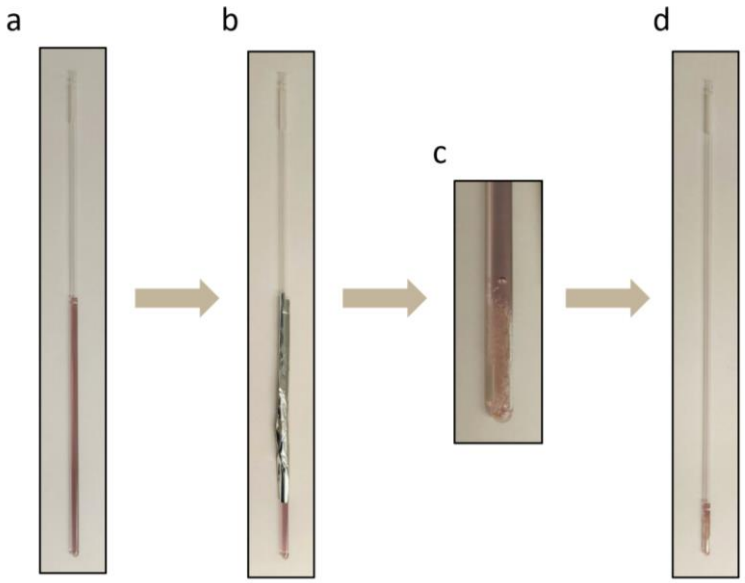

Supplementary figure 41 | Testing for FROMP. **a,** NMR tube filled with a DCPD/***cis*-Ru-P(OBn)$_3$/AuBP$_{850}$** (20 OD) formulation. **b,** The described NMR tube partially covered. **c,** The unprotected area polymerized after NIR irradiation. **d,** In the protected area the still liquid formulation could be poured out.

11.3 Supplementary Figure 42: Low OD films

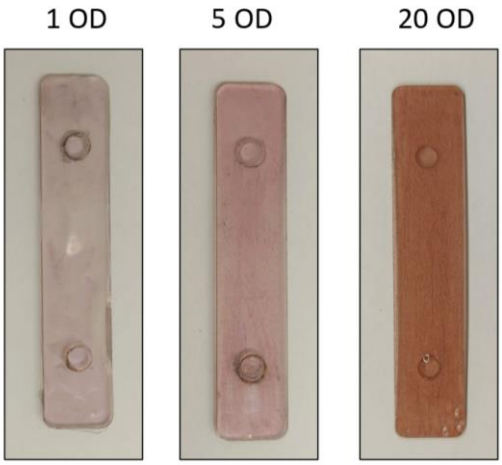

Supplementary figure 42 | Low OD PPCs with substantially less coloration than the 20 OD PPC. The 20 OD film image was taken from supplementary figure 48. The 1 OD sample could be polymerized photothermally with approximately 13 ppm of gold.

11.4 Supplementary Figure 43: p-DCPD/AuNR and p-DCPD/CB films

Supplementary figure 43 | **Left,** Fully cured film containing **AuNR$_{850}$** (20 OD). **Right,** Fully cured film containing carbon black (260 ppm).

12. Molding technique

12.1 Procedure

A DCPD/***cis*-Ru-P(OBn)$_3$**/AuBP formulation was prepared as detailed in section 9.1. The formulation was inserted into the desired mold (NMR tube or metal mold) and exposed to 365 nm light for 15-45 minutes (for small film molds 15 minutes, large film and dog-bone mold 30 minutes and NMR tubes 45 minutes) until a soft polymer film is obtained. The soft film was then shaped to the desired form (or left in the original mold) and exposed to 850 nm or 660 nm LED (1-5 mins) depending on LSPR activation wavelength.

12.2 Supplementary Figure 44: p-DCPD films

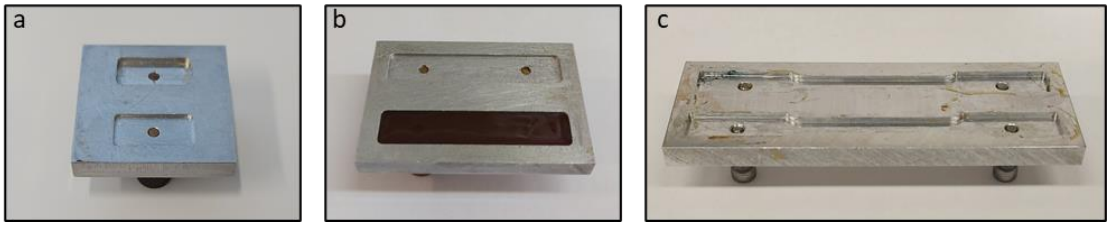

Supplementary figure 44 | Three types of films were prepared as part of this research using the templates seen above. **a,** "Small film" rectangular aluminum template (2.5 cm × 1cm × 1mm). Used for the synthesis of the films seen in figure 3 of the article. These films were later cut manually to fit the LED illumination area. **b,** "Large film" rectangular aluminum template (5cm × 1cm × 1mm). Used for the synthesis of DMA analysis samples. DCPD/***cis*-Ru-P(OBn)$_3$/AuBP$_{850}$** formulation can be seen in the template. **c,** "Dog-bone" aluminum template. Used for the synthesis of UTM analysis samples.

12.3 Knot and coil

The knot and coil seen in figure three of the article were molded using 3 mm NMR tubes. After "soft" polymerization the tubes were broken carefully and the resulting p-DCPD-AuBP composite was shaped as shown in supplementary videos 2 and 3.

13. ROMP of cyclooctene

Supplementary Table 4

Entry	Activation method	NMR Conversion (%)	SEC Results				Active catalyst (%)
			Mn (kDa)	Mw (kDa)	PDI (Mw/Mn)	rh(v)z (nm)	
1	Oil bath	70	360	420	1.1	30	**18**
2	NIR irradiation	93	70	90	1.3	15	**114**

13.1 Procedure

A solution containing 0.5 M cyclooctene, 0.1 mol% ***cis*-Ru-P(OBn)$_3$** and **AuBP$_{850}$** (5 OD) was prepared in toluene. The mixture was then irradiated with an NIR LED (100 watt, 850nm) for 45 min to 80 °C. For the control sample an identical solution was prepared including AuBPs and heated in an oil bath to the same temperature.

13.2 Supplementary Figures 45, 46: NMR conversion

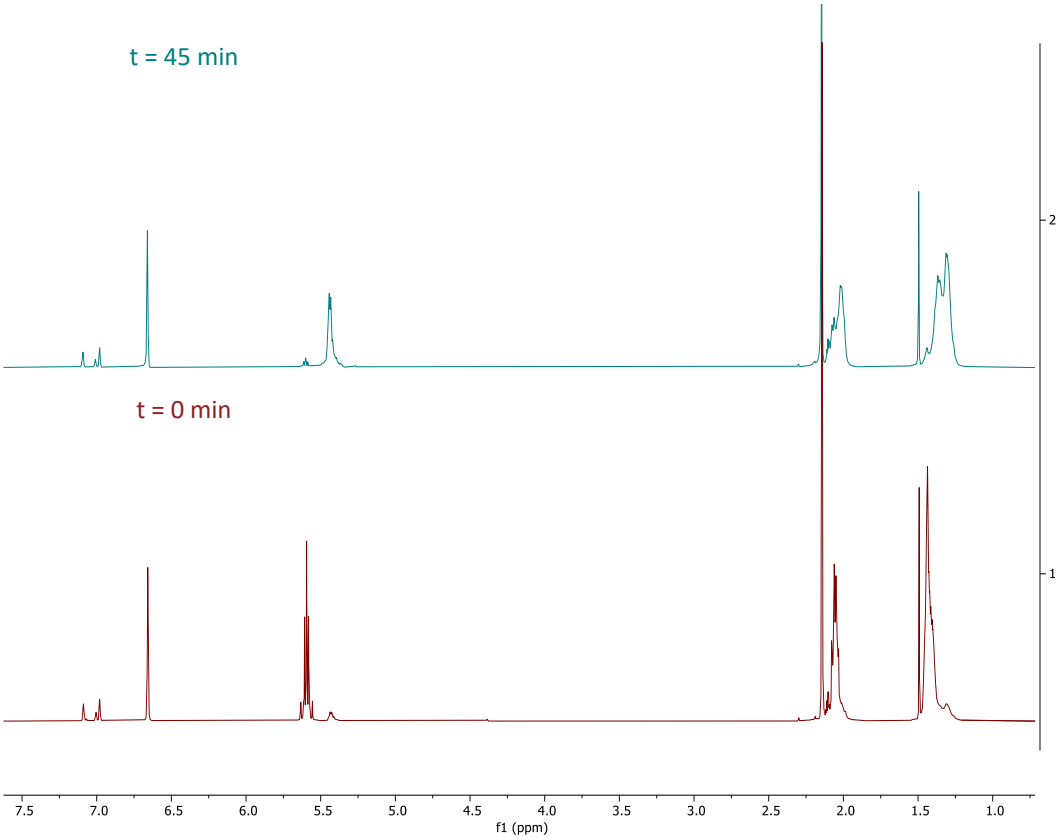

Supplementary figure 45 | NMR results of NIR activated cyclooctene ROMP at t=0 and t=45 minutes. Peak integration shows 93 % conversion.

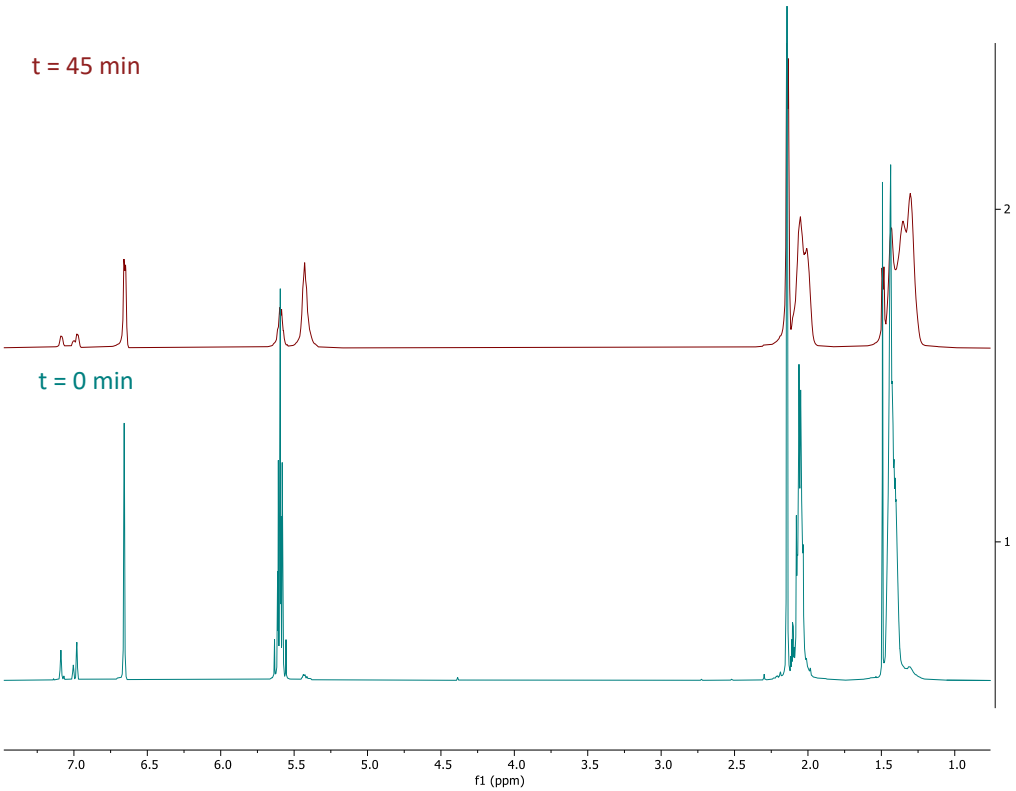

Supplementary figure 46 | NMR results of conventionally activated (oil bath) cyclooctene ROMP at t=0 and t=45 minutes. Peak integration shows 70 % conversion.

13.3 Supplementary Figure 47: SEC results

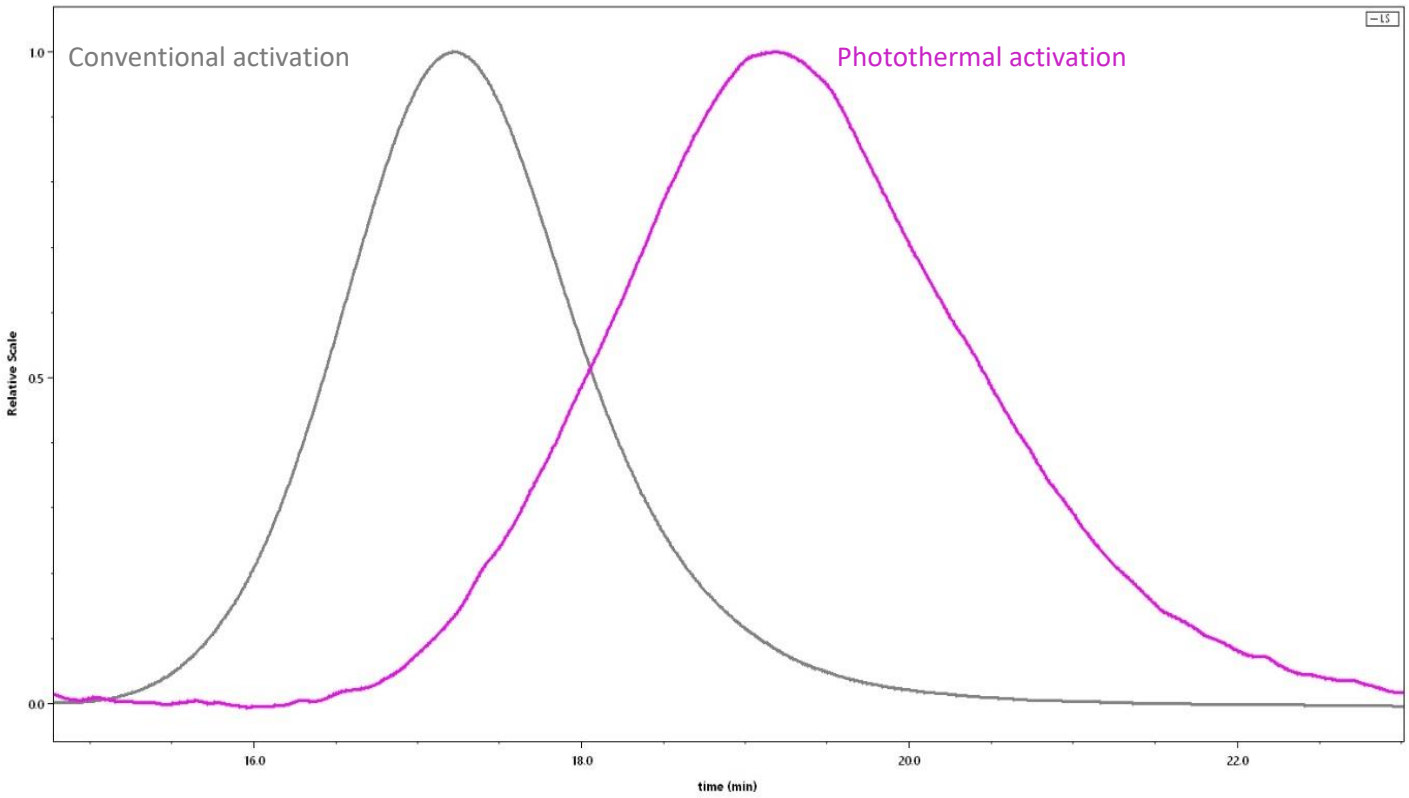

Supplementary figure 47 | SEC chromatogram produced from the light scattering (LS) detector, of cyclooctene ROMP experiments. Analysis shown in supplementary table 4.

14. Homogeneity of AuBPs in solutions and polymers

14.1 Procedure for solution uniform distribution test

The reaction solution was prepared as described in section 6.1 with **AuBP$_{850}$** and the RCM substrate appearing in entry 1 of table 1. The 0.5 ml solution was then split into three equal volume fractions and their absorbance was measured (diluted 50 times to obtain optimal conditions) to compare the concentration of AuBPs (supplementary fig. 47a and b). All three spectra showed the characteristic AuBP$_{850}$ peak with minor deviations that can be expected when considering slight errors in volume are practically unavoidable, confirming that the original solution was homogenous. Additional validation was obtained by carrying out the reaction separately in each fraction. GC-MS confirmed 99% conversion for all three RCM reactions.

14.2 Procedure for testing uniform distribution in polymer composites

A 20 OD **PPC$_{850}$** film was prepared as described in section 12.1. We then cut the film into three sections and ensured they had an equal thickness so that the absorbance could be compared. The absorbance spectra were then obtained and showed staggering similarity almost completely overlapping. This indicates the AuBPs are very uniformly distributed throughout the PPC.

14.3 Supplementary Figure 48: Uniform distribution test

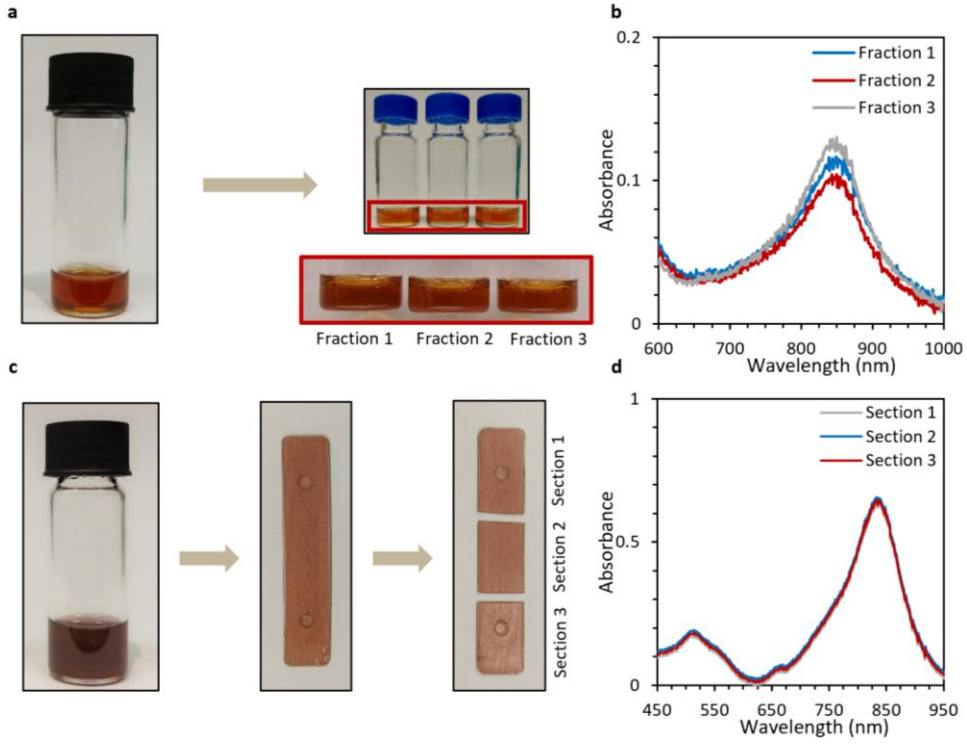

Supplementary figure 48 | Uniform distribution test. **a,** Images of the RCM reaction solution before and after splitting. In red outline a zoomed-in image of the fractions. **b,** Absorbance spectra of fractions 1-3. **c,** From left to right, images of: DCPD/***cis*-Ru-P(OBn)$_3$/AuBP$_{850}$** (20 OD) formulation prior to irradiation; fully cured PPC film; and the film cut into 3 sections. **d,** Absorbance spectra of sections 1-3 (not normalized).

15. Patterning technique

15.1 Procedure

A DCPD/***cis*-Ru-P(OBn)$_3$**/AuBP formulation was prepared as detailed in section 9.1. The formulation was drop casted uniformly on a microscope slide and a DLP projector (Supplementary figure 31) was used to irradiate UV light (365 nm) according to the desired pattern for 2 minutes. The exposure to UV light initiated "soft" polymerization matching the selected pattern. The slide was then washed carefully with ethyl acetate or acetone to dispose of unreacted formulation and dried under air.

15.2 Supplementary Figure 49: System set-up

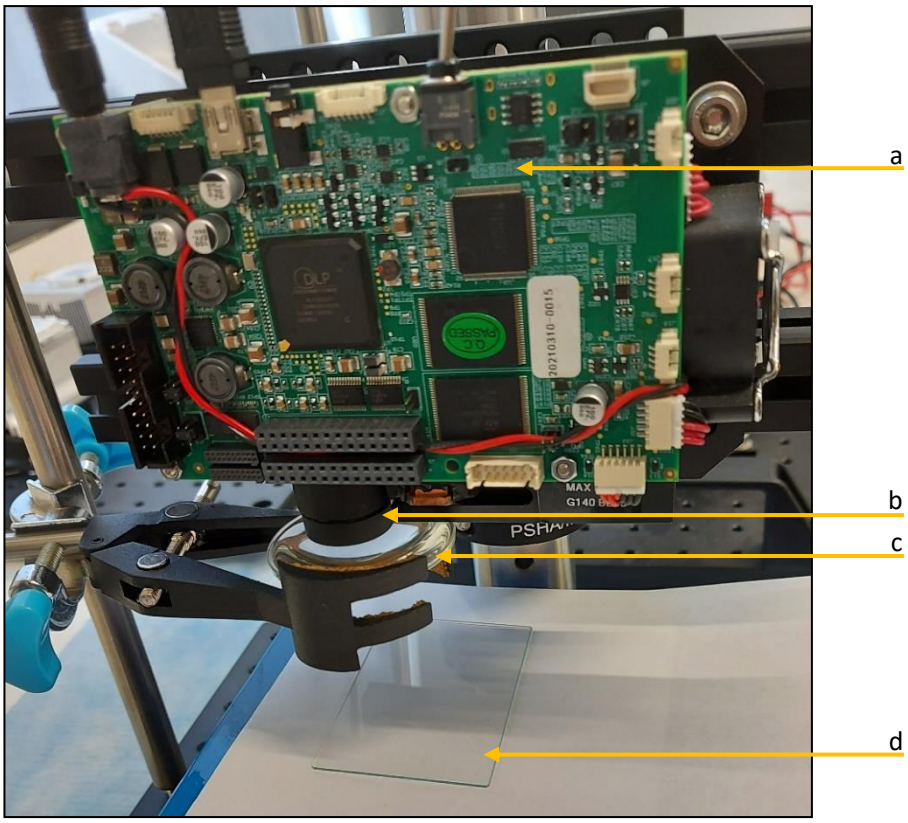

Supplementary figure 49 | DCPD patterning system set up. A Texas Instruments® Lightcrafter 4500MKII DLP projector was used as detailed above. Complementary with the hardware that can be seen in the image the system consists also of a software that was used to design patterns and set exposure times. **a,** DLP projector hardware. **b,** 365 nm LED. **c,** Glass lens used for focusing image. **d,** microscope slide where polymer formulations are spread.

16. Photonic Vials

16.1 Procedure

A DCPD/**cis-Ru-P(OBn)$_3$/AuBP$_{850}$** formulation was poured into a 2 mL dram vial. A glass insert tube was then placed inside the vial, and the formulation was allowed to reach the top of the vial. The DCPD/**cis-Ru-P(OBn)$_3$/AuBP$_{850}$** was fully polymerized by irradiating 850 nm light (100-watt LED) for 5 minutes. The curing of the DCPD-AuBP composite afforded a reaction vessel (the insert) coated by the photo-responsive material, the photonic vial.

0.1 M reaction mixture of diethyl diallyl malonate in toluene was placed inside the photonic vial with a 1 mol% of ***cis*-Ru-SCF$_3$**. The vials were exposed to the corresponding activation light (5-watt 850 nm or 660 nm LED) for 15 minutes and reached a temperature of 100 °C. Additionally, this reaction was also carried out with **AuBP$_{850}$** directly in the solution as described for previous RCM reactions. The substrate and catalyst concentrations were kept identical, 5 OD of **AuBP$_{850}$** were added and the reaction was done at a volume of 0.5 ml.

16.2 Supplementary Figures 50, 51: GC-MS results for reactions in photonic vials

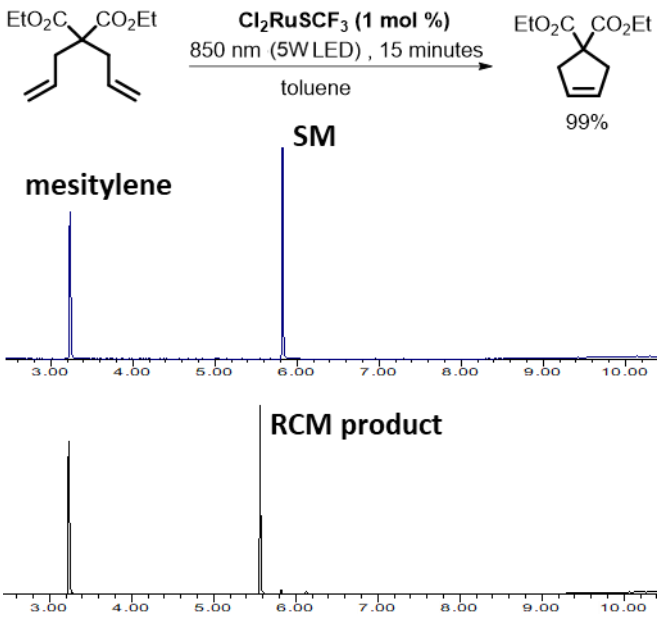

Supplementary figure 50 | GC-MS results of reaction mixture in **AuBP$_{850}$** photonic vial before and after exposure to activation light.

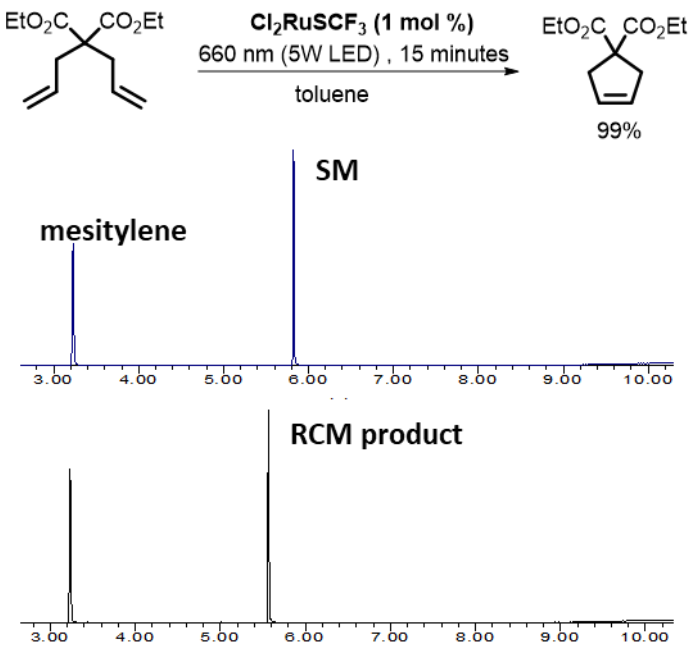

Supplementary figure 51 | GC-MS results of reaction mixture in **AuBP$_{660}$** photonic vial before and after exposure to activation light.

16.3 Supplementary Figure 52: GC-MS results for reaction with AuBPs in solution

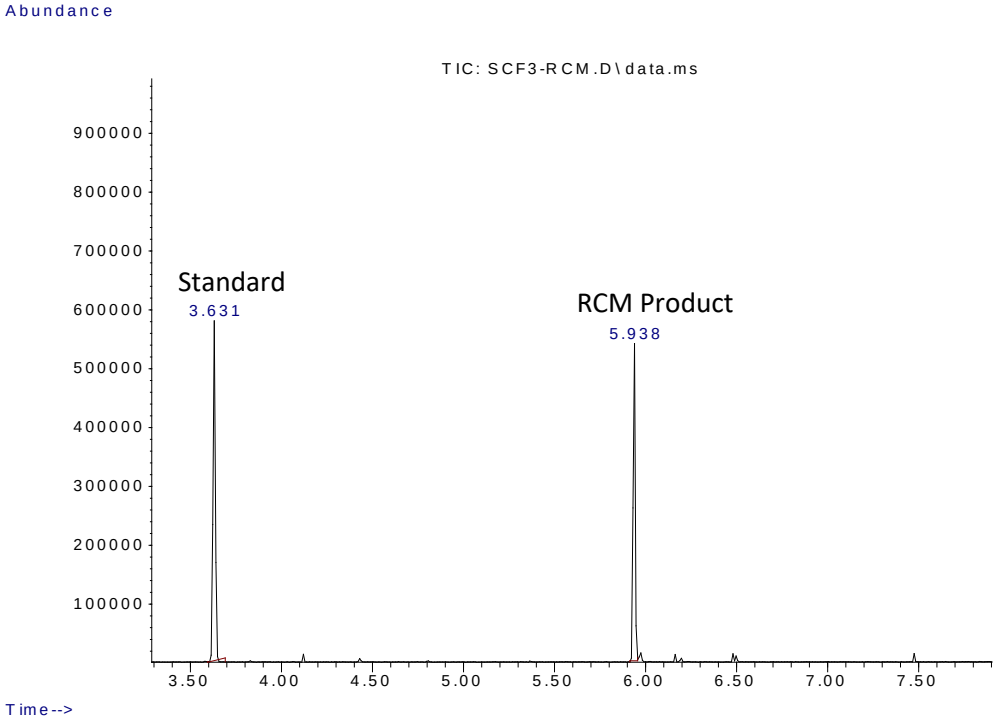

Supplementary figure 52 | GC-MS results of reaction mixture where **AuBP$_{850}$** was inserted directly into the solution. Peak integration showed 99 % conversion.

17. Photo-responsive characterization

17.1 Supplementary Figure 53: Heating/Cooling cycle zoom-in

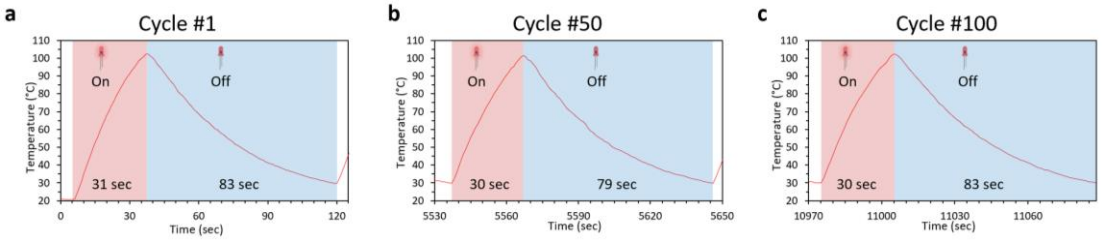

Supplementary figure 53 | Zoom-in on heating/cooling cycles. To help assess individual cycles more accurately, three representative cycles have been enlarged. a, Zoom-in on cycle number 1 from **figure 3c**. Red background representing the LED is on and the heating process is taking place. Blue background indicating the LED is off and the polymer is cooling. **b,** as in **a** for cycle number 50. **c,** as in **a** for cycle number 100.

17.2 Supplementary Figure 54: Procedure

To assess the heating capacity and durability of the photo-responsive feature observed when irradiating the AuBP embedded polymer, a DCPD film containing 850 nm AuBPs at 20 OD was irradiated so that upon reaching 100 °C the LED turned off and when cooling back to 30 °C the LED turned on and reinitiated the plasmonic heating response. The illumination was done with a 100 W 850 nm LED and the temperature was monitored by the system described in section 5.

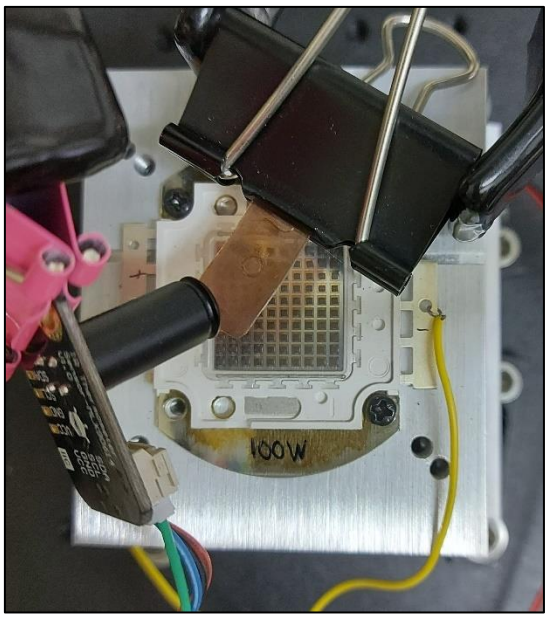

Supplementary figure 54 | Image showing the composite polymer film, 100 W 850 nm LED and thermocouple.

18. “Soft” polymer composition

18.1 Procedure

Initially, a 100 mg UV treated film was stirred in THF for 72 hours. After drying the film, it was weighed and determined that 18 % of the original mass was left undissolved. The THF filtrate was analysed with SEC and showed the presence of a high molecular weight polymer. An identical film was stirred in ethyl acetate and the solvent was analysed by GC-MS showing the presence of unreacted DCPD. To find the ratio between DCPD monomer and pDCPD, an additional film was prepared, stirred in deuterated THF (72 hours) and analysed by NMR.

18.2 Supplementary Figure 55: SEC results

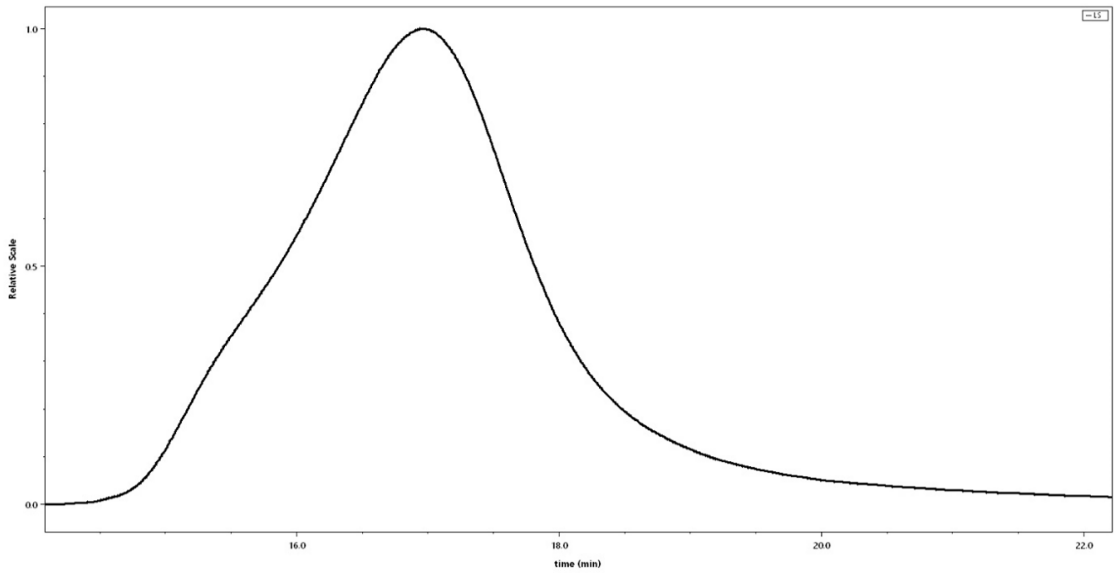

Mn (kDa)	Mw (kDa)	PDI (Mw/Mn)	rh(v)z (nm)
1504	1670	1.11	53

Supplementary figure 55 | SEC chromatogram produced from the light scattering (LS) detector, of the filtrate. Results derived from the analysis shown below.

18.3 Supplementary Figure 56: GC-MS results

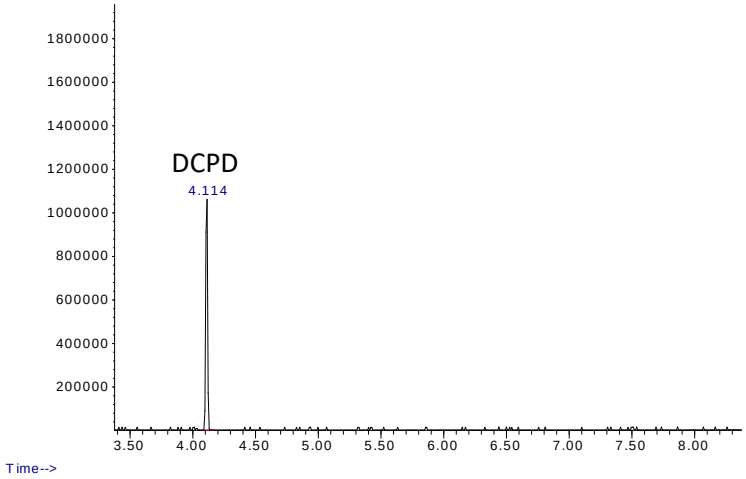

Supplementary figure 56 | GC-MS indicating the presence of DCPD.

18.4 Supplementary Figure 57: NMR results

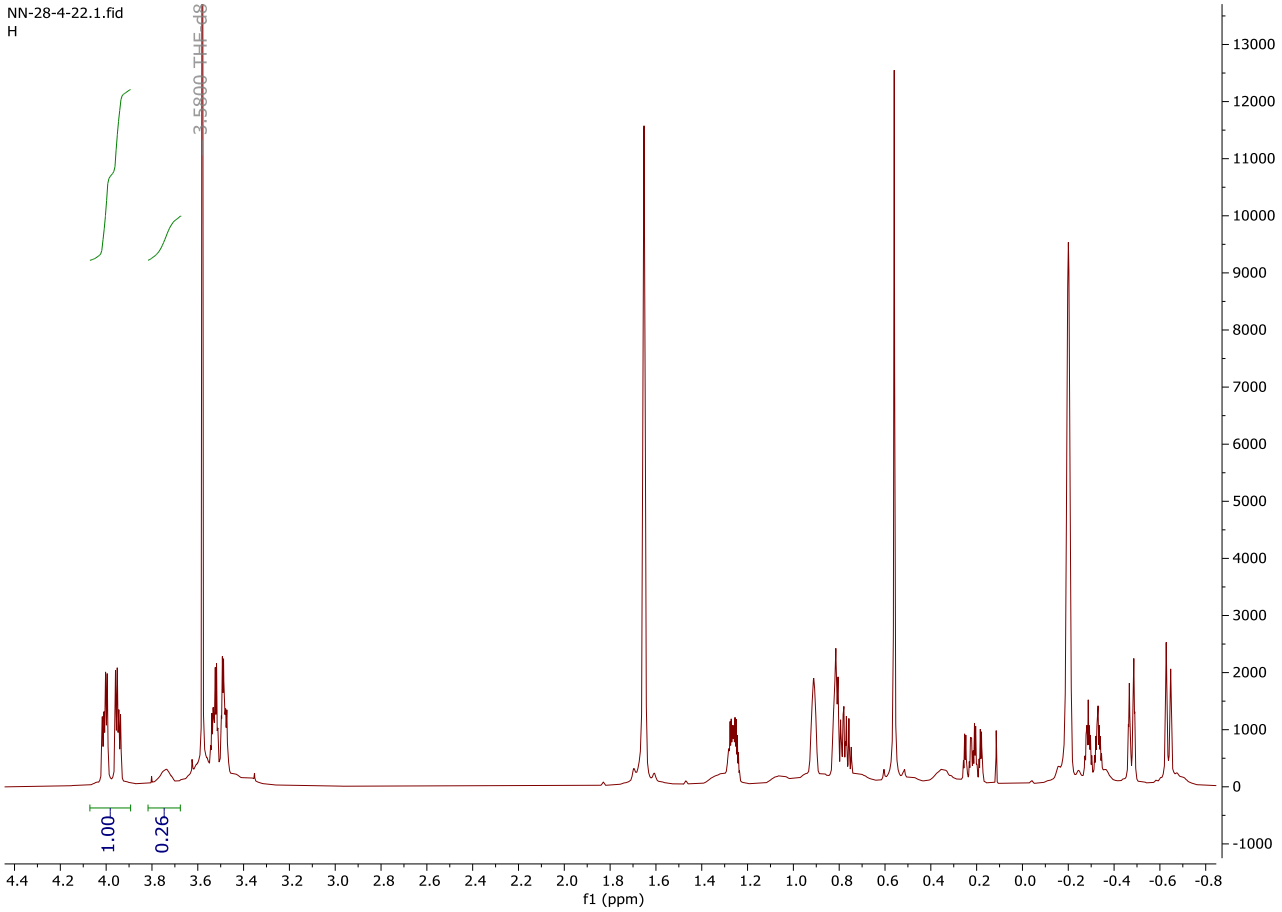

Supplementary figure 57 | NMR showing the ratio between DCPD and dissolved polymer in deuterated THF filtrate.

18.5 Supplementary Figure 58: DMA results

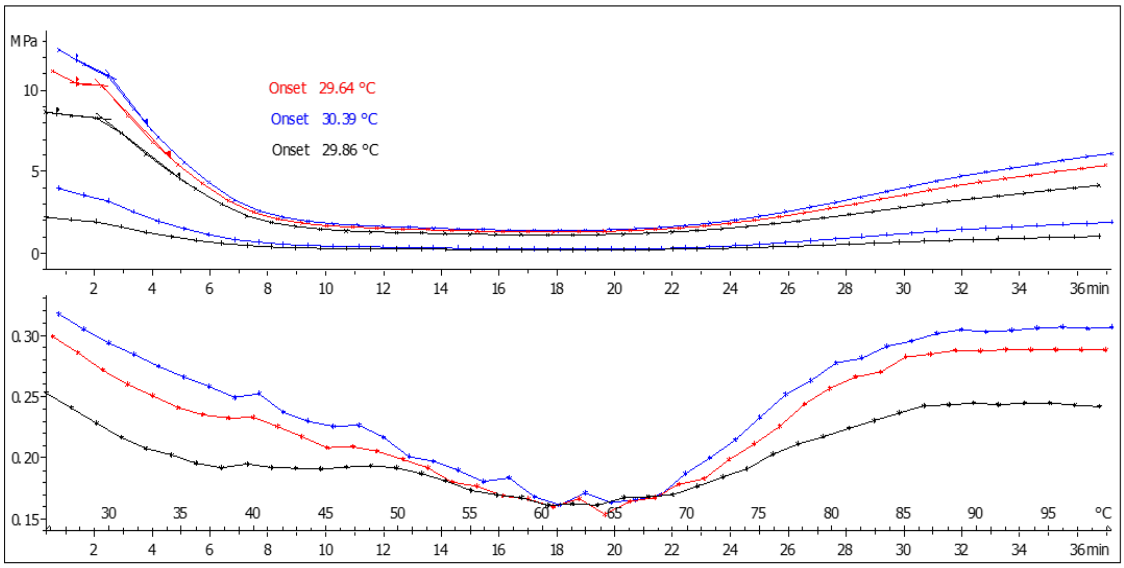

Supplementary figure 58 | DMA curves of "soft" polymer sample. **Top,** storage modulus (E') and loss modulus (E'') curves; **bottom,** Tan delta (δ) curves. Colour codes: Black: at 1 Hz; Red: at 5 Hz; Blue: at 10 Hz.

19. Mechanical characterization

19.1 Supplementary Figures 59-69: DMA data

Supplementary Table 5

Entry	Formulation	Curing	Sample 1		Sample 2	
			Onset	Tan δ	Onset	Tan δ
1	p-DCPD/***cis*-Ru-P(OBn)$_3$**/No AuBPs	oven	85 °C	91 °C	81 °C	85 °C
2	p-DCPD/***cis*-Ru-P(OBn)$_3$/AuBP$_{660}$**	oven	85 °C	86 °C	88 °C	90 °C
3	p-DCPD/***cis*-Ru-P(OBn)$_3$/AuBP$_{660}$**	LED	113 °C	119 °C	114 °C	121 °C
4	p-DCPD/***cis*-Ru-P(OBn)$_3$/AuBP$_{850}$**	oven	86 °C	90 °C	85 °C	88 °C
5	p-DCPD/***cis*-Ru-P(OBn)$_3$/AuBP$_{850}$**	LED	122 °C	128 °C	118 °C	130 °C

DMA films were initially exposed to 365 nm light for 30 minutes. Then, curing of the films was obtained at 90 °C for 30 minutes by irradiating LSPR activation light (AuBP containing films) or by oven (control films). All films containing AuBPs were prepared with a final

concentration of 20 OD. Two identical films (samples 1 and 2) were prepared and tested for each entry.

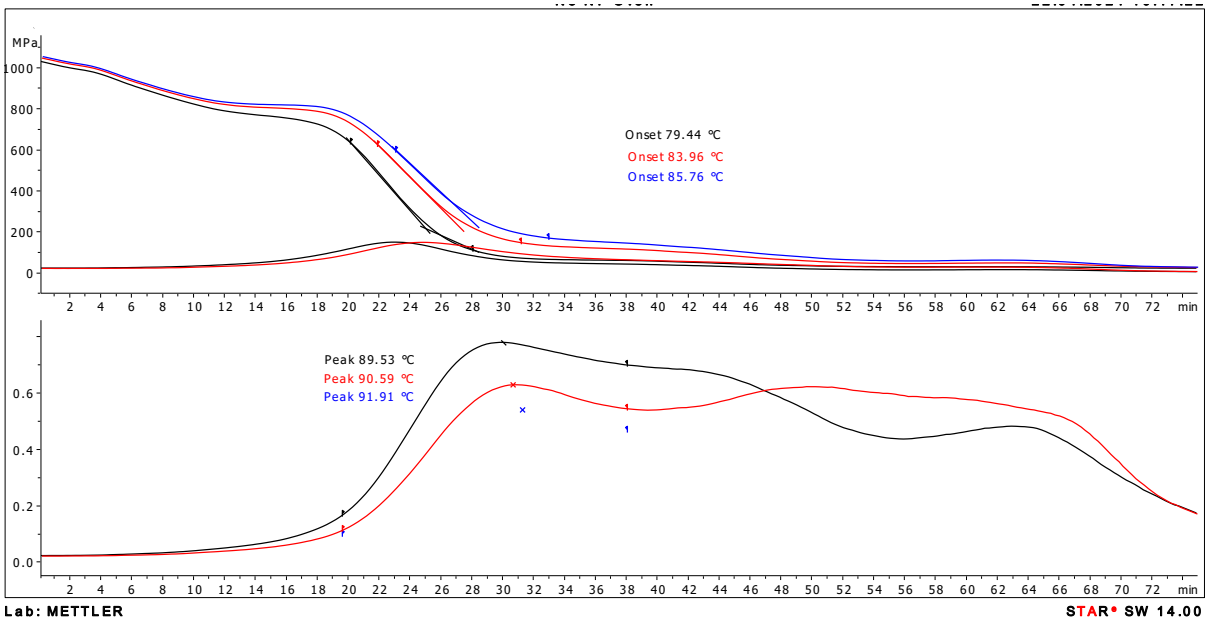

Supplementary figure 59 | DMA curves of table 5 entry 1, sample 1: **Top,** storage modulus (*E'*) and loss modulus (*E''*) curves; **bottom,** Tan delta (δ) curves. Colour codes: Black: at 1 Hz; Red: at 5 Hz; Blue: at 10 Hz.

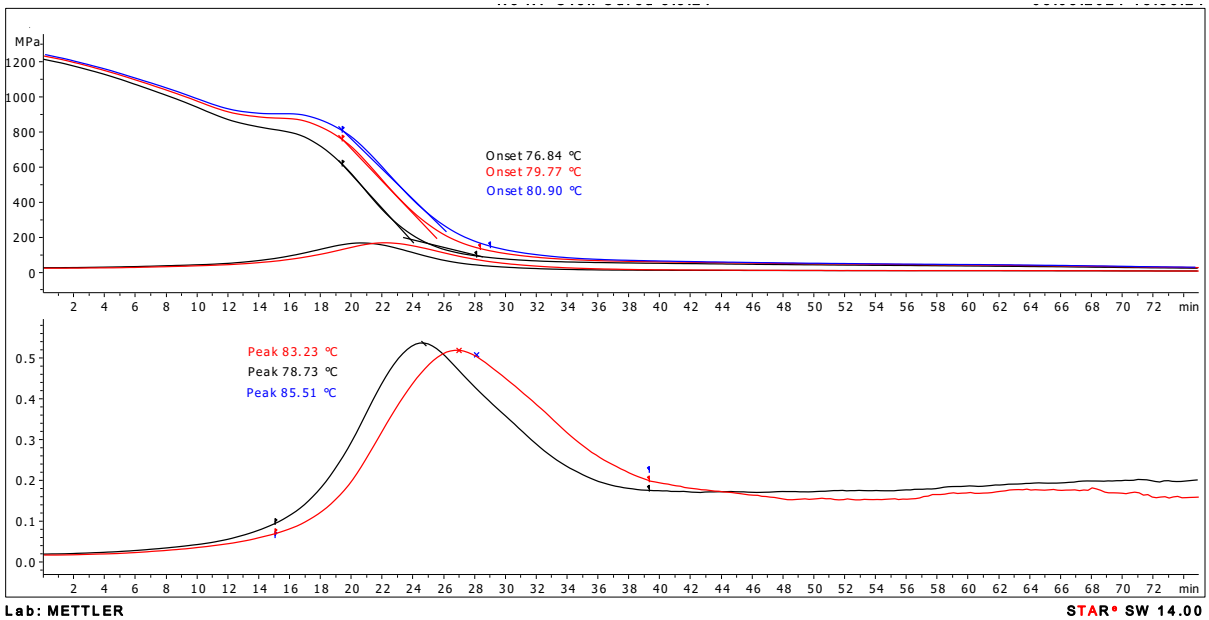

Supplementary figure 60 | DMA curves of table 5 entry 1, sample 2: **Top,** storage modulus (*E'*) and loss modulus (*E''*) curves; **bottom,** Tan delta (δ) curves. Colour codes: Black: at 1 Hz; Red: at 5 Hz; Blue: at 10 Hz.

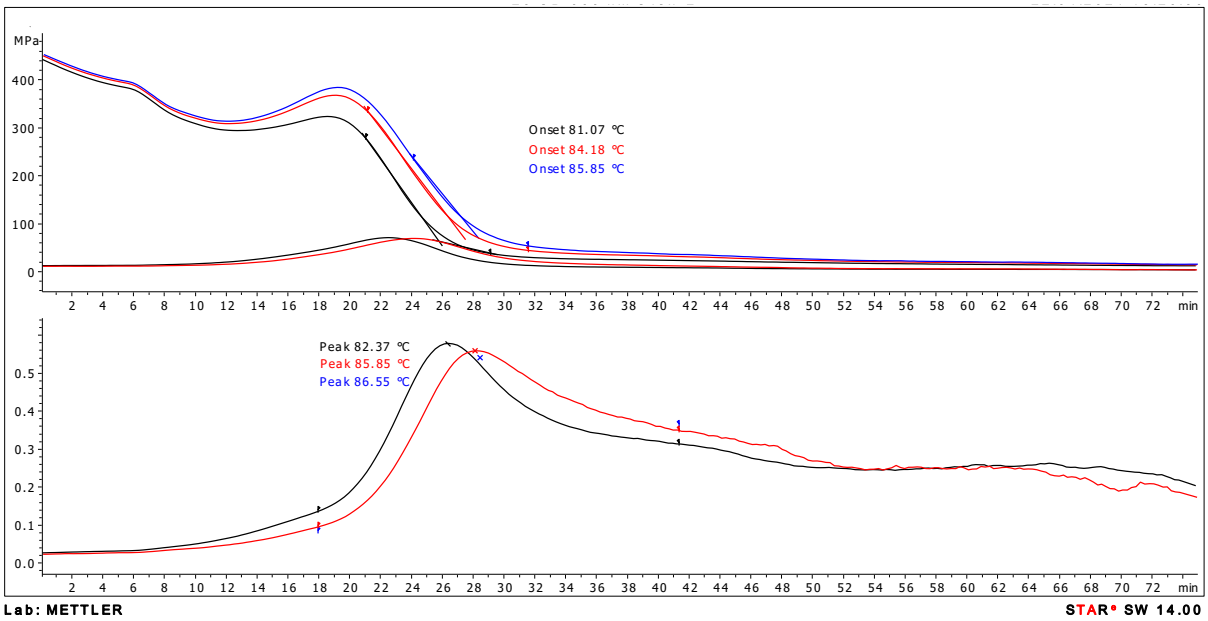

Supplementary figure 61 | DMA curves of table 5 entry 2, sample 1: **Top,** storage modulus (*E'*) and loss modulus (*E''*) curves; **bottom,** Tan delta (δ) curves. Colour codes: Black: at 1 Hz; Red: at 5 Hz; Blue: at 10 Hz.

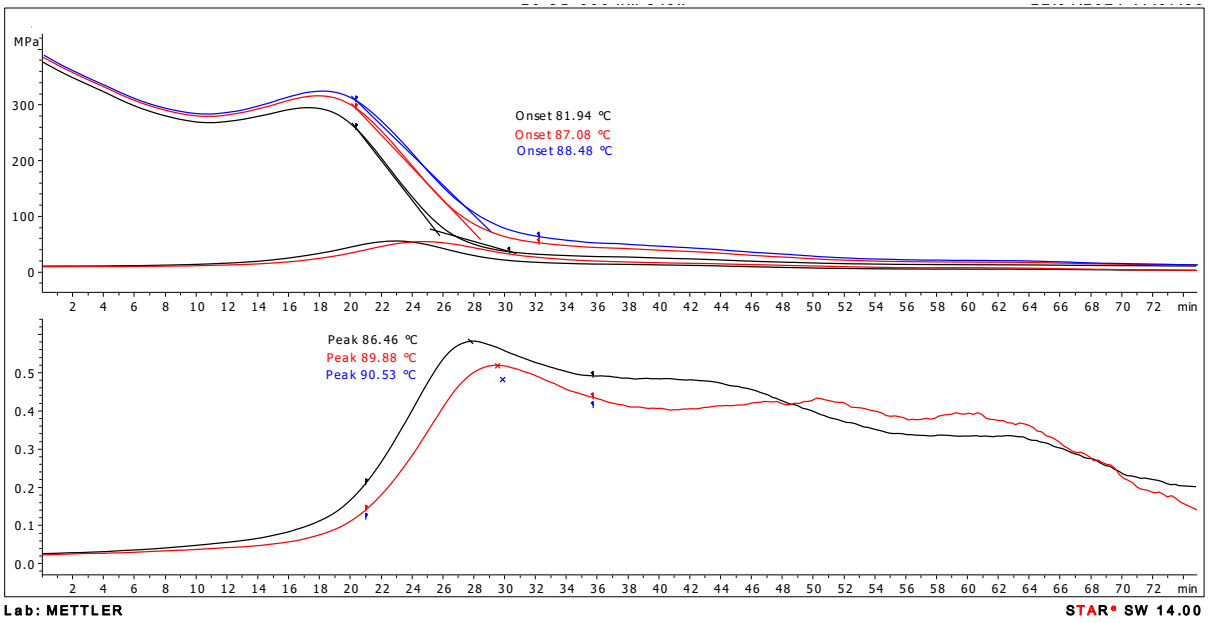

Supplementary figure 62 | DMA curves of table 5 entry 2, sample 2: **Top,** storage modulus (*E'*) and loss modulus (*E''*) curves; **bottom,** Tan delta (δ) curves. Colour codes: Black: at 1 Hz; Red: at 5 Hz; Blue: at 10 Hz.

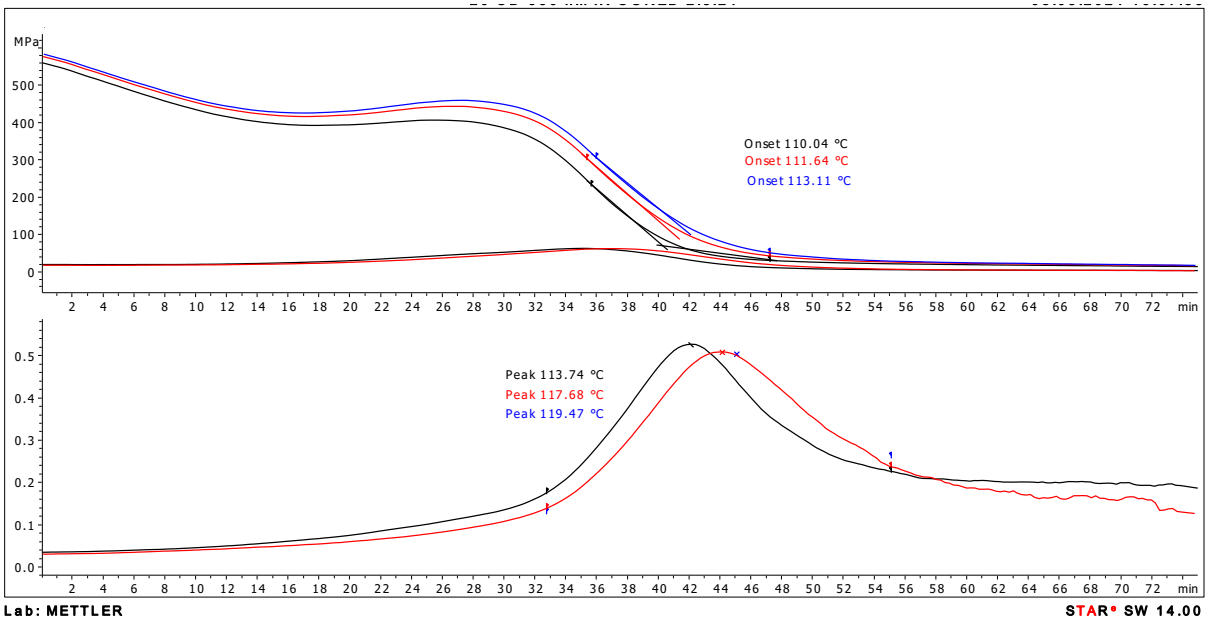

Supplementary figure 63 | DMA curves of table 5 entry 3, sample 1: **Top,** storage modulus (*E'*) and loss modulus (*E''*) curves; **bottom,** Tan delta (δ) curves. Colour codes: Black: at 1 Hz; Red: at 5 Hz; Blue: at 10 Hz.

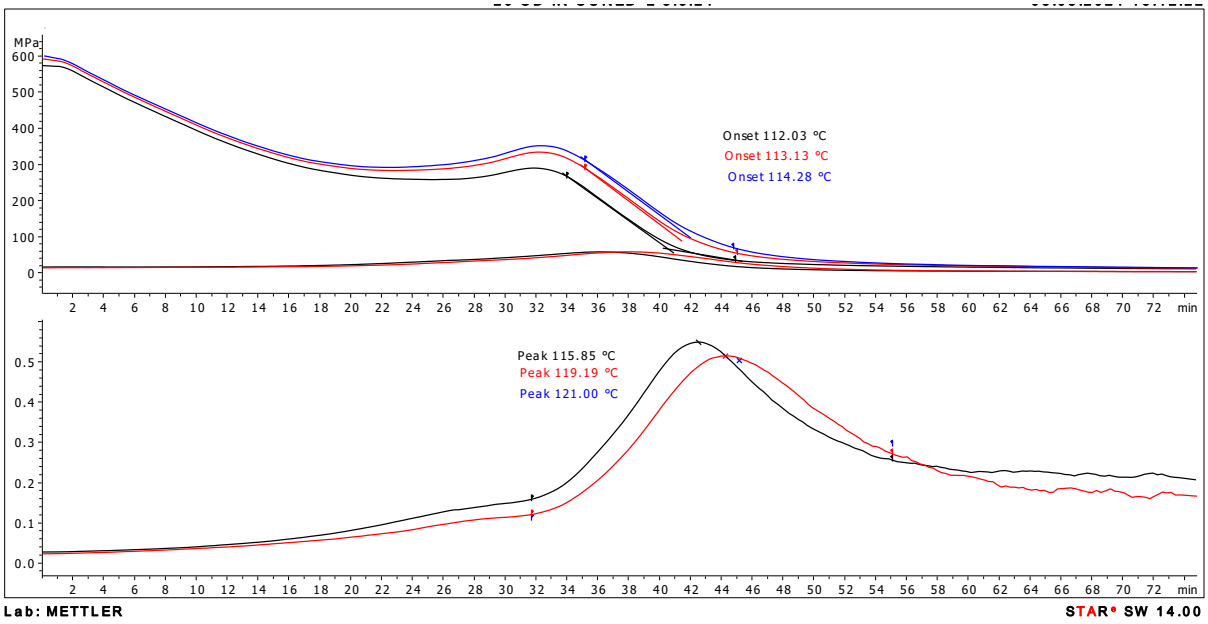

Supplementary figure 64 | DMA curves of table 5 entry 3, sample 2: **Top,** storage modulus (*E'*) and loss modulus (*E''*) curves; **bottom,** Tan delta (δ) curves. Colour codes: Black: at 1 Hz; Red: at 5 Hz; Blue: at 10 Hz.

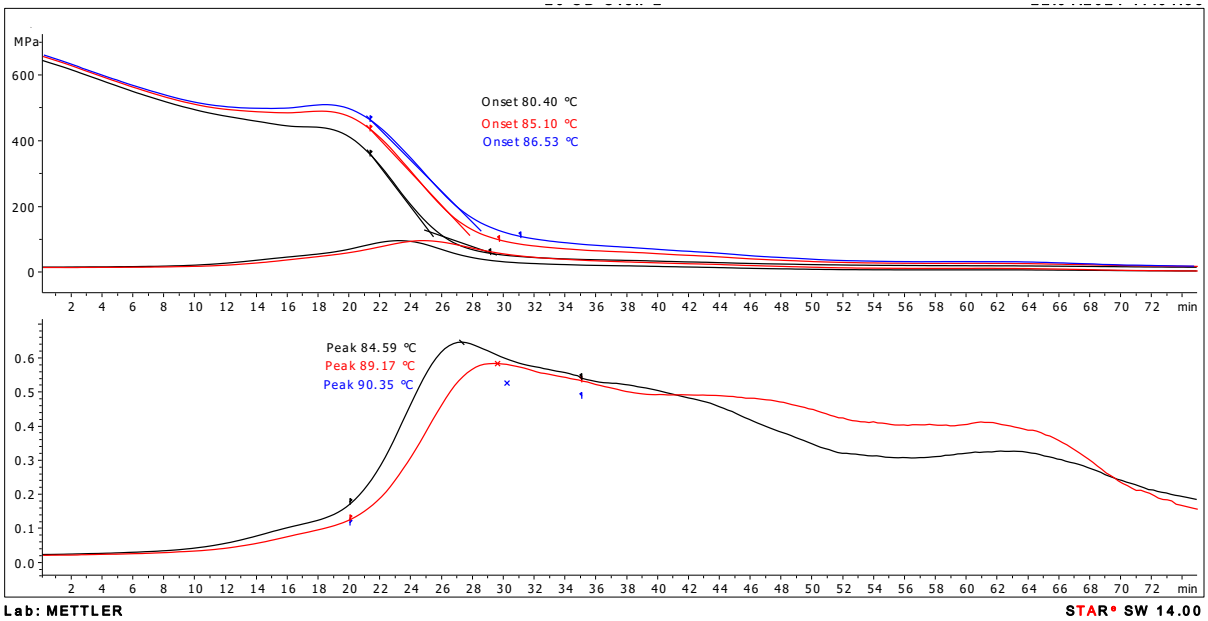

Supplementary figure 65 | DMA curves of table 5 entry 4, sample 1: **Top,** storage modulus (*E'*) and loss modulus (*E''*) curves; **bottom,** Tan delta (δ) curves. Colour codes: Black: at 1 Hz; Red: at 5 Hz; Blue: at 10 Hz.

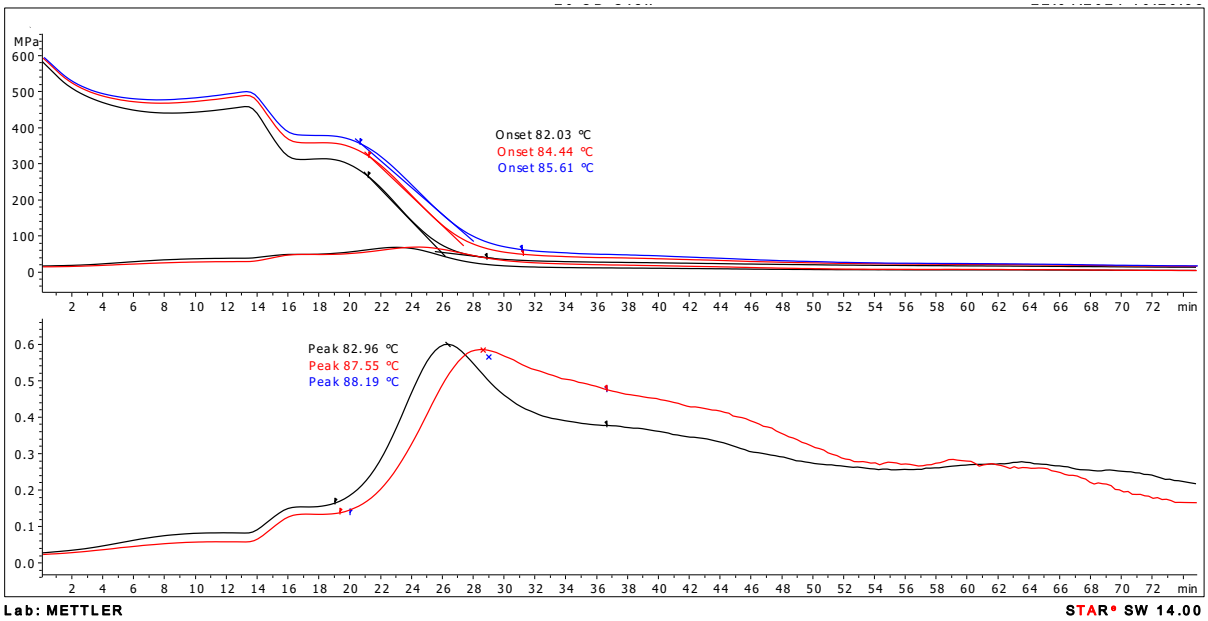

Supplementary figure 66 | DMA curves of table 5 entry 4, sample 2: **Top,** storage modulus (*E'*) and loss modulus (*E''*) curves; **bottom,** Tan delta (δ) curves. Colour codes: Black: at 1 Hz; Red: at 5 Hz; Blue: at 10 Hz.

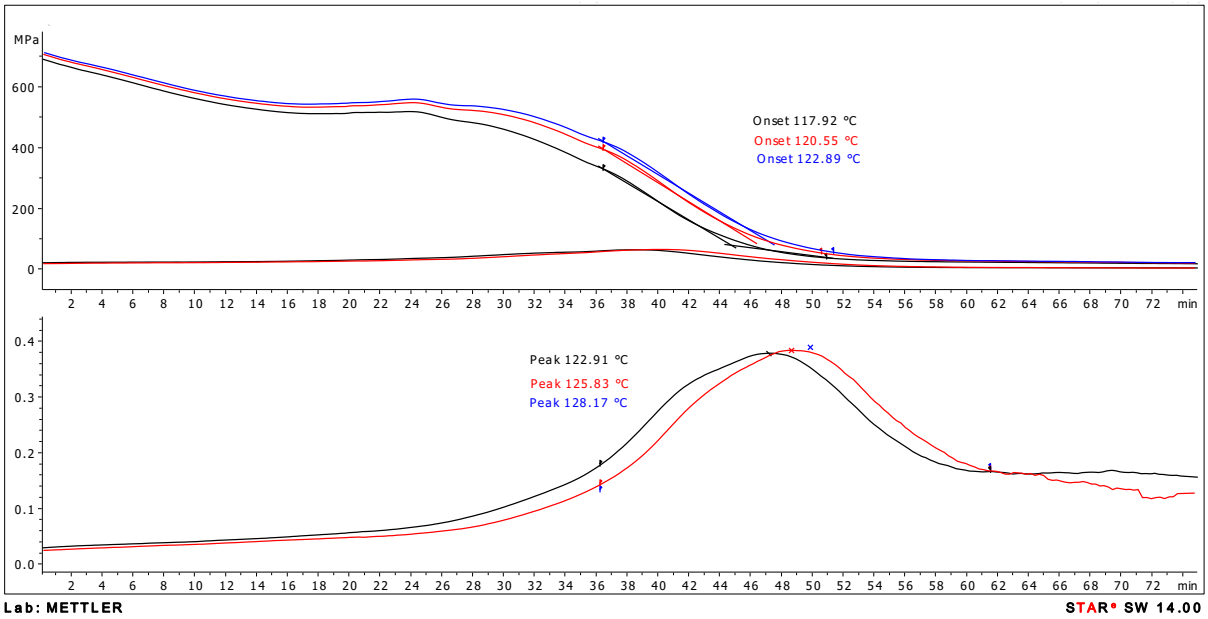

Supplementary figure 67 | DMA curves of table 5 entry 5, sample 1: **Top,** storage modulus (*E'*) and loss modulus (*E''*) curves; **bottom,** Tan delta (δ) curves. Colour codes: Black: at 1 Hz; Red: at 5 Hz; Blue: at 10 Hz.

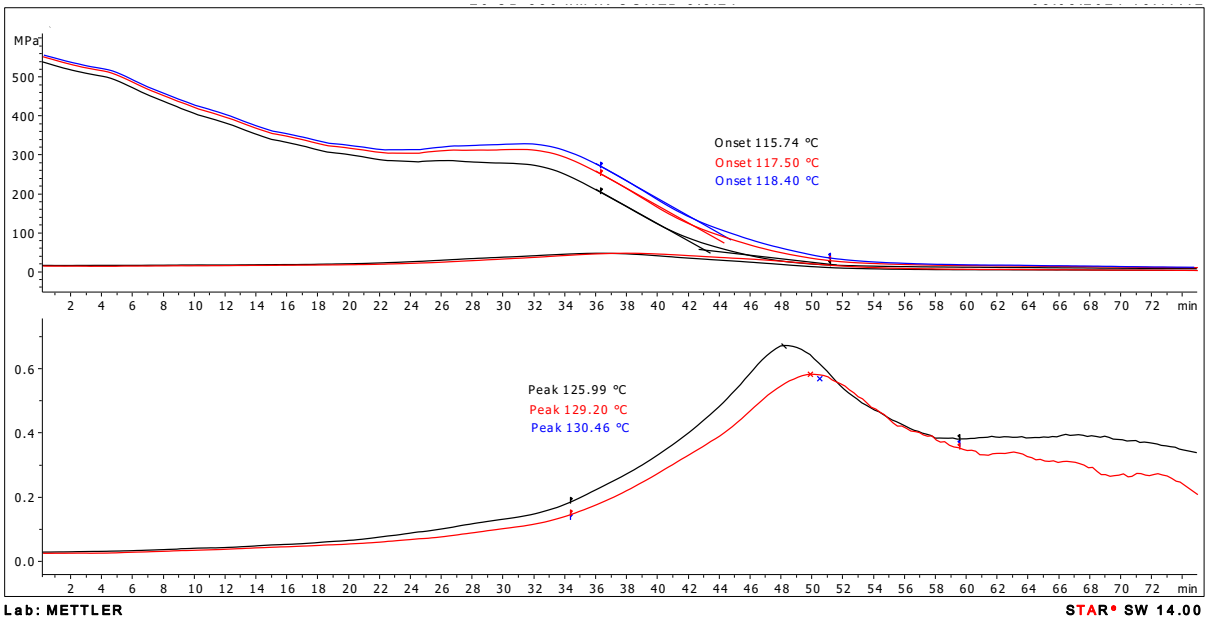

Supplementary figure 68 | DMA curves of table 5 entry 5, sample 2: **Top,** storage modulus (*E'*) and loss modulus (*E''*) curves; **bottom,** Tan delta (δ) curves. Colour codes: Black: at 1 Hz; Red: at 5 Hz; Blue: at 10 Hz.

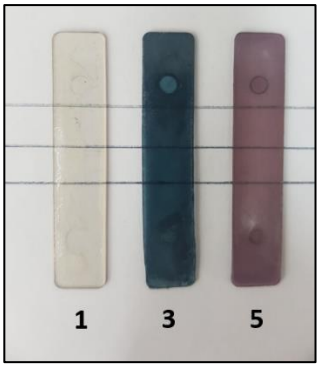

Supplementary figure 69 | Images of polymeric films (table 5 entries 1, 3, 5). Lines drawn underneath the polymers to highlight transparency.

19.2 Supplementary Figures 70, 71: Tensile test data

Supplementary Table 6

	Entry	Formulation	Curing	Width (mm)	Thickness (mm)	Ultimate force (N)	Ultimate tensile strength (MPa)	Average UTM (MPa)
	1			6.20	1.40	230.0	26.5	
a	2		Oven	6.00	1.30	238.7	30.6	29.4 ± 2.0
	3	p-DCPD/***cis*-Ru-P(OBn)$_3$/AuBP$_{660}$**		6.00	1.40	260.0	31.0	
	4			6.20	1.40	361.9	41.7	
b	5		LED	6.20	1.25	412.5	53.2	47.3 ± 4.7
	6			6.00	1.20	338.2	47.0	
	7	p-DCPD/***cis*-Ru-P(OBn)$_3$**/No AuBPs		6.00	1.55	262.4	28.2	
c	8		Oven	6.00	1.55	250.0	26.9	28.6 ± 1.5
	9			6.00	1.55	284.3	30.6	
	10			5.94	1.18	275.0	39.2	
d	11		LED	6.10	1.23	322.7	43.0	40.7 ± 1.6
	12	p-DCPD/***cis*-Ru-P(OBn)$_3$/AuBP$_{850}$**		5.98	1.25	298.2	39.9	
	13			6.20	1.78	265.8	24.1	
e	14		Oven	6.20	1.78	263.8	23.9	25.0 ± 1.5
	15			6.00	1.73	281.6	27.1	

The UTM was calculated to be the ratio of the ultimate force and the cross-section at the point of failure ($UTM(MPa) = \frac{UM(N)}{Thickness(mm) * Width(mm)}$).

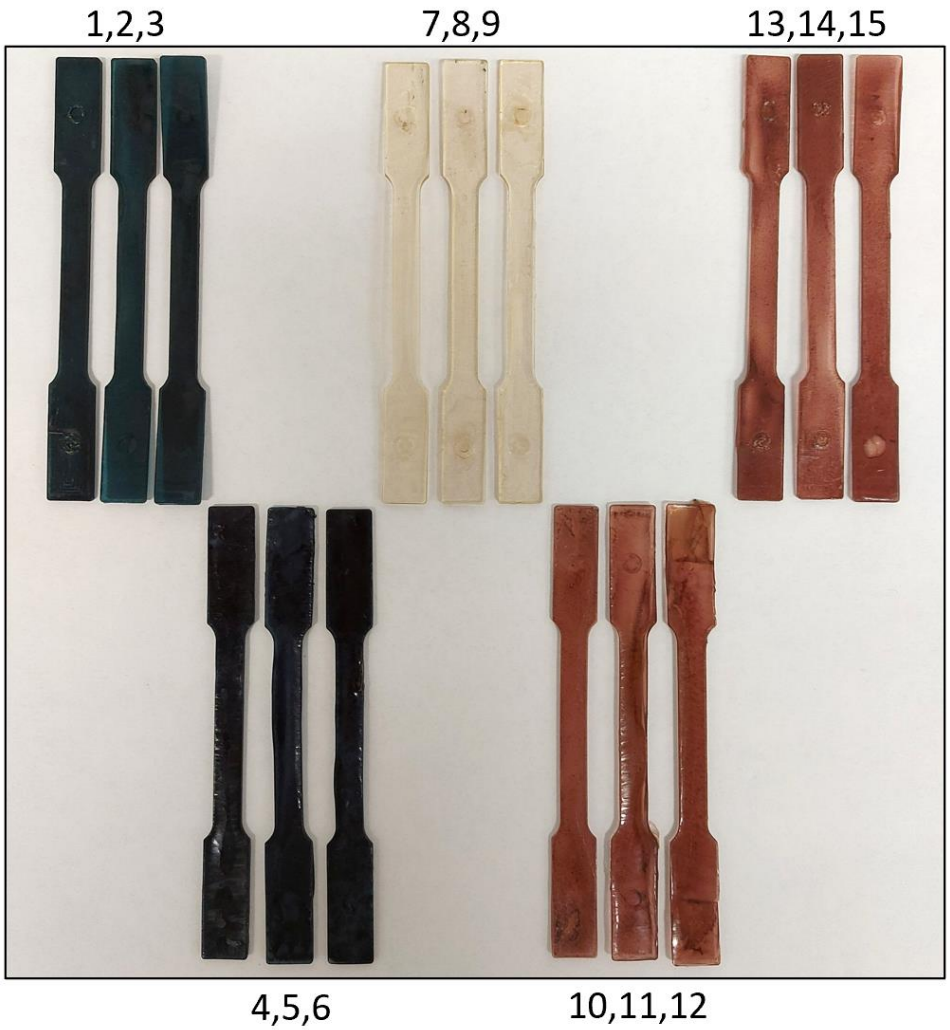

Supplementary figure 70 | Image of PPC dog-bone samples numbered to match supplementary table 6.

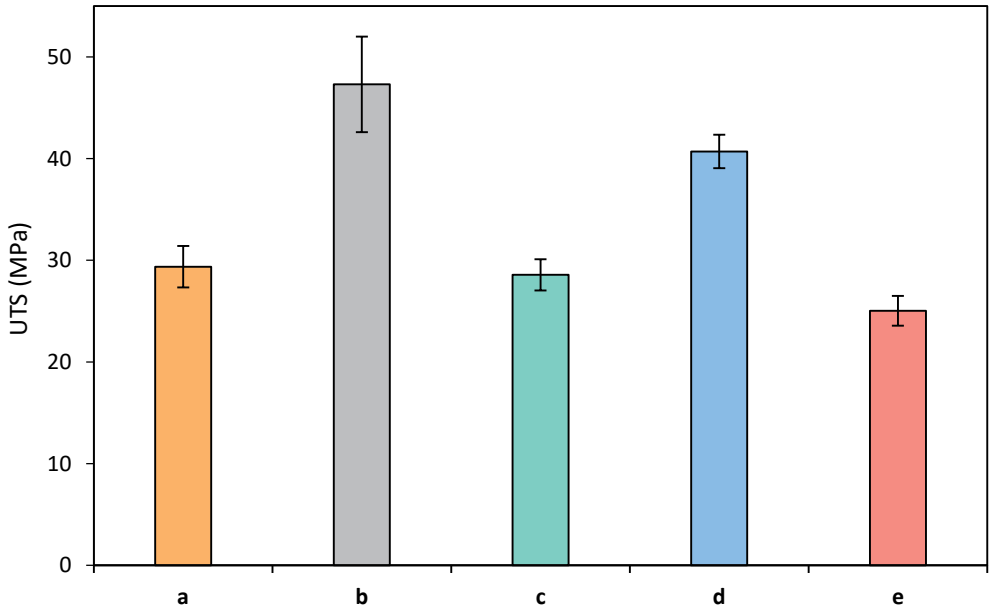

Supplementary figure 71 | Ultimate tensile strength of PPC samples tested from the data presented in supplementary table 6. Error bars represent the standard deviation according to the data in supplementary table 6 (last column titled Average UTM).

19.3 Supplementary Figures 72-81: SEM characterization

Four SEM samples were imaged to assess the influence of plasmon induced curing on the polymer structure at the nano scale.

Supplementary Table 7

Sample	Formulation	Curing
1	p-DCPD/***cis*-Ru-P(OBn)$_3$/AuBP$_{850}$**	LED
2	p-DCPD/***cis*-Ru-P(OBn)$_3$/AuBP$_{850}$**	Oven
3	p-DCPD/***cis*-Ru-P(OBn)$_3$/AuBP$_{660}$**	LED
4	p-DCPD/***cis*-Ru-P(OBn)$_3$/AuBP$_{660}$**	Oven

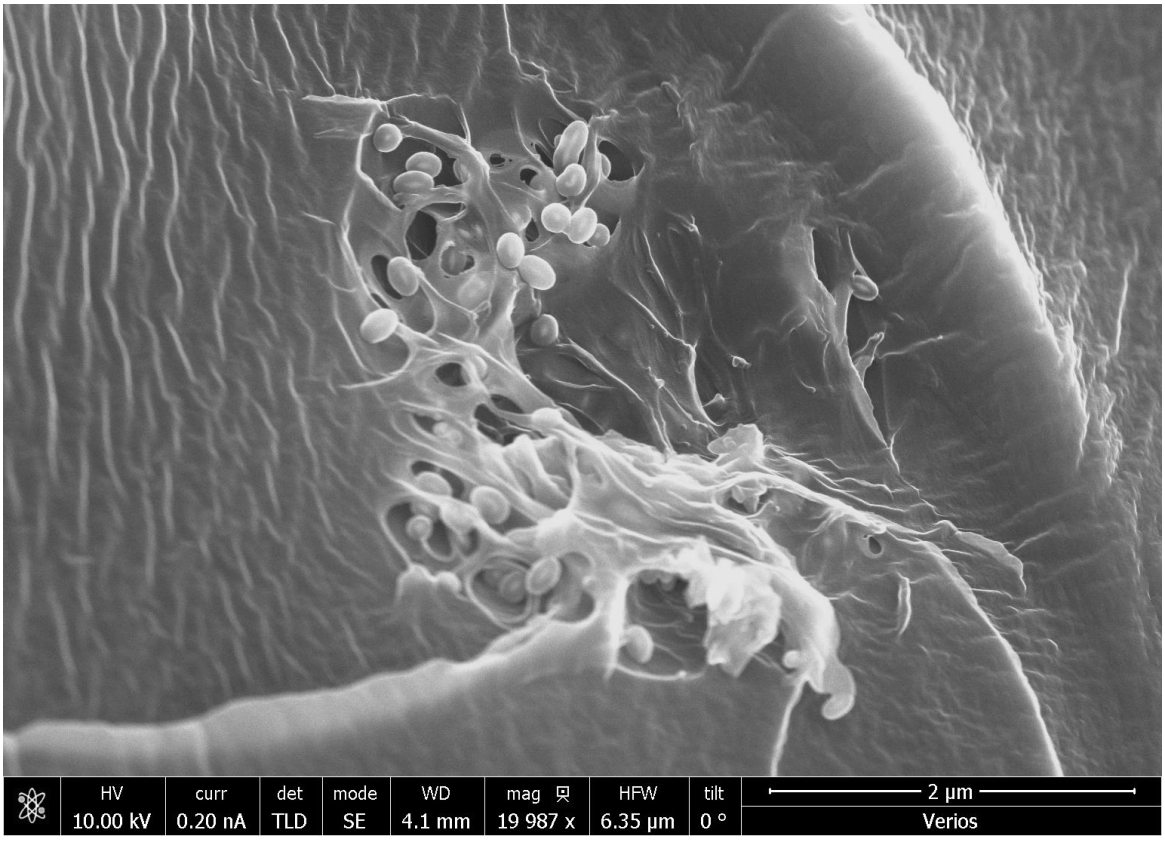

Supplementary figure 72 | SEM image of sample 1 table 7.

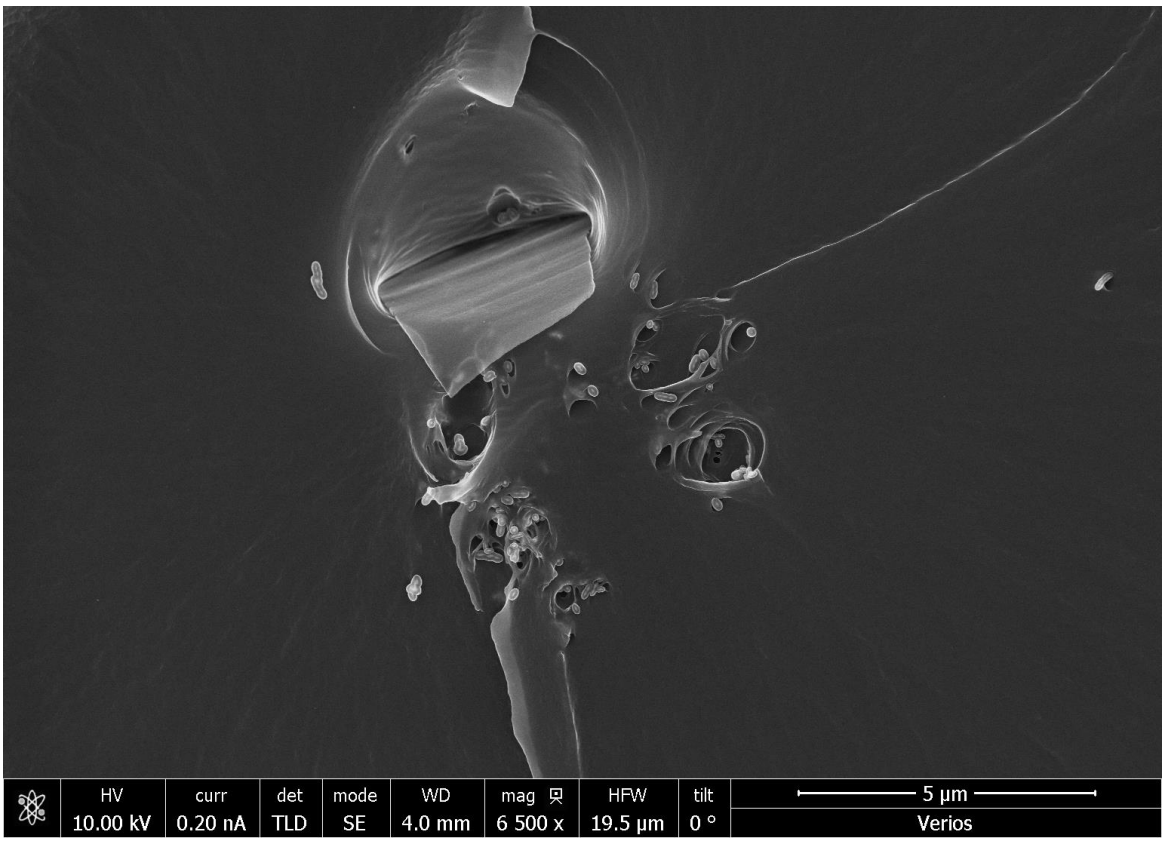

Supplementary figure 73 | SEM image of sample 1 table 7.

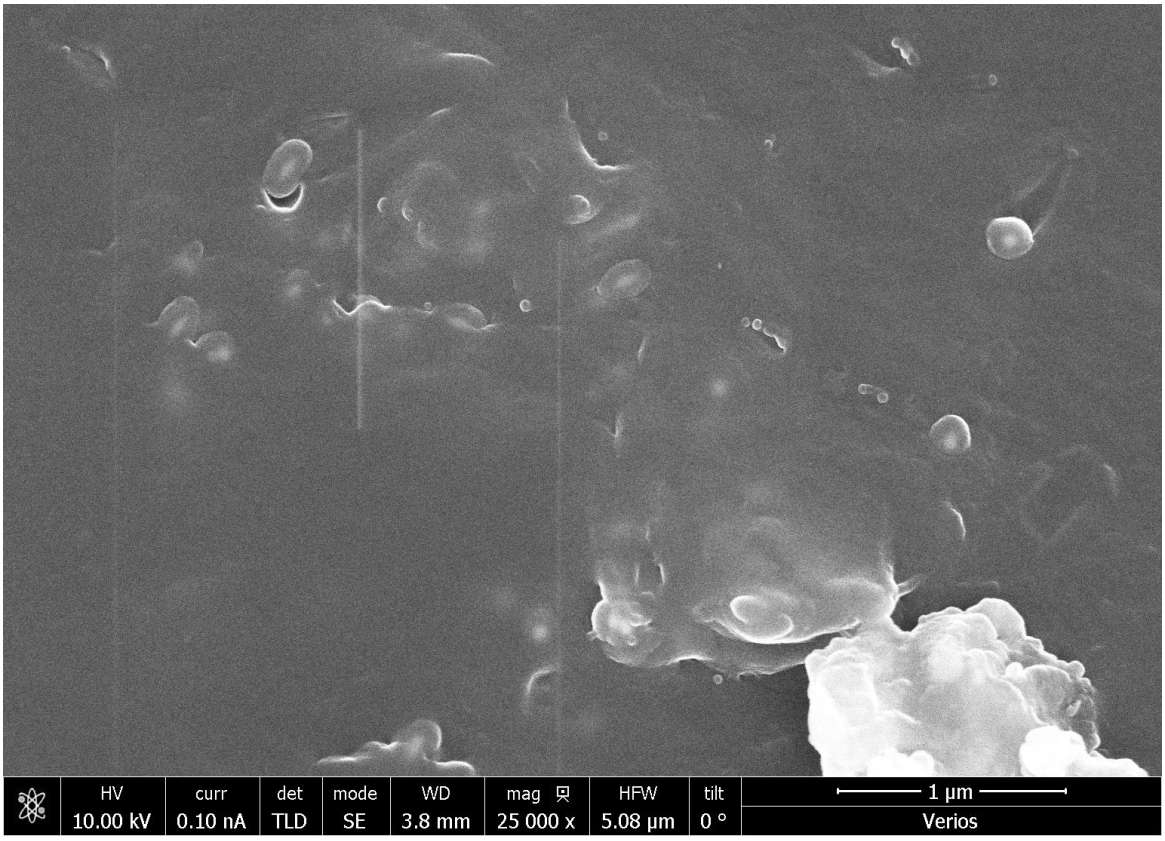

Supplementary figure 74 | SEM image of sample 2 table 7.

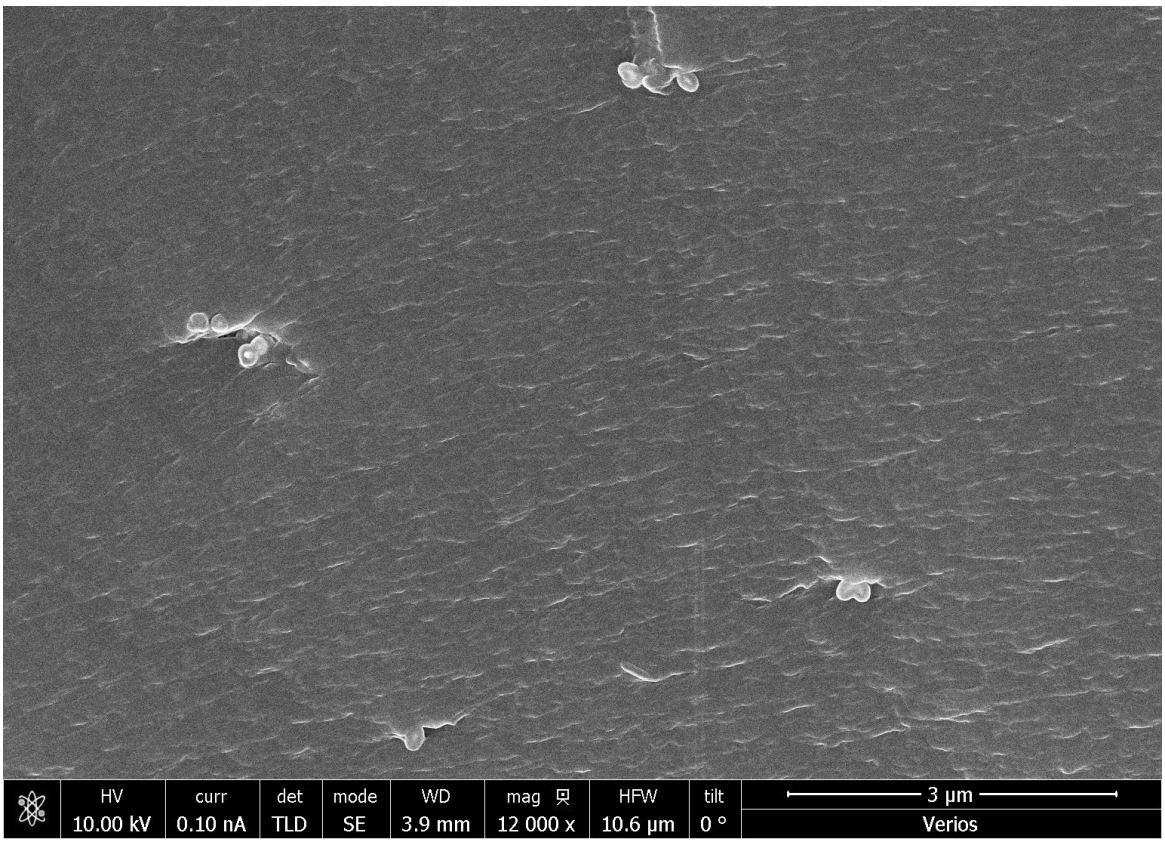

Supplementary figure 75 | SEM image of sample 2 table 7.

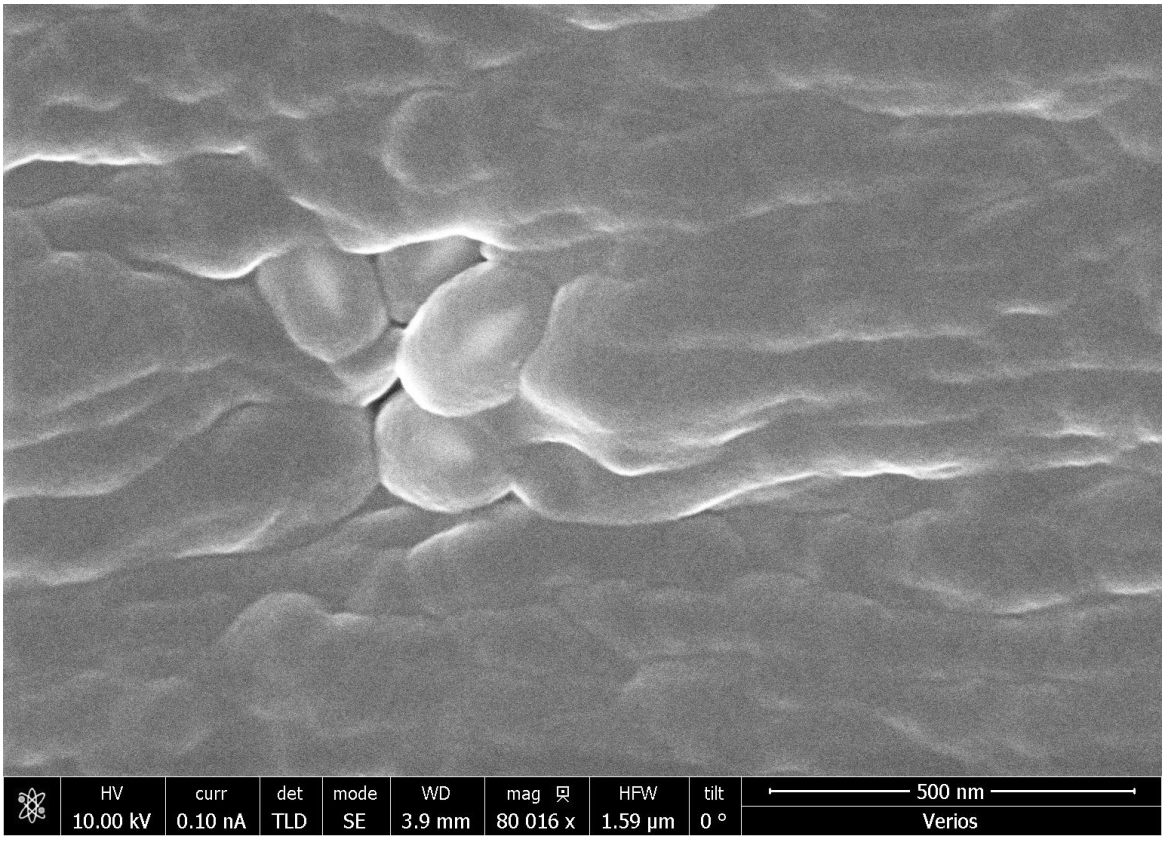

Supplementary figure 76 | SEM image of sample 2 table 7.

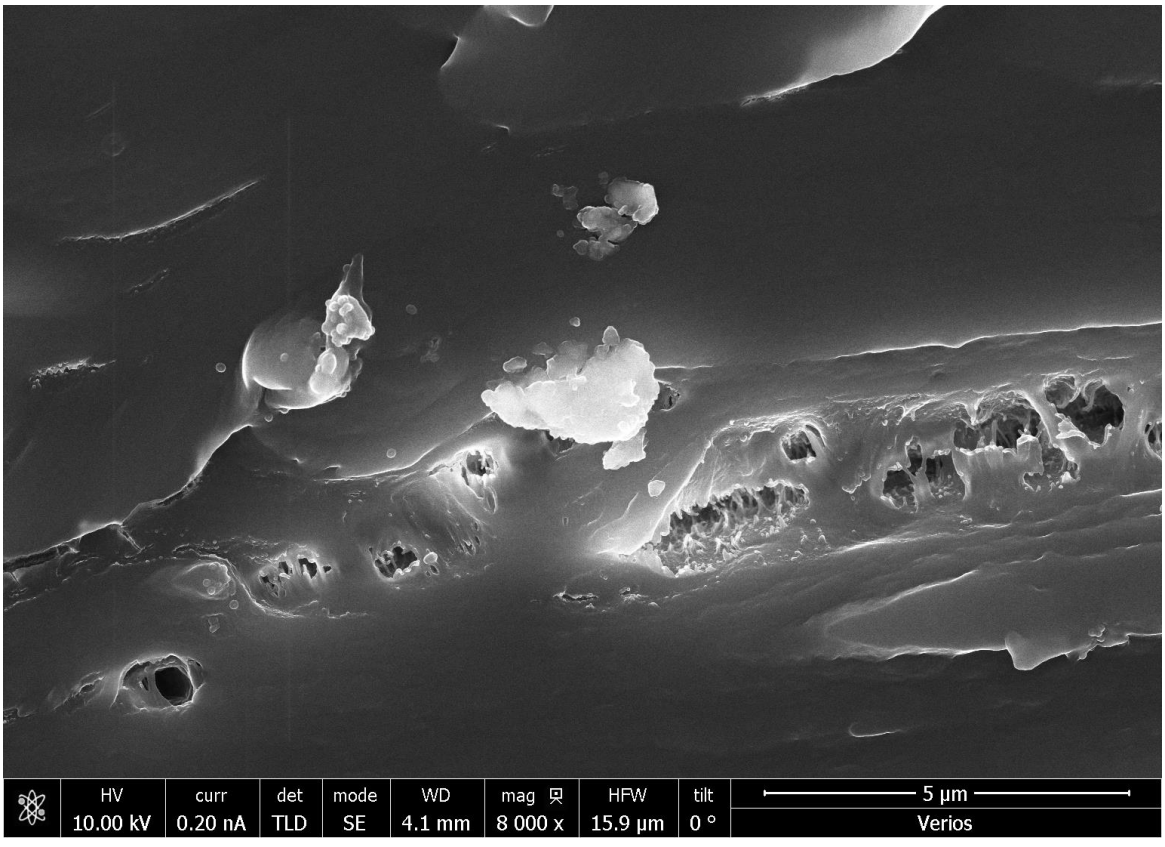

Supplementary figure 77 | SEM image of sample 3 table 7.

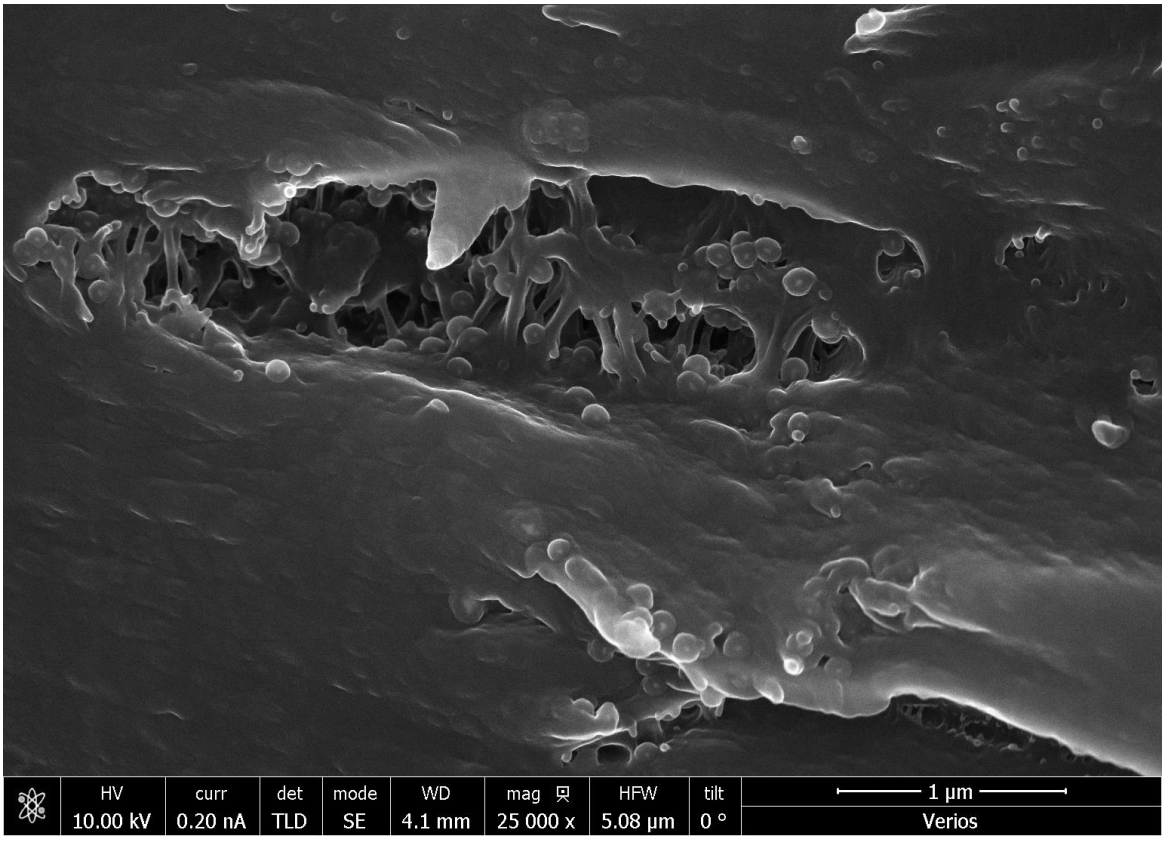

Supplementary figure 78 | SEM image of sample 3 table 7.

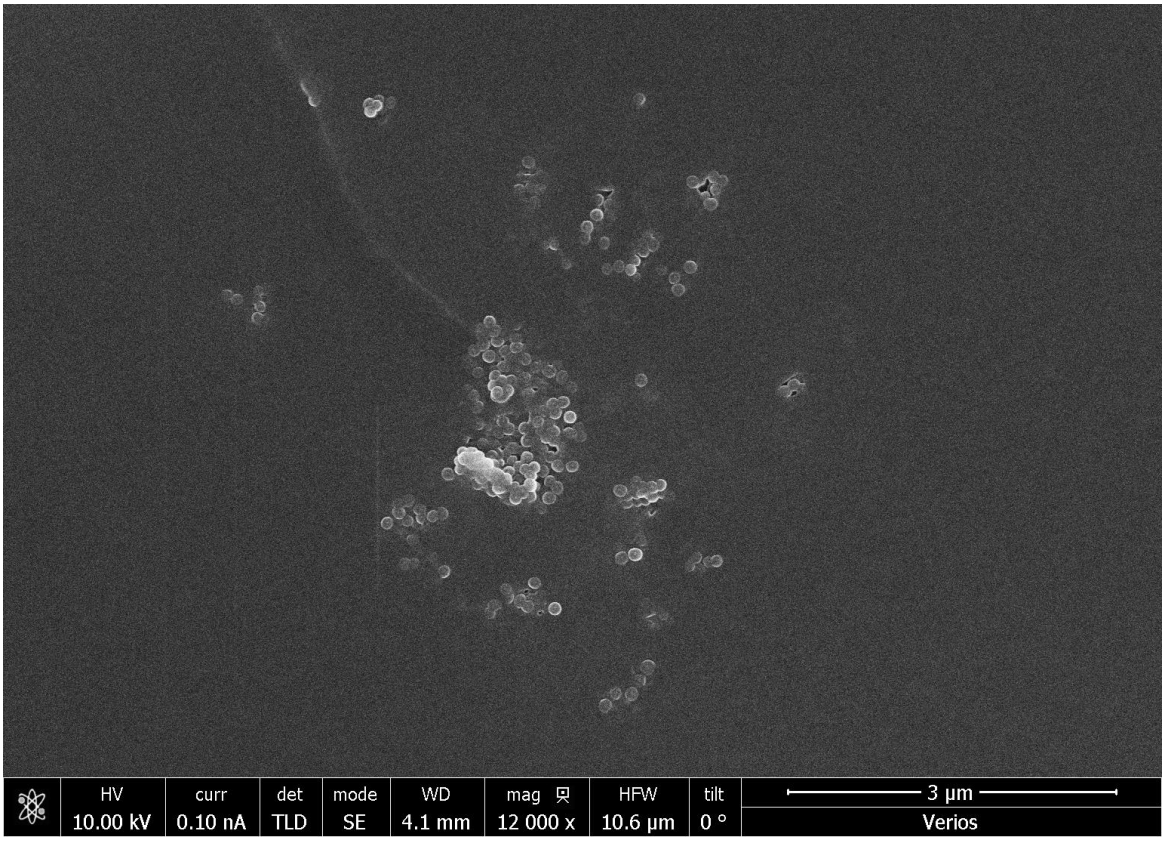

Supplementary figure 79 | SEM image of sample 4 table 7.

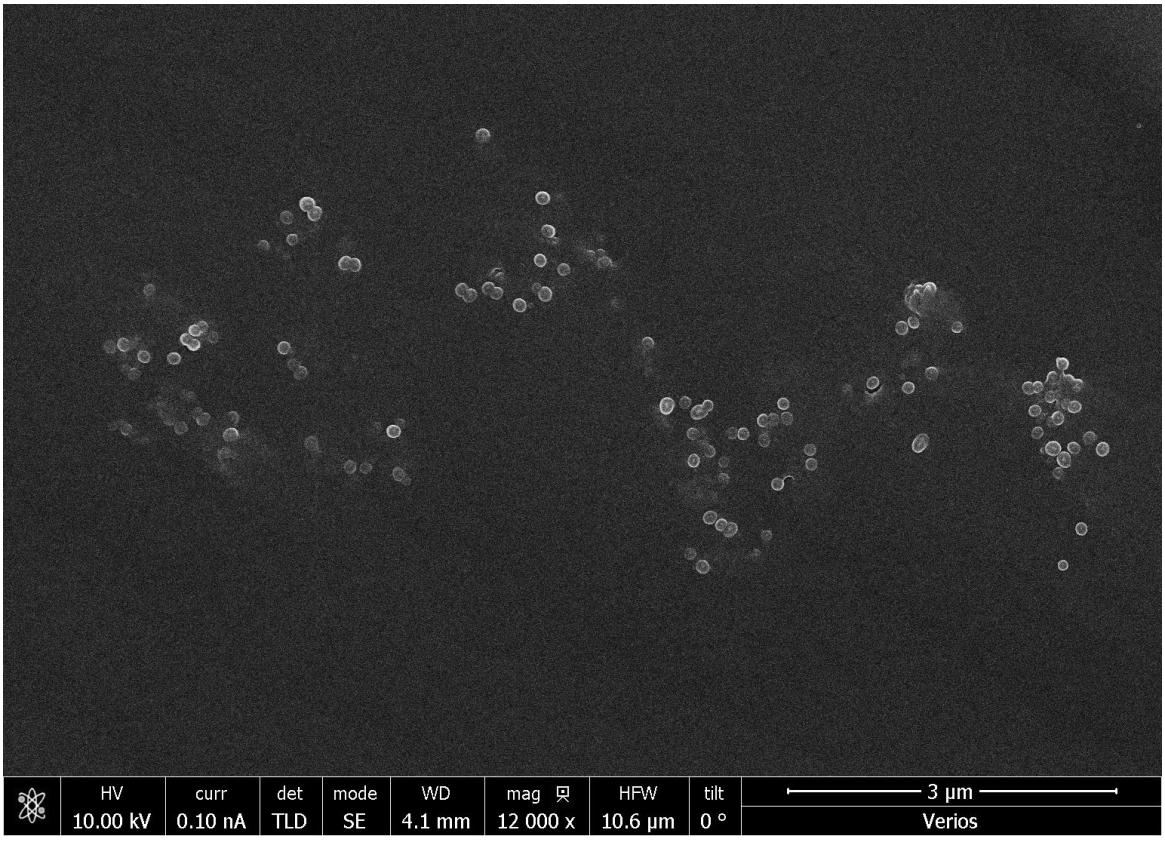

Supplementary figure 80 | SEM image of sample 4 table 7.

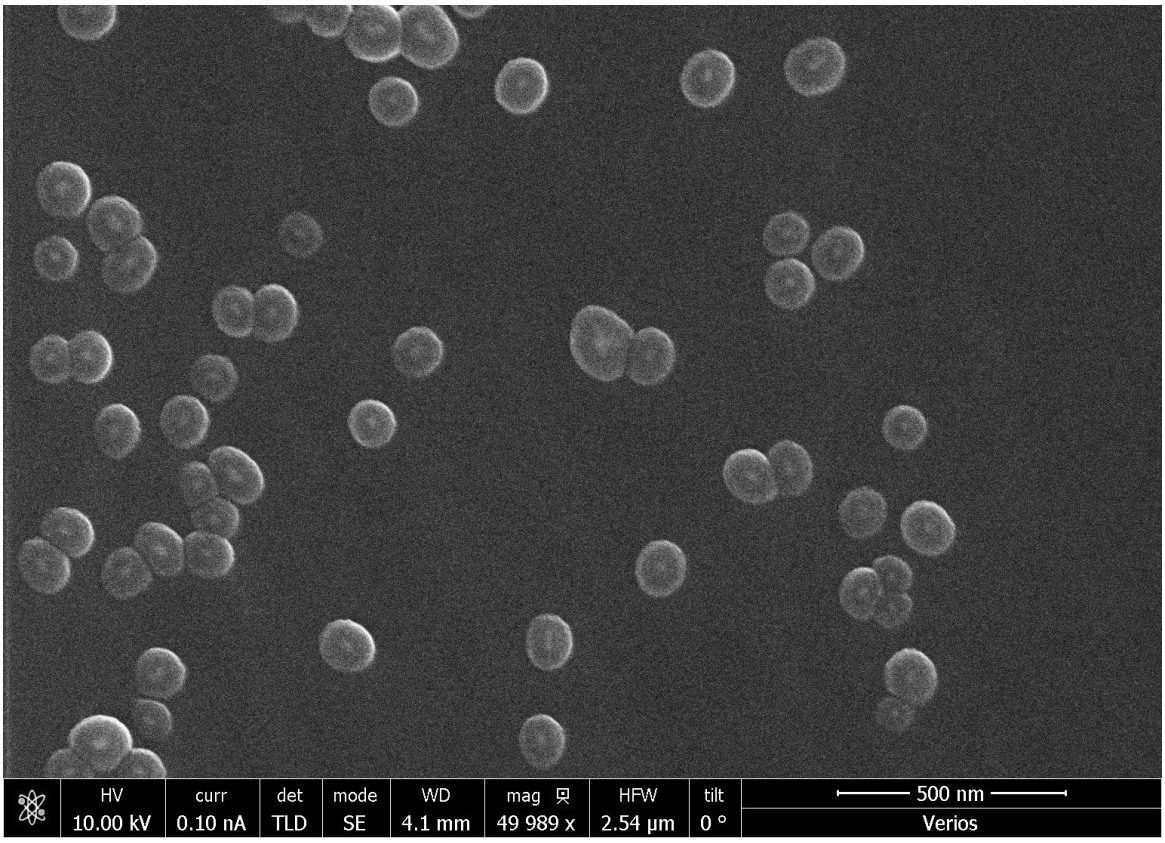

Supplementary figure 81 | SEM image of sample 4 table 7.

20. Supplementary Videos

Supplementary Video 1 | Side by side videos of a PPC_{850} film (20 OD) while being irradiated with 850 nm LED (100 W). On the left, normal recording. On the right, the thermal camera (Flir one) recording including its temperature reading.

Supplementary Video 2 | Preparation process of photoresponsive PPC_{660} (20 OD) coil. Initially, the "soft" polymer is shaped. After the shaping is complete photothermal curing was achieved by irradiating with 660 nm LED (200 W). Finally, the coils toughness was demonstrated.

Supplementary Video 3 | Preparation process of photoresponsive PPC_{850} (20 OD) knot. Initially, the "soft" polymer was shaped into a knot. It was then irradiated with an 850 nm LED (100 W) until photothermal curing was complete. Finally, the knots toughness was demonstrated, and one can clearly see that cured sections are rigid and non-cured sections are flexible.

Supplementary Video 4 | Side by side video of a funnel blocked by the photoresponsive jojoba derived wax (embedded with **$AuBP_{850}$** at 10 OD). The funnel was filled with water and then irradiated with an 850 nm LED (100 W). The wax's photothermal response caused its melting and the water was spilled. This simple demonstration hints at potential applications for materials of this type.

21. Supplementary References

1. Sánchez-Iglesias, A. *et al.* High-Yield Seeded Growth of Monodisperse Pentatwinned Gold Nanoparticles through Thermally Induced Seed Twinning. *J. Am. Chem. Soc.* **139**, 107–110 (2017).
2. Eivgi, O., Vaisman, A., Nechmad, N. B., Baranov, M. and Lemcoff, N. G., Latent Ruthenium Benzylidene Phosphite Complexes for Visible Light Induced Olefin Metathesis, *ACS Catal.*, **10**, 2033-2038, (2020).
3. Ginzburg, Y., Anaby, A., Vidavsky, Y., Diesendruck, C.E., Ben-Asuly, A., Goldberg, I. and Lemcoff, N.G., Widening the Latency Gap in Chelated Ruthenium Olefin Metathesis Catalysts, *Organometallics*, **30**, 3430 – 3437, (2011).
4. Jana, N., Gram-Scale Synthesis of Soluble, Near-Monodisperse Gold Nanorods and Other Anisotropic Nanoparticles, Small, **1**, 875-882, (2005).